

Gaussian Belief Propagation: Theory and Application

Thesis for the degree of

DOCTOR of PHILOSOPHY

by

Danny Bickson

SUBMITTED TO THE SENATE OF
THE HEBREW UNIVERSITY OF JERUSALEM

October 2008

**This work was carried out under the supervision of
Prof. Danny Dolev and Prof. Dahlia Malkhi**

Acknowledgements

I would first like to thank my advisors, Prof. Danny Dolev and Prof. Dahlia Malkhi. Danny Dolev encouraged me to follow this interesting research direction, had infinite time to meet and our brainstorming sessions were always valuable and enjoyable. Dahlia Malkhi encouraged me to do a Ph.D., worked with me closely at the first part of my Ph.D., and was always energetic and inspiring. My time as an intern in Microsoft Research, Silicon Valley, will never be forgotten, in the period where my research skills were immensely improved.

I would like to thank Prof. Yair Weiss, for teaching highly interesting courses and introducing me to the graphical models world. Also for continuous support in answering millions of questions.

Prof. Scott Kirkpatrick introduced me to the world of statistical physics, mainly using the Evergrow project. It was a pleasure working with him, specifically watching his superb management skills which could defeat every obstacle. In this project, I've also met Prof. Erik Aurell from SICS/KTH and we had numerous interesting discussions about Gaussians, the bread-and-butter of statistical physics.

I am lucky that I had the opportunity to work with Dr. Ori Shental from USCD. Ori introduced me into the world of information theory and together we had a fruitful joint research.

Further thanks to Prof. Yuval Shavitt from Tel Aviv university, for serving in my Ph.D. committee, and for fruitful discussions.

The support vector regression work was done when I was intern in IBM Research Haifa Lab. Thanks to Elad Yom-Tov and Oded Margalit for their encouragement and for our enjoyable joint work.

I thank Prof. Andrea Montanari for sharing his multiuser detection code.

Finally I would like to thank my wife Ravit, for her continuous support.

Abstract

The canonical problem of solving a system of linear equations arises in numerous contexts in information theory, communication theory, and related fields. In this contribution, we develop a solution based upon Gaussian belief propagation (GaBP) that does not involve direct matrix inversion. The iterative nature of our approach allows for a distributed message-passing implementation of the solution algorithm. In the first part of this thesis, we address the properties of the GaBP solver, including convergence, exactness, computational complexity, message-passing efficiency and its relation to classical solution methods including numerical examples. We further relate to several other algorithms and explore their connection to the GaBP algorithm.

In the second part we give three applications to illustrate the applicability of the GaBP algorithm to very large computer networks: Peer-to-Peer rating, linear detection and distributed computation of support vector regression. Using extensive simulations on up to 1,024 CPUs in parallel using IBM Bluegene supercomputer we demonstrate the attractiveness and applicability of the GaBP algorithm, using real life network topologies with up to millions of nodes and hundreds of millions of communication links.

Contents

1	Introduction	1
1.1	Material Covered in this Thesis	2
1.2	Preliminaries: Notations and Definitions	3
1.2.1	Linear Algebra	3
1.2.2	Graphical Models	4
1.3	Problem Formulation	5
	Part 1: Theory	6
2	The GaBP Algorithm	7
2.1	From Linear Algebra to Probabilistic Inference	7
2.2	Belief Propagation	8
2.3	GaBP Algorithm	9
2.4	Max-Product Rule	11
2.5	Properties	13
2.6	Convergence	13
2.7	Complexity and Efficiency	14
2.8	The GaBP-Based Solver and Classical Solution Methods	15
2.8.1	Gaussian Elimination	15
2.8.2	Iterative Methods	18
2.8.3	Jacobi Method	18
2.8.4	Gauss-Seidel	19
3	Numerical Examples	20
3.1	Toy Linear System	20
3.2	Non PSD Example	22
3.3	2D Poisson's	22
4	Relation to other algorithms	29
4.1	Montanari's Linear Detection	29
4.2	Frey's LPP Algorithm	31
4.3	Consensus Propagation	33

4.4	Quadratic Min-Sum	35
Part 2: Applications		37
5	Peer-to-Peer Rating	38
5.1	Framework	39
5.2	Quadratic Cost Functions	40
5.2.1	Peer-to-Peer rating	42
5.2.2	Spatial Ranking	43
5.2.3	Personalized PageRank	44
5.2.4	Information Centrality	44
5.3	Experimental results	45
5.3.1	Rating Benchmark	47
6	Linear Detection	49
6.1	GaBP Extension	54
6.1.1	Distributed Iterative Computation of the MMSE Detector	55
6.1.2	Relation to factor graph	56
6.1.3	New convergence results	57
7	Support vector regression	59
7.1	SVM Classification	59
7.2	KRR Problem	61
7.3	Previous Approaches	61
7.4	GaBP Algorithm Convergence	63
7.5	Convergence in Asynchronous Settings	63
7.6	Experimental Results	64
7.7	Discussion	67
8	Appendices	68
8.1	Proof of Lemma 10	68
8.2	Integrating over x_i	69
8.3	Maximizing over x_i	69
8.4	Weiss vs. Johnson	70
8.5	Proof of Theorem 21	71
8.6	Proof of Theorem 22	71
8.7	Proof of Theorem 17	72
8.8	Proof of Theorem 26	72
8.9	GaBP code in matlab	72
8.9.1	The file gabp.m	72
8.9.2	The file run_gabp.m	74

Chapter 1

Introduction

Solving a system of linear equations $\mathbf{Ax} = \mathbf{b}$ is one of the most fundamental problems in algebra, with countless applications in the mathematical sciences and engineering. In this thesis, we propose an efficient distributed iterative algorithm for solving systems of linear equations.

The problem of solving linear system of equations is described as follows. Given an observation vector $\mathbf{b} \in \mathbb{R}^m$ and the data matrix $\mathbf{A} \in \mathbb{R}^{m \times n}$ ($m \geq n \in \mathbb{Z}$), a unique solution, $\mathbf{x} = \mathbf{x}^* \in \mathbb{R}^n$, exists if and only if the data matrix \mathbf{A} has full column rank. Assuming a nonsingular matrix \mathbf{A} , the system of equations can be solved either directly or in an iterative manner. Direct matrix inversion methods, such as Gaussian elimination (LU factorization, [1]-Ch. 3) or band Cholesky factorization ([1]-Ch. 4), find the solution with a finite number of operations, typically, for a dense $n \times n$ matrix, of the order of n^3 . The former is particularly effective for systems with unstructured dense data matrices, while the latter is typically used for structured dense systems.

Iterative methods [2] are inherently simpler, requiring only additions and multiplications, and have the further advantage that they can exploit the sparsity of the matrix \mathbf{A} to reduce the computational complexity as well as the algorithmic storage requirements [3]. By comparison, for large, sparse and amorphous data matrices, the direct methods are impractical due to the need for excessive matrix reordering operations.

The main drawback of the iterative approaches is that, under certain conditions, they converge only asymptotically to the exact solution \mathbf{x}^* [2]. Thus, there is the risk that they may converge slowly, or not at all. In practice, however, it has been found that they often converge to the exact solution or a good approximation after a relatively small number of iterations.

A powerful and efficient iterative algorithm, belief propagation (BP, [4]), also known as the sum-product algorithm, has been very successfully used to solve, either exactly or approximately, inference problems in probabilistic graphical models [5].

In this thesis, we reformulate the general problem of solving a linear system of algebraic equations as a probabilistic inference problem on a suitably-defined graph. We believe that this is the first time that an explicit connection between these two ubiquitous problems has been established¹. Furthermore, for the first time, we provide a full step-by-step derivation of the

¹Recently, we have found out the work of Moallemi and Van Roy [6] which discusses the connection between the Min-Sum message passing algorithm and solving quadratic programs. Both works [7, 6] were published in

GaBP algorithm from the belief propagation algorithm.

As an important consequence, we demonstrate that Gaussian BP (GaBP) provides an efficient, distributed approach to solving a linear system that circumvents the potentially complex operation of direct matrix inversion. Using the seminal work of Weiss and Freeman [8] and some recent related developments [9, 10, 6], we address the convergence and exactness properties of the proposed GaBP solver. Other properties of the GaBP solver, as computational complexity, message-passing efficiency and its relation to classical solution methods are also investigated.

We provide several applications for our GaBP solver.

The first application we investigate (Chapter 5) is the rating of nodes in a Peer-to-Peer network. We propose a unifying family of quadratic cost functions to be used in Peer-to-Peer ratings. We show that our approach is general, since it captures many of the existing algorithms in the fields of visual layout, collaborative filtering and Peer-to-Peer rating, among them Koren spectral layout algorithm, Katz method, Spatial ranking, Personalized PageRank and Information Centrality. Besides of the theoretical interest in finding common basis of algorithms that where not linked before, we allow a single efficient implementation for computing those various rating methods, using the GaBP solver. We provide simulation results on top of real life topologies including the MSN Messenger social network.

In Chapter 6 we consider the problem of linear detection using a decorrelator in a code-division multiple-access (CDMA) system. Through the use of the iterative message-passing formulation, we implement the decorrelator detector in a distributed manner. This example allows us to quantitatively compare the new GaBP solver with the classical iterative solution methods that have been previously investigated in the context of a linear implementation of CDMA demodulation [11, 12, 13]. We show that the GaBP-based decorrelator yields faster convergence than these conventional methods. Furthermore, the GaBP convergence is further accelerated by incorporating the linear-algebraic methods of Aitken and Steffensen [14] into the GaBP-based scheme. As far as we know, this represents the first time these acceleration methods have been examined within the framework of message-passing algorithms.

A third application from the field of learning is the support vector regression, described in Chapter 7. We show how to compute kernel ridge regression using our GaBP solver. For demonstrating the applicability of our approach we used a cluster of IBM BlueGene computers with up to 1,024 CPUs in parallel on very large data sets consisting of millions of data points.

1.1 Material Covered in this Thesis

This thesis is divided into two parts. The first part discusses the theory of Gaussian belief propagation algorithm and covers the following papers: [7, 15, 16, 17].

The second part discusses several applications that where covered in the following papers: [18, 19, 20, 21, 22].

Below we briefly outline some other related papers that did not fit into this thesis main

parallel, and the algorithms where derived independently, using different techniques. In Section 4.4 we discuss the connection between the two algorithms, and show they are equivalent.

theme. We have looked at belief propagation at the using discrete distribution as a basis for various distributed algorithms: clustering [23], data placement [24, 25] Peer-to-Peer streaming media [26] and wireless settings [27]. The other major topic we worked on is Peer-to-Peer networks, especially content distribution networks (CDNs). The Julia content distribution network is described on [28, 29]. A modified version of Julia using network coding [30]. Tulip is a Peer-to-Peer overlay that enables fast routing and searching [31]. The eMule protocol specification is found on [32]. An implementation of a distributed testbed on eight European clusters is found on [33].

1.2 Preliminaries: Notations and Definitions

1.2.1 Linear Algebra

We shall use the following linear-algebraic notations and definitions. The operator $\{\cdot\}^T$ stands for a vector or matrix transpose, the matrix \mathbf{I}_n is an $n \times n$ identity matrix, while the symbols $\{\cdot\}_i$ and $\{\cdot\}_{ij}$ denote entries of a vector and matrix, respectively. Let $\mathbf{M} \in \mathbb{R}^{n \times n}$ be a real symmetric square matrix and $\mathbf{A} \in \mathbb{R}^{m \times n}$ be a real (possibly rectangular) matrix. Let

Definition 1 (Pseudoinverse). *The Moore-Penrose pseudoinverse matrix of the matrix \mathbf{A} , denoted by \mathbf{A}^\dagger , is defined as*

$$\mathbf{A}^\dagger \triangleq (\mathbf{A}^T \mathbf{A})^{-1} \mathbf{A}^T. \quad (1.1)$$

Definition 2 (Spectral radius). *The spectral radius of the matrix \mathbf{M} , denoted by $\rho(\mathbf{M})$, is defined to be the maximum of the absolute values of the eigenvalues of \mathbf{M} , i.e.,*

$$\rho(\mathbf{M}) \triangleq \max_{1 \leq i \leq s} (|\lambda_i|), \quad (1.2)$$

where $\lambda_1, \dots, \lambda_s$ are the eigenvalues of the matrix \mathbf{M} .

Definition 3 (Diagonal dominance). *The matrix \mathbf{M} is*

1. *weakly diagonally dominant if*

$$|M_{ii}| \geq \sum_{j \neq i} |M_{ij}|, \forall i, \quad (1.3)$$

2. *strictly diagonally dominant if*

$$|M_{ii}| > \sum_{j \neq i} |M_{ij}|, \forall i, \quad (1.4)$$

3. irreducibly diagonally dominant if \mathbf{M} is irreducible², and

$$|M_{ii}| \geq \sum_{j \neq i} |M_{ij}|, \forall i, \quad (1.5)$$

with strict inequality for at least one i .

Definition 4 (PSD). The matrix \mathbf{M} is positive semi-definite (PSD) if and only if for all non-zero real vectors $\mathbf{z} \in \mathbb{R}^n$,

$$\mathbf{z}^T \mathbf{M} \mathbf{z} \geq 0. \quad (1.6)$$

Definition 5 (Residual). For a real vector $\mathbf{x} \in \mathbb{R}^n$, the residual, $\mathbf{r} = \mathbf{r}(\mathbf{x}) \in \mathbb{R}^m$, of a linear system is $\mathbf{r} = \mathbf{A} \mathbf{x} - \mathbf{b}$.

The standard norm of the residual, $\|\mathbf{r}\|_p (p = 1, 2, \dots, \infty)$, is a good measure of the accuracy of a vector \mathbf{x} as a solution to the linear system. In our experimental study, the Frobenius norm (i.e., $p = 2$) per equation is used, $\|\mathbf{r}\|_F/m = \sqrt{\sum_{i=1}^m r_i^2}/m$.

Definition 6. The condition number, κ , of the matrix \mathbf{M} is defined as

$$\kappa_p \triangleq \|\mathbf{M}\|_p \|\mathbf{M}\|_p^{-1}. \quad (1.7)$$

For \mathbf{M} being a normal matrix (i.e., $\mathbf{M}^T \mathbf{M} = \mathbf{M} \mathbf{M}^T$), the condition number is given by

$$\kappa = \kappa_2 = \left| \frac{\lambda_{max}}{\lambda_{min}} \right|, \quad (1.8)$$

where λ_{max} and λ_{min} are the maximal and minimal eigenvalues of \mathbf{M} , respectively.

Even though a system is nonsingular it could be ill-conditioned. Ill-conditioning means that a small perturbation in the data matrix \mathbf{A} , or the observation vector \mathbf{b} , causes large perturbations in the solution, \mathbf{x}^* . This determines the difficulty of solving the problem. The condition number is a good measure of the ill-conditioning of the matrix. The better the conditioning of a matrix the condition number is smaller, going to unity. The condition number of a non-invertible (singular) matrix is set arbitrarily to infinity.

1.2.2 Graphical Models

We will make use of the following terminology and notation in the discussion of the GaBP algorithm. Given the data matrix \mathbf{A} and the observation vector \mathbf{b} , one can write explicitly the Gaussian density function, $p(\mathbf{x})$, and its corresponding graph \mathcal{G} consisting of edge potentials

² A matrix is said to be reducible if there is a permutation matrix \mathbf{P} such that $\mathbf{P} \mathbf{M} \mathbf{P}^T$ is block upper triangular. Otherwise, it is irreducible.

(compatibility functions) ψ_{ij} and self potentials ('evidence') ϕ_i . These graph potentials are simply determined according to the following pairwise factorization of the Gaussian function (2.1)

$$p(\mathbf{x}) \propto \prod_{i=1}^n \phi_i(x_i) \prod_{\{i,j\}} \psi_{ij}(x_i, x_j), \quad (1.9)$$

resulting in $\psi_{ij}(x_i, x_j) \triangleq \exp(-x_i A_{ij} x_j)$ and $\phi_i(x_i) \triangleq \exp(b_i x_i - A_{ii} x_i^2 / 2)$. The edges set $\{i, j\}$ includes all non-zero entries of \mathbf{A} for which $i > j$. The set of graph nodes $N(i)$ denotes the set of all the nodes neighboring the i th node (excluding node i). The set $N(i) \setminus j$ excludes the node j from $N(i)$.

1.3 Problem Formulation

Let $\mathbf{A} \in \mathbb{R}^{m \times n}$ ($m, n \in \mathbb{N}^*$) be a full column rank, $m \times n$ real-valued matrix, with $m \geq n$, and let $\mathbf{b} \in \mathbb{R}^m$ be a real-valued vector. Our objective is to efficiently find a solution \mathbf{x}^* to the linear system of equations $\mathbf{A}\mathbf{x} = \mathbf{b}$ given by

$$\mathbf{x}^* = \mathbf{A}^\dagger \mathbf{b}. \quad (1.10)$$

Assumption 7. *The matrix \mathbf{A} is square (i.e., $m = n$) and symmetric.*

For the case of square matrices the pseudoinverse matrix is nothing but the data matrix inverse, i.e., $\mathbf{A}^\dagger = \mathbf{A}^{-1}$. For any linear system of equations with a unique solution, Assumption 7 conceptually entails no loss of generality, as can be seen by considering the invertible system defined by the new symmetric (and PSD) matrix $\mathbf{A}^T_{n \times m} \mathbf{A}_{m \times n} \mapsto \mathbf{A}_{n \times n}$ and vector $\mathbf{A}^T_{n \times m} \mathbf{b}_{m \times 1} \mapsto \mathbf{b}_{n \times 1}$. However, this transformation involves an excessive computational complexity of $\mathcal{O}(n^2 m)$ and $\mathcal{O}(nm)$ operations, respectively. Furthermore, a sparse data matrix may become dense due to the transformation, an undesired property as far as complexity concerns. Thus, we first limit the discussion to the solution of the popular case of square matrices. In Section 6.1.1 the proposed GaBP solver is extended to the more general case of linear systems with rectangular $m \times n$ full rank matrices.

Part 1: Theory

Chapter 2

The GaBP-Based Solver Algorithm

In this section, we show how to derive the iterative, Gaussian BP-based algorithm that we propose for solving the linear system

$$\mathbf{A}_{n \times n} \mathbf{x}_{n \times 1} = \mathbf{b}_{n \times 1}.$$

2.1 From Linear Algebra to Probabilistic Inference

We begin our derivation by defining an undirected graphical model (*i.e.*, a Markov random field), \mathcal{G} , corresponding to the linear system of equations. Specifically, let $\mathcal{G} = (\mathcal{X}, \mathcal{E})$, where \mathcal{X} is a set of nodes that are in one-to-one correspondence with the linear system's variables $\mathbf{x} = \{x_1, \dots, x_n\}^T$, and where \mathcal{E} is a set of undirected edges determined by the non-zero entries of the (symmetric) matrix \mathbf{A} .

Using this graph, we can translate the problem of solving the linear system from the algebraic domain to the domain of probabilistic inference, as stated in the following theorem.

Proposition 8. *The computation of the solution vector \mathbf{x}^* is identical to the inference of the vector of marginal means $\mu \triangleq \{\mu_1, \dots, \mu_n\}$ over the graph \mathcal{G} with the associated joint Gaussian probability density function $p(\mathbf{x}) \sim \mathcal{N}(\mu, \mathbf{A}^{-1})$.*

Proof. Another way of solving the set of linear equations $\mathbf{A}\mathbf{x} - \mathbf{b} = \mathbf{0}$ is to represent it by using a quadratic form $q(\mathbf{x}) \triangleq \mathbf{x}^T \mathbf{A}\mathbf{x}/2 - \mathbf{b}^T \mathbf{x}$. As the matrix \mathbf{A} is symmetric, the derivative of the quadratic form w.r.t. the vector \mathbf{x} is given by the vector $\partial q/\partial \mathbf{x} = \mathbf{A}\mathbf{x} - \mathbf{b}$. Thus equating $\partial q/\partial \mathbf{x} = \mathbf{0}$ gives the global minimum \mathbf{x}^* of this convex function, which is nothing but the desired solution to $\mathbf{A}\mathbf{x} = \mathbf{b}$.

Next, one can define the following joint Gaussian probability density function

$$p(\mathbf{x}) \triangleq \mathcal{Z}^{-1} \exp(-q(\mathbf{x})) = \mathcal{Z}^{-1} \exp(-\mathbf{x}^T \mathbf{A}\mathbf{x}/2 + \mathbf{b}^T \mathbf{x}), \quad (2.1)$$

where \mathcal{Z} is a distribution normalization factor. Denoting the vector $\mu \triangleq \mathbf{A}^{-1}\mathbf{b}$, the Gaussian

density function can be rewritten as

$$\begin{aligned}
 p(\mathbf{x}) &= \mathcal{Z}^{-1} \exp(\mu^T \mathbf{A} \mu / 2) \\
 &\times \exp(-\mathbf{x}^T \mathbf{A} \mathbf{x} / 2 + \mu^T \mathbf{A} \mathbf{x} - \mu^T \mathbf{A} \mu / 2) \\
 &= \zeta^{-1} \exp(-(\mathbf{x} - \mu)^T \mathbf{A} (\mathbf{x} - \mu) / 2) \\
 &= \mathcal{N}(\mu, \mathbf{A}^{-1}),
 \end{aligned} \tag{2.2}$$

where the new normalization factor $\zeta \triangleq \mathcal{Z} \exp(-\mu^T \mathbf{A} \mu / 2)$. It follows that the target solution $\mathbf{x}^* = \mathbf{A}^{-1} \mathbf{b}$ is equal to $\mu \triangleq \mathbf{A}^{-1} \mathbf{b}$, the mean vector of the distribution $p(\mathbf{x})$, as defined above (2.1).

Hence, in order to solve the system of linear equations we need to infer the marginal densities, which must also be Gaussian, $p(x_i) \sim \mathcal{N}(\mu_i = \{\mathbf{A}^{-1} \mathbf{b}\}_i, P_i^{-1} = \{\mathbf{A}^{-1}\}_{ii})$, where μ_i and P_i are the marginal mean and inverse variance (sometimes called the precision), respectively. \square

According to Proposition 8, solving a deterministic vector-matrix linear equation translates to solving an inference problem in the corresponding graph. The move to the probabilistic domain calls for the utilization of BP as an efficient inference engine.

Remark 9. *Defining a jointly Gaussian probability density function, immediately yields an implicit assumption on the positive semi-definiteness of the precision matrix \mathbf{A} , in addition to the symmetry assumption. However, we would like to stress out that this assumption emerges only for exposition purposes, so we can use the notion of ‘Gaussian probability’, but the derivation of the GaBP solver itself does not use this assumption. See the numerical example of the exact GaBP-based solution of a system with a symmetric, but not positive semi-definite, data matrix \mathbf{A} in Section 3.2.*

2.2 Belief Propagation

Belief propagation (BP) is equivalent to applying Pearl’s local message-passing algorithm [4], originally derived for exact inference in trees, to a general graph even if it contains cycles (loops). BP has been found to have outstanding empirical success in many applications, e.g., in decoding Turbo codes and low-density parity-check (LDPC) codes. The excellent performance of BP in these applications may be attributed to the sparsity of the graphs, which ensures that cycles in the graph are long, and inference may be performed as if it were a tree.

The BP algorithm functions by passing real-valued messages across edges in the graph and consists of two computational rules, namely the ‘sum-product rule’ and the ‘product rule’. In contrast to typical applications of BP in coding theory [34], our graphical representation resembles to a pairwise Markov random field [5] with a single type of propagating messages, rather than a factor graph [35] with two different types of messages, originated from either the variable node or the factor node. Furthermore, in most graphical model representations used in the information theory literature the graph nodes are assigned with discrete values, while in this contribution we deal with nodes corresponding to continuous variables. Thus, for a graph \mathcal{G}

composed of potentials ψ_{ij} and ϕ_i as previously defined, the conventional sum-product rule becomes an integral-product rule [8] and the message $m_{ij}(x_j)$, sent from node i to node j over their shared edge on the graph, is given by

$$m_{ij}(x_j) \propto \int_{x_i} \psi_{ij}(x_i, x_j) \phi_i(x_i) \prod_{k \in \mathcal{N}(i) \setminus j} m_{ki}(x_i) dx_i. \quad (2.3)$$

The marginals are computed (as usual) according to the product rule

$$p(x_i) = \alpha \phi_i(x_i) \prod_{k \in \mathcal{N}(i)} m_{ki}(x_i), \quad (2.4)$$

where the scalar α is a normalization constant. Note that the propagating messages (and the graph potentials) do not have to describe valid (*i.e.*, normalized) density probability functions, as long as the inferred marginals do.

2.3 The Gaussian BP Algorithm

Gaussian BP is a special case of continuous BP, where the underlying distribution is Gaussian. Now, we derive the Gaussian BP update rules by substituting Gaussian distributions into the continuous BP update equations.

Given the data matrix \mathbf{A} and the observation vector \mathbf{b} , one can write explicitly the Gaussian density function, $p(\mathbf{x})$ (2.2), and its corresponding graph \mathcal{G} . Using the graph definition and a certain (arbitrary) pairwise factorization of the Gaussian function (2.2), the edge potentials (compatibility functions) and self potentials ('evidence') ϕ_i are determined to be

$$\psi_{ij}(x_i, x_j) \triangleq \exp(-x_i A_{ij} x_j), \quad (2.5)$$

$$\phi_i(x_i) \triangleq \exp(b_i x_i - A_{ii} x_i^2 / 2), \quad (2.6)$$

respectively. Note that by completing the square, one can observe that

$$\phi_i(x_i) \propto \mathcal{N}(\mu_{ii} = b_i / A_{ii}, P_{ii}^{-1} = A_{ii}^{-1}). \quad (2.7)$$

The graph topology is specified by the structure of the matrix \mathbf{A} , *i.e.* the edges set $\{i, j\}$ includes all non-zero entries of \mathbf{A} for which $i > j$.

Before describing the inference algorithm performed over the graphical model, we make the elementary but very useful observation that the product of Gaussian densities over a common variable is, up to a constant factor, also a Gaussian density.

Lemma 10. *Let $f_1(x)$ and $f_2(x)$ be the probability density functions of a Gaussian random variable with two possible densities $\mathcal{N}(\mu_1, P_1^{-1})$ and $\mathcal{N}(\mu_2, P_2^{-1})$, respectively. Then their product, $f(x) = f_1(x)f_2(x)$ is, up to a constant factor, the probability density function of a Gaussian random variable with distribution $\mathcal{N}(\mu, P^{-1})$, where*

$$\mu = P^{-1}(P_1\mu_1 + P_2\mu_2), \quad (2.8)$$

$$P^{-1} = (P_1 + P_2)^{-1}. \quad (2.9)$$

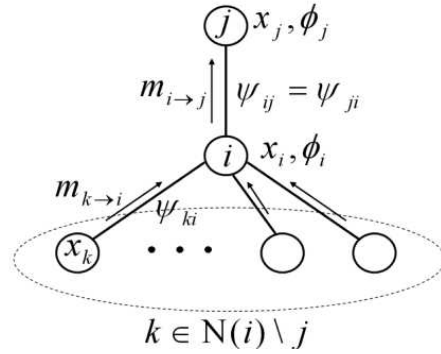


Figure 2.1: Belief propagation message flow

The proof of this lemma is found in Appendix 8.1.

Fig. 2.1 plots a portion of a certain graph, describing the neighborhood of node i . Each node (empty circle) is associated with a variable and self potential ϕ , which is a function of this variable, while edges go with the pairwise (symmetric) potentials Ψ . Messages are propagating along the edges on both directions (only the messages relevant for the computation of m_{ij} are drawn in Fig. 2.1). Looking at the right hand side of the integral-product rule (2.3), node i needs to first calculate the product of all incoming messages, except for the message coming from node j . Recall that since $p(\mathbf{x})$ is jointly Gaussian, the factorized self potentials $\phi_i(x_i) \propto \mathcal{N}(\mu_{ii}, P_{ii}^{-1})$ (2.7) and similarly all messages $m_{ki}(x_i) \propto \mathcal{N}(\mu_{ki}, P_{ki}^{-1})$ are of Gaussian form as well.

As the terms in the product of the incoming messages and the self potential in the integral-product rule (2.3) are all a function of the same variable, x_i (associated with the node i), then, according to the multivariate extension of Lemma 10,

$$\phi_i(x_i) \prod_{k \in N(i) \setminus j} m_{ki}(x_i) \quad (2.10)$$

is proportional to a certain Gaussian distribution, $\mathcal{N}(\mu_{i \setminus j}, P_{i \setminus j}^{-1})$. Applying the multivariate version of the product precision expression in (2.9), the update rule for the inverse variance is given by (over-braces denote the origin of each of the terms)

$$P_{i \setminus j} = \overbrace{P_{ii}}^{\phi_i(x_i)} + \sum_{k \in N(i) \setminus j} \overbrace{P_{ki}}^{m_{ki}(x_i)}, \quad (2.11)$$

where $P_{ii} \triangleq A_{ii}$ is the inverse variance a-priori associated with node i , via the precision of $\phi_i(x_i)$, and P_{ki} are the inverse variances of the messages $m_{ki}(x_i)$. Similarly using (2.8) for the multivariate case, we can calculate the mean

$$\mu_{i \setminus j} = P_{i \setminus j}^{-1} \left(\overbrace{P_{ii} \mu_{ii}}^{\phi_i(x_i)} + \sum_{k \in N(i) \setminus j} \overbrace{P_{ki} \mu_{ki}}^{m_{ki}(x_i)} \right), \quad (2.12)$$

where $\mu_{ii} \triangleq b_i/A_{ii}$ is the mean of the self potential and μ_{ki} are the means of the incoming messages.

Next, we calculate the remaining terms of the message $m_{ij}(x_j)$, including the integration over x_i . After some algebraic manipulation (deferred to Appendix 8.2), using the Gaussian integral

$$\int_{-\infty}^{\infty} \exp(-ax^2 + bx)dx = \sqrt{\pi/a} \exp(b^2/4a), \quad (2.13)$$

we find that the messages $m_{ij}(x_j)$ are proportional to normal distribution with precision and mean

$$P_{ij} = -A_{ij}^2 P_{i \setminus j}^{-1}, \quad (2.14)$$

$$\mu_{ij} = -P_{ij}^{-1} A_{ij} \mu_{i \setminus j}. \quad (2.15)$$

These two scalars represent the messages propagated in the Gaussian BP-based algorithm.

Finally, computing the product rule (2.4) is similar to the calculation of the previous product (2.10) and the resulting mean (2.12) and precision (2.11), but including all incoming messages. The marginals are inferred by normalizing the result of this product. Thus, the marginals are found to be Gaussian probability density functions $\mathcal{N}(\mu_i, P_i^{-1})$ with precision and mean

$$P_i = \overbrace{P_{ii}}^{\phi_i(x_i)} + \sum_{k \in \mathcal{N}(i)} \overbrace{P_{ki}}^{m_{ki}(x_i)}, \quad (2.16)$$

$$\mu_i = P_i^{-1} \left(\overbrace{P_{ii} \mu_{ii}}^{\phi_i(x_i)} + \sum_{k \in \mathcal{N}(i)} \overbrace{P_{ki} \mu_{ki}}^{m_{ki}(x_i)} \right), \quad (2.17)$$

respectively. The derivation of the GaBP-based solver algorithm is concluded by simply substituting the explicit derived expressions of $P_{i \setminus j}$ (2.11) into P_{ij} (2.14), $\mu_{i \setminus j}$ (2.12) and P_{ij} (2.14) into μ_{ij} (2.15) and $P_{i \setminus j}$ (2.11) into μ_i (2.17).

The message passing in the GaBP solver can be performed subject to any scheduling. We refer to two conventional messages updating rules: parallel (flooding or synchronous) and serial (sequential, asynchronous) scheduling. In the parallel scheme, messages are stored in two data structures: messages from the previous iteration round, and messages from the current round. Thus, incoming messages do not affect the result of the computation in the current round, since it is done on messages that were received in the previous iteration round. Unlike this, in the serial scheme, there is only one data structure, so incoming messages in this round, change the result of the computation. In a sense it is exactly like the difference between the Jacobi and Gauss-Seidel algorithms, to be discussed in the following. Some in-depth discussions about parallel vs. serial scheduling in the BP context can be found in the work of Elidan *et al.* [36].

2.4 Max-Product Rule

A well-known alternative version to the sum-product BP is the max-product (a.k.a. min-sum) algorithm [37]. In this variant of BP, maximization operation is performed rather than marginal-

Algorithm 1.

1. <i>Initialize:</i>	<ul style="list-style-type: none"> ✓ Set the neighborhood $N(i)$ to include $\forall k \neq i \exists A_{ki} \neq 0$. ✓ Set the scalar fixes $P_{ii} = A_{ii}$ and $\mu_{ii} = b_i/A_{ii}, \forall i$. ✓ Set the initial $N(i) \ni k \rightarrow i$ scalar messages $P_{ki} = 0$ and $\mu_{ki} = 0$. ✓ Set a convergence threshold ϵ.
2. <i>Iterate:</i>	<ul style="list-style-type: none"> ✓ Propagate the $N(i) \ni k \rightarrow i$ messages P_{ki} and $\mu_{ki}, \forall i$ (under certain scheduling). ✓ Compute the $N(j) \ni i \rightarrow j$ scalar messages $P_{ij} = -A_{ij}^2 / (P_{ii} + \sum_{k \in N(i) \setminus j} P_{ki})$, $\mu_{ij} = (P_{ii}\mu_{ii} + \sum_{k \in N(i) \setminus j} P_{ki}\mu_{ki}) / A_{ij}$.
3. <i>Check:</i>	<ul style="list-style-type: none"> ✓ If the messages P_{ij} and μ_{ij} did not converge (w.r.t. ϵ), return to Step 2. ✓ Else, continue to Step 4.
4. <i>Infer:</i>	<ul style="list-style-type: none"> ✓ Compute the marginal means $\mu_i = (P_{ii}\mu_{ii} + \sum_{k \in N(i)} P_{ki}\mu_{ki}) / (P_{ii} + \sum_{k \in N(i)} P_{ki}), \forall i$. (✓ Optionally compute the marginal precisions $P_i = P_{ii} + \sum_{k \in N(i)} P_{ki}$)
5. <i>Solve:</i>	<ul style="list-style-type: none"> ✓ Find the solution $x_i^* = \mu_i, \forall i$.

ization, *i.e.*, variables are eliminated by taking maxima instead of sums. For Trellis trees (*e.g.*, graphically representing convolutional codes or ISI channels), the conventional sum-product BP algorithm boils down to performing the BCJR algorithm [38], resulting in the most probable symbol, while its max-product counterpart is equivalent to the Viterbi algorithm [39], thus inferring the most probable sequence of symbols [35].

In order to derive the max-product version of the proposed GaBP solver, the integral(sum)-product rule (2.3) is replaced by a new rule

$$m_{ij}(x_j) \propto \arg \max_{x_i} \psi_{ij}(x_i, x_j) \phi_i(x_i) \prod_{k \in N(i) \setminus j} m_{ki}(x_i) dx_i. \quad (2.18)$$

Computing $m_{ij}(x_j)$ according to this max-product rule, one gets (the exact derivation is deferred to Appendix 8.3)

$$m_{ij}(x_j) \propto \mathcal{N}(\mu_{ij} = -P_{ij}^{-1} A_{ij} \mu_{i \setminus j}, P_{ij}^{-1} = -A_{ij}^{-2} P_{i \setminus j}), \quad (2.19)$$

which is identical to the messages derived for the sum-product case (2.14)-(2.15). Thus interestingly, as opposed to ordinary (discrete) BP, the following property of the GaBP solver emerges.

Corollary 11. *The max-product (Eq. 8.6) and sum-product (Eq. 2.3) versions of the GaBP solver are identical.*

2.5 Convergence and Exactness

In ordinary BP, convergence does not entail exactness of the inferred probabilities, unless the graph has no cycles. Luckily, this is not the case for the GaBP solver. Its underlying Gaussian nature yields a direct connection between convergence and exact inference. Moreover, in contrast to BP the convergence of GaBP is not limited for tree or sparse graphs and can occur even for dense (fully-connected) graphs, adhering to certain rules discussed in the following.

We can use results from the literature on probabilistic inference in graphical models [8, 9, 10] to determine the convergence and exactness properties of the GaBP-based solver. The following two theorems establish sufficient conditions under which GaBP is guaranteed to converge to the exact marginal means.

Theorem 12. [8, Claim 4] *If the matrix \mathbf{A} is strictly diagonally dominant, then GaBP converges and the marginal means converge to the true means.*

This sufficient condition was recently relaxed to include a wider group of matrices.

Theorem 13. [9, Proposition 2] *If the spectral radius of the matrix \mathbf{A} satisfies*

$$\rho(|\mathbf{I}_n - \mathbf{A}|) < 1, \quad (2.20)$$

then GaBP converges and the marginal means converge to the true means. (The assumption here is that the matrix \mathbf{A} is first normalized by multiplying with \mathbf{D}^{-1} , where $\mathbf{D} = \text{diag}(\mathbf{A})$.)

A third and weaker sufficient convergence condition (relative to Theorem 13) which characterizes the convergence of the variances is given in [6, Theorem 2]: For each row in the matrix \mathbf{A} , if $A_{ii}^2 > \sum_{j \neq i} A_{ij}^2$ then the variances converge. Regarding the means, additional condition related to Theorem 13 is given.

There are many examples of linear systems that violate these conditions, for which GaBP converges to the exact means. In particular, if the graph corresponding to the system is acyclic (*i.e.*, a tree), GaBP yields the exact marginal means (and variances [8]), regardless of the value of the spectral radius of the matrix [8]. Another example, where the graph is fully-connected, is discussed in the following section. However, in contrast to conventional iterative methods derived from linear algebra, understanding the conditions for exact convergence and quantifying the convergence rate of the GaBP solver remain intriguing open problems.

2.6 Convergence Acceleration

Further speed-up of GaBP can be achieved by adapting known acceleration techniques from linear algebra, such as Aitken's method and Steffensen's iterations [14]. Consider a sequence $\{x_n\}$

(e.g., obtained by using GaBP iterations) linearly converging to the limit \hat{x} , and $x_n \neq \hat{x}$ for $n \geq 0$. According to Aitken's method, if there exists a real number a such that $|a| < 1$ and $\lim_{n \rightarrow \infty} (x_n - \hat{x}) / (x_{n-1} - \hat{x}) = a$, then the sequence $\{y_n\}$ defined by

$$y_n = x_n - \frac{(x_{n+1} - x_n)^2}{x_{n+2} - 2x_{n+1} + x_n}$$

converges to \hat{x} faster than $\{x_n\}$ in the sense that $\lim_{n \rightarrow \infty} |(\hat{x} - y_n) / (\hat{x} - x_n)| = 0$. Aitken's method can be viewed as a generalization of over-relaxation, since one uses values from three, rather than two, consecutive iteration rounds. This method can be easily implemented in GaBP as every node computes values based only on its own history.

Steffensen's iterations incorporate Aitken's method. Starting with x_n , two iterations are run to get x_{n+1} and x_{n+2} . Next, Aitken's method is used to compute y_n , this value replaces the original x_n , and GaBP is executed again to get a new value of x_{n+1} . This process is repeated iteratively until convergence. We remark that, although the convergence rate is improved with these enhanced algorithms, the region of convergence of the accelerated GaBP solver remains unchanged.

2.7 Computational Complexity and Message-Passing Efficiency

For a dense matrix \mathbf{A} each node out of the n nodes sends a unique message to every other node on the fully-connected graph. This recipe results in a total of n^2 messages per iteration round.

The computational complexity of the GaBP solver as described in Algorithm 1 for a dense linear system, in terms of operations (multiplications and additions) per iteration round, is shown in Table 2.1. In this case, the total number of required operations per iteration is $\mathcal{O}(n^3)$. This number is obtained by evaluating the number of operations required to generate a message multiplied by the number of messages. Based on the summation expressions for the propagating messages P_{ij} and μ_{ij} , it is easily seen that it takes $\mathcal{O}(n)$ operations to compute such a message. In the dense case, the graph is fully-connected resulting in $\mathcal{O}(n^2)$ propagating messages.

In order to estimate the total number of operations required for the GaBP algorithm to solve the linear system, we have to evaluate the number of iterations required for convergence. It is known [40] that the number of iterations required for an iterative solution method is $\mathcal{O}(f(\kappa))$, where $f(\kappa)$ is a function of the condition number of the data matrix \mathbf{A} . Hence the total complexity of the GaBP solver can be expressed by $\mathcal{O}(n^3) \times \mathcal{O}(f(\kappa))$. The analytical evaluation of the convergence rate function $f(\kappa)$ is a challenging open problem. However, it can be upper bounded by $f(\kappa) < \kappa$. furthermore, based on our experimental study, described in Section 3, we can conclude that $f(\kappa) \leq \sqrt{\kappa}$. Thus, the total complexity of the GaBP solve in this case is $\mathcal{O}(n^3) \times \mathcal{O}(\sqrt{\kappa})$. For well-conditioned (as opposed to ill-conditioned) data matrices the condition number is $\mathcal{O}(1)$. Thus, for well-conditioned linear systems the total complexity is $\mathcal{O}(n^3)$, i.e., the complexity is cubic, the same order as for direct solution methods, like Gaussian elimination.

Algorithm	Operations per msg	msgs	Total operations per iteration
Naive GaBP (Algorithm 1)	$\mathcal{O}(n)$	$\mathcal{O}(n^2)$	$\mathcal{O}(n^3)$
Broadcast GaBP (Algorithm 2)	$\mathcal{O}(n)$	$\mathcal{O}(n)$	$\mathcal{O}(n^2)$

Table 2.1: Computational complexity of the GaBP solver for dense $n \times n$ matrix \mathbf{A} .

At first sight, this result may be considered disappointing, with no complexity gain w.r.t. direct matrix inversion. Luckily, the GaBP implementation as described in Algorithm 1 is a naive one, thus termed naive GaBP. In this implementation we did not take into account the correlation between the different messages transmitted from a certain node i . These messages, computed by summation, distinct from one another in only two summation terms.

Instead of sending a message composed of the pair of μ_{ij} and P_{ij} , a node can broadcast the aggregated sums

$$\tilde{P}_i = P_{ii} + \sum_{k \in \mathcal{N}(i)} P_{ki}, \quad (2.21)$$

$$\tilde{\mu}_i = \tilde{P}_i^{-1} (P_{ii}\mu_{ii} + \sum_{k \in \mathcal{N}(i)} P_{ki}\mu_{ki}). \quad (2.22)$$

Consequently, each node can retrieve locally the $P_{i \setminus j}$ (2.11) and $\mu_{i \setminus j}$ (2.12) from the sums by means of a subtraction

$$P_{i \setminus j} = \tilde{P}_i - P_{ji}, \quad (2.23)$$

$$\mu_{i \setminus j} = \tilde{\mu}_i - P_{i \setminus j}^{-1} P_{ji} \mu_{ji}. \quad (2.24)$$

The rest of the algorithm remains the same. On dense graphs, the broadcast version sends $\mathcal{O}(n)$ messages per round, instead of $\mathcal{O}(n^2)$ messages in the GaBP algorithm.

2.8 The GaBP-Based Solver and Classical Solution Methods

2.8.1 Gaussian Elimination

Proposition 14. *The GaBP-based solver (Algorithm 1) for a system of linear equations represented by a tree graph is identical to the renowned Gaussian elimination algorithm (a.k.a. LU factorization, [40]).*

Proof. Consider a set of n linear equations with n unknown variables, a unique solution and a tree graph representation. We aim at computing the unknown variable associated with the root

Algorithm 2.

1. <i>Initialize:</i>	<ul style="list-style-type: none"> ✓ Set the neighborhood $N(i)$ to include $\forall k \neq i \exists A_{ki} \neq 0$. ✓ Set the scalar fixes $P_{ii} = A_{ii}$ and $\mu_{ii} = b_i/A_{ii}, \forall i$. ✓ Set the initial $i \rightarrow N(i)$ broadcast messages $\tilde{P}_i = 0$ and $\tilde{\mu}_i = 0$. ✓ Set the initial $N(i) \ni k \rightarrow i$ internal scalars $P_{ki} = 0$ and $\mu_{ki} = 0$. ✓ Set a convergence threshold ϵ.
2. <i>Iterate:</i>	<ul style="list-style-type: none"> ✓ Broadcast the aggregated sum messages $\tilde{P}_i = P_{ii} + \sum_{k \in N(i)} P_{ki}$, $\tilde{\mu}_i = \tilde{P}_i^{-1} (P_{ii}\mu_{ii} + \sum_{k \in N(i)} P_{ki}\mu_{ki}), \forall i$ (under certain scheduling). ✓ Compute the $N(j) \ni i \rightarrow j$ internal scalars $P_{ij} = -A_{ij}^2 / (\tilde{P}_i - P_{ji})$, $\mu_{ij} = (\tilde{P}_i\tilde{\mu}_i - P_{ji}\mu_{ji}) / A_{ij}$.
3. <i>Check:</i>	<ul style="list-style-type: none"> ✓ If the internal scalars P_{ij} and μ_{ij} did not converge (w.r.t. ϵ), return to Step 2. ✓ Else, continue to Step 4.
4. <i>Infer:</i>	<ul style="list-style-type: none"> ✓ Compute the marginal means $\mu_i = (P_{ii}\mu_{ii} + \sum_{k \in N(i)} P_{ki}\mu_{ki}) / (P_{ii} + \sum_{k \in N(i)} P_{ki}) = \tilde{\mu}_i, \forall i$. (✓ Optionally compute the marginal precisions $P_i = P_{ii} + \sum_{k \in N(i)} P_{ki} = \tilde{P}_i$)
5. <i>Solve:</i>	<ul style="list-style-type: none"> ✓ Find the solution $x_i^* = \mu_i, \forall i$.

node. Without loss of generality as the tree can be drawn with any of the other nodes being its root. Let us enumerate the nodes in an ascending order from the root to the leaves (see, e.g., Fig. 2.2).

As in a tree each child node (*i.e.*, all nodes but the root) has only one parent node and based on the top-down ordering, it can be easily observed that the tree graph's corresponding data matrix \mathbf{A} must have one and only one non-zero entry in the upper triangular portion of its columns. Moreover, for a leaf node this upper triangular entry is the only non-zero off-diagonal entry in the whole column. See, for example, the data matrix associated with the tree graph

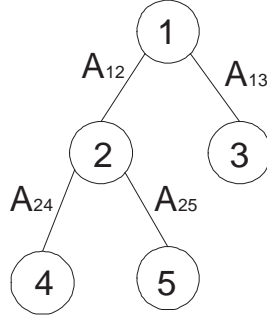


Figure 2.2: Example topology of a tree with 5 nodes

depicted in Fig 2.2

$$\begin{pmatrix} A_{11} & \mathbf{A_{12}} & \mathbf{A_{13}} & 0 & 0 \\ A_{12} & A_{22} & 0 & \mathbf{A_{24}} & \mathbf{A_{25}} \\ A_{13} & 0 & A_{33} & 0 & 0 \\ 0 & A_{24} & 0 & A_{44} & 0 \\ 0 & A_{25} & 0 & 0 & A_{55} \end{pmatrix}, \quad (2.25)$$

where the non-zero upper triangular entries are in bold and among these the entries corresponding to leaves are underlined.

Now, according to GE we would like to lower triangulate the matrix \mathbf{A} . This is done by eliminating these entries from the leaves to the root. Let l be a leaf node, i be its parent and j be its parent (l 'th node grandparent). Then, the l 'th row is multiplied by $-A_{li}/A_{ll}$ and added to the i 'th row. in this way the A_{li} entry is being eliminated. However, this elimination, transforms the i 'th diagonal entry to be $A_{ii} \rightarrow A_{ii} - A_{li}^2/A_{ll}$, or for multiple leaves connected to the same parent $A_{ii} \rightarrow A_{ii} - \sum_{l \in \mathcal{N}(i)} A_{li}^2/A_{ll}$. In our example,

$$\begin{pmatrix} A_{11} & A_{12} & 0 & 0 & 0 \\ A_{12} & A_{22} - A_{13}^2/A_{33} - A_{24}^2/A_{44} - A_{25}^2/A_{55} & 0 & 0 & 0 \\ A_{13} & 0 & A_{33} & 0 & 0 \\ 0 & A_{24} & 0 & A_{44} & 0 \\ 0 & A_{25} & 0 & 0 & A_{55} \end{pmatrix}. \quad (2.26)$$

Thus, in a similar manner, eliminating the parent i yields the multiplication of the j 'th diagonal term by $-A_{ij}^2/(A_{ii} - \sum_{l \in \mathcal{N}(i)} A_{li}^2/A_{ll})$. Recalling that $P_{ii} = A_{ii}$, we see that the last expression is identical to the update rule of P_{ij} in GaBP. Again, in our example

$$\begin{pmatrix} B & 0 & 0 & 0 & 0 \\ 0 & C & 0 & 0 & 0 \\ A_{13} & 0 & A_{33} & 0 & 0 \\ 0 & A_{24} & 0 & A_{44} & 0 \\ 0 & A_{25} & 0 & 0 & A_{55} \end{pmatrix}, \quad (2.27)$$

where $B = A_{11} - A_{12}^2/(A_{22} - A_{13}^2/A_{33} - A_{24}^2/A_{44} - A_{25}^2/A_{55})$, $C = A_{22} - A_{13}^2/A_{33} - A_{24}^2/A_{44} - A_{25}^2/A_{55}$. Now the matrix is fully lower triangulated. To put differently in terms of GaBP, the P_{ij}

messages are subtracted from the diagonal P_{ii} terms to triangulate the data matrix of the tree. Performing the same row operations on the right hand side column vector \mathbf{b} , it can be easily seen that we equivalently get that the outcome of the row operations is identical to the GaBP solver's μ_{ij} update rule. These updates/row operations can be repeated, in the general case, until the matrix is lower triangulated.

Now, in order to compute the value of the unknown variable associated with the root node, all we have to do is divide the first diagonal term by the transformed value of b_1 , which is identical to the infer stage in the GaBP solver (note that by definition all the nodes connected to the root are its children, as it does not have parent node). In the example

$$x_1^* = \frac{A_{11} - A_{12}^2/(A_{22} - A_{13}^2/A_{33} - A_{24}^2/A_{44} - A_{25}^2/A_{55})}{b_{11} - A_{12}/(b_{22} - A_{13}/A_{33} - A_{24}/A_{44} - A_{25}/A_{55})} \quad (2.28)$$

Note that the rows corresponding to leaves remain unchanged.

To conclude, in the tree graph case, the 'iterative' stage (stage 2 on algorithm 1) of the GaBP solver actually performs lower triangulation of the matrix, while the 'infer' stage (stage 4) reduces to what is known as forward substitution. Evidently, using an opposite ordering, one can get the complementary upper triangulation and back substitution, respectively. \square

It is important to note, that based on this proposition, the GaBP solver can be viewed as GE ran over an unwrapped version (*i.e.*, a computation tree) of a general loopy graph.

2.8.2 Iterative Methods

Iterative methods that can be expressed in the simple form

$$\mathbf{x}^{(t)} = \mathbf{B}\mathbf{x}^{(t-1)} + \mathbf{c}, \quad (2.29)$$

where neither the iteration matrix \mathbf{B} nor the vector \mathbf{c} depend upon the iteration number t , are called stationary iterative methods. In the following, we discuss three main stationary iterative methods: the Jacobi method, the Gauss-Seidel (GS) method and the successive overrelaxation (SOR) method. The GaBP-based solver, in the general case, can not be written in this form, thus can not be categorized as a stationary iterative method.

Proposition 15. [40] *Assuming $\mathbf{I} - \mathbf{B}$ is invertible, then the iteration 2.29 converges (for any initial guess, $\mathbf{x}^{(0)}$).*

2.8.3 Jacobi Method

The Jacobi method (Gauss, 1823, and Jacobi 1845, [2]), a.k.a. the simultaneous iteration method, is the oldest iterative method for solving a square linear system of equations $\mathbf{A}\mathbf{x} = \mathbf{b}$. The method assumes that $\forall_i A_{ii} \neq 0$. It's complexity is $\mathcal{O}(n^2)$ per iteration. A sufficient convergence condition for the Jacobi method is that for any starting vector \mathbf{x}_0 as long as $\rho(\mathbf{D}^{-1}(\mathbf{L} + \mathbf{U})) < 1$. Where $\mathbf{D} = \text{diag}\{\mathbf{A}\}$, \mathbf{L}, \mathbf{U} are upper and lower triangular matrices of \mathbf{A} . A second sufficient convergence condition is that \mathbf{A} is diagonally dominant.

Proposition 16. *The GaBP-based solver (Algorithm 1)*

1. with inverse variance messages arbitrarily set to zero, i.e., $P_{ij} = 0, i \in N(j), \forall j$;
2. incorporating the message received from node j when computing the message to be sent from node i to node j , i.e. replacing $k \in N(i) \setminus j$ with $k \in N(i)$,

is identical to the Jacobi iterative method.

Proof. Arbitrarily setting the precisions to zero, we get in correspondence to the above derivation,

$$P_{i \setminus j} = P_{ii} = A_{ii}, \quad (2.30)$$

$$P_{ij} \mu_{ij} = -A_{ij} \mu_{i \setminus j}, \quad (2.31)$$

$$\mu_i = A_{ii}^{-1} (b_i - \sum_{k \in N(i)} A_{ki} \mu_{k \setminus i}). \quad (2.32)$$

Note that the inverse relation between P_{ij} and $P_{i \setminus j}$ (2.14) is no longer valid in this case.

Now, we rewrite the mean $\mu_{i \setminus j}$ (2.12) without excluding the information from node j ,

$$\mu_{i \setminus j} = A_{ii}^{-1} (b_i - \sum_{k \in N(i)} A_{ki} \mu_{k \setminus i}). \quad (2.33)$$

Note that $\mu_{i \setminus j} = \mu_i$, hence the inferred marginal mean μ_i (2.32) can be rewritten as

$$\mu_i = A_{ii}^{-1} (b_i - \sum_{k \neq i} A_{ki} \mu_k), \quad (2.34)$$

where the expression for all neighbors of node i is replaced by the redundant, yet identical, expression $k \neq i$. This fixed-point iteration is identical to the renowned Jacobi method, concluding the proof. \square

Proposition 16 can be viewed also as a probabilistic proof of Jacobi. The fact that Jacobi iterations can be obtained as a special case of the GaBP solver further indicates the richness of the proposed algorithm. Note, that the GaBP algorithm converges to the exact solution also for nonsymmetric matrices in this form.

2.8.4 Gauss-Seidel

The Gauss-Seidel method converges for any starting vector x_0 if $\rho((L + D)^{-1}U) < 1$. This condition holds, for example, for diagonally dominant matrices as well as for positive definite ones. It is necessary, however, that the diagonal terms in the matrix are greater (in magnitude) than the other terms.

The successive overrelaxation (SOR) method aims to further refine the Gauss-Seidel method, by adding a damping parameter $0 < \alpha < 1$:

$$x_i^t = \alpha x_i^{t-1} + (1 - \alpha) GS_i, \quad (2.35)$$

where GS_i is the Gauss-Seidel update computed by node i . Damping has previously shown to be a heuristic for accelerating belief propagation as well [41].

Chapter 3

Numerical Examples

Our experimental study includes four numerical examples and two possible applications. In all examples, but the Poisson's equation 3.8, \mathbf{b} is assumed to be an m -length all-ones observation vector. For fairness in comparison, the initial guess in all experiments, for the various solution methods under investigation, is taken to be the same and is arbitrarily set to be equal to the value of the vector \mathbf{b} . The stopping criterion in all experiments determines that for all propagating messages (in the context the GaBP solver) or all n tentative solutions (in the context of the compared iterative methods) the absolute value of the difference should be less than $\epsilon \leq 10^{-6}$. As for terminology, in the following performing GaBP with parallel (flooding or synchronous) message scheduling is termed 'parallel GaBP', while GaBP with serial (sequential or asynchronous) message scheduling is termed 'serial GaBP'.

3.1 Numerical Example: Toy Linear System: 3×3 Equations

Consider the following 3×3 linear system

$$\underbrace{\begin{pmatrix} A_{xx} = 1 & A_{xy} = -2 & A_{xz} = 3 \\ A_{yx} = -2 & A_{yy} = 1 & A_{yz} = 0 \\ A_{zx} = 3 & A_{zy} = 0 & A_{zz} = 1 \end{pmatrix}}_{\mathbf{A}} \underbrace{\begin{pmatrix} x \\ y \\ z \end{pmatrix}}_{\mathbf{x}} = \underbrace{\begin{pmatrix} -6 \\ 0 \\ 2 \end{pmatrix}}_{\mathbf{b}}. \quad (3.1)$$

We would like to find the solution to this system, $\mathbf{x}^* = \{x^*, y^*, z^*\}^T$. Inverting the data matrix \mathbf{A} , we directly solve

$$\underbrace{\begin{pmatrix} x^* \\ y^* \\ z^* \end{pmatrix}}_{\mathbf{x}^*} = \underbrace{\begin{pmatrix} -1/12 & -1/6 & 1/4 \\ -1/6 & 2/3 & 1/2 \\ 1/4 & 1/2 & 1/4 \end{pmatrix}}_{\mathbf{A}^{-1}} \underbrace{\begin{pmatrix} -6 \\ 0 \\ 2 \end{pmatrix}}_{\mathbf{b}} = \begin{pmatrix} 1 \\ 2 \\ -1 \end{pmatrix}. \quad (3.2)$$

Alternatively, we can now run the GaBP solver. Fig. 3.1 displays the graph, corresponding to the data matrix \mathbf{A} , and the message-passing flow. As $A_{yz} = A_{zy} = 0$, this graph is a cycle-free tree, thus GaBP is guaranteed to converge in a finite number of rounds. As demonstrated in the following, in this example GaBP converges only in two rounds, which equals the tree's diameter. Each propagating message, m_{ij} , is described by two scalars μ_{ij} and P_{ij} , standing for the mean and precision of this distribution. The evolution of the propagating means and precisions, until convergence, is described in Table 3.1, where the notation $t = 0, 1, 2, 3$ denotes the iteration rounds. Converged values are written in bold.

Message	Computation	t=0	t=1	t=2	t=3
P_{xy}	$-A_{xy}^2/(P_{xx} + P_{zx})$	0	-4	1/2	1/2
P_{yx}	$-A_{yx}^2/(P_{yy})$	0	-4	-4	-4
P_{xz}	$-A_{xz}^2/(P_{zz})$	0	-9	3	3
P_{zx}	$-A_{zx}^2/(P_{xx} + P_{yx})$	0	-9	-9	-9
μ_{xy}	$(P_{xx}\mu_{xx} + P_{zx}\mu_{zx})/A_{xy}$	0	3	6	6
μ_{yx}	$P_{yy}\mu_{yy}/A_{yx}$	0	0	0	0
μ_{xz}	$(P_{xx}\mu_{xx} + P_{yx}\mu_{yx})/A_{xz}$	0	-2	-2	-2
μ_{zx}	$P_{zz}\mu_{zz}/A_{zx}$	0	2/3	2/3	2/3

Table 3.1: Evolution of means and precisions on a tree with three nodes

Next, following the GaBP solver algorithm, we infer the marginal means. For exposition purposes we also present in Table 3.2 the tentative solutions at each iteration round.

Solution	Computation	t=0	t=1	t=2	t=3
μ_x	$(P_{xx}\mu_{xx} + P_{zx}\mu_{zx} + P_{yx}\mu_{yx})/(P_{xx} + P_{zx} + P_{yx})$	-6	1	1	1
μ_y	$(P_{yy}\mu_{yy} + P_{xy}\mu_{xy})/(P_{yy} + P_{xy})$	0	4	2	2
μ_z	$(P_{zz}\mu_{zz} + P_{xz}\mu_{xz})/(P_{zz} + P_{xz})$	2	-5/2	-1	-1

Table 3.2: Tentative means computed on each iteration until convergence

Thus, as expected, the GaBP solution $\mathbf{x}^* = \{x^* = 1, y^* = 2, z^* = -1\}^T$ is identical to what is found taking the direct approach. Note that as the linear system is described by a tree graph, then for this particular case, the inferred precision is also exact

$$P_x = P_{xx} + P_{yx} + P_{zx} = -12, \quad (3.3)$$

$$P_y = P_{yy} + P_{xy} = 3/2, \quad (3.4)$$

$$P_z = P_{zz} + P_{xz} = 4. \quad (3.5)$$

$$(3.6)$$

and gives $\{P_x^{-1} = \{\mathbf{A}^{-1}\}_{xx} = -1/12, P_y^{-1} = \{\mathbf{A}^{-1}\}_{yy} = 2/3, P_z^{-1} = \{\mathbf{A}^{-1}\}_{zz} = 1/4\}^T$, i.e. the true diagonal values of the data matrix's inverse, \mathbf{A}^{-1} .

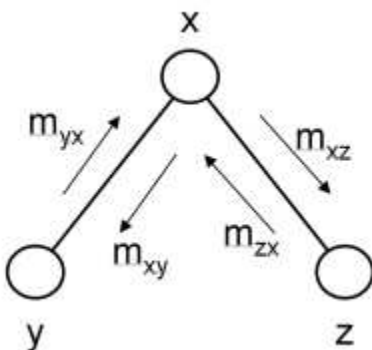


Figure 3.1: A tree topology with three nodes

3.2 Numerical Example: Symmetric Non-PSD Data Matrix

Consider the case of a linear system with a symmetric, but non-PSD data matrix

$$\begin{pmatrix} 1 & 2 & 3 \\ 2 & 2 & 1 \\ 3 & 1 & 1 \end{pmatrix}. \quad (3.7)$$

Table 3.3 displays the number of iterations required for convergence for the iterative methods under consideration. The classical methods diverge, even when aided with acceleration techniques. This behavior (at least without the acceleration) is not surprising in light of Theorem 13. Again we observe that serial scheduling of the GaBP solver is superior parallel scheduling and that applying Steffensen iterations reduces the number of iterations in 45% in both cases. Note that SOR cannot be defined when the matrix is not PSD. By definition CG works only for symmetric PSD matrices. because the solution is a saddle point and not a minimum or maximum.

3.3 Application Example: 2-D Poisson's Equation

One of the most common partial differential equations (PDEs) encountered in various areas of exact sciences and engineering (e.g., heat flow, electrostatics, gravity, fluid flow, quantum mechanics, elasticity) is Poisson's equation. In two dimensions, the equation is

$$\Delta u(x, y) = f(x, y), \quad (3.8)$$

for $\{x, y\} \in \Omega$, where

$$\Delta(\cdot) = \frac{\partial^2(\cdot)}{\partial x^2} + \frac{\partial^2(\cdot)}{\partial y^2}. \quad (3.9)$$

Algorithm	Iterations t
Jacobi, GS, SR, Jacobi+Aitkens, Jacobi+Steffensen	—
Parallel GaBP	38
Serial GaBP	25
Parallel GaBP+Steffensen	21
Serial GaBP+Steffensen	14

Table 3.3: Symmetric non-PSD 3×3 data matrix. Total number of iterations required for convergence (threshold $\epsilon = 10^{-6}$) for GaBP-based solvers vs. standard methods.

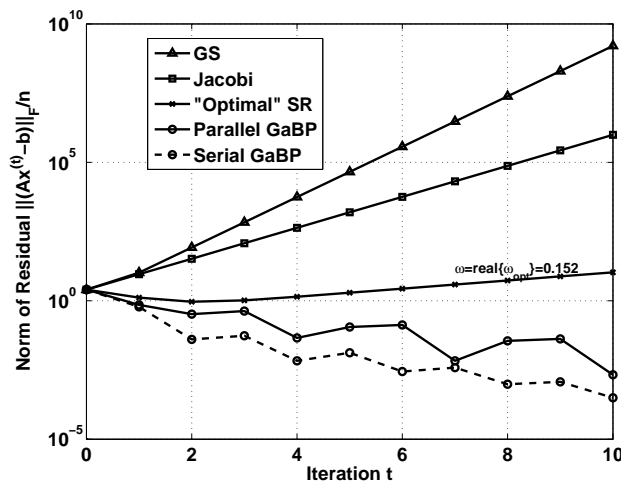


Figure 3.2: Convergence rate for a 3×3 symmetric non-PSD data matrix. The Frobenius norm of the residual per equation, $\|Ax^t - b\|_F/n$, as a function of the iteration t for GS (triangles and solid line), Jacobi (squares and solid line), SR (stars and solid line), parallel GaBP (circles and solid line) and serial GaBP (circles and dashed line) solvers.

is the Laplacean operator and Ω is a bounded domain in \mathbb{R}^2 . The solution is well defined only under boundary conditions, *i.e.*, the value of $u(x, y)$ on the boundary of Ω is specified. We consider the simple (Dirichlet) case of $u(x, y) = 0$ for $\{x, y\}$ on the boundary of Ω . This equation describes, for instance, the steady-state temperature of a uniform square plate with the boundaries held at temperature $u = 0$, and $f(x, y)$ equaling the external heat supplied at point $\{x, y\}$.

The poisson's PDE can be discretized by using finite differences. An $p+1 \times p+1$ square grid on Ω with size (arbitrarily) set to unity is used, where $h \triangleq 1/(p+1)$ is the grid spacing. We let

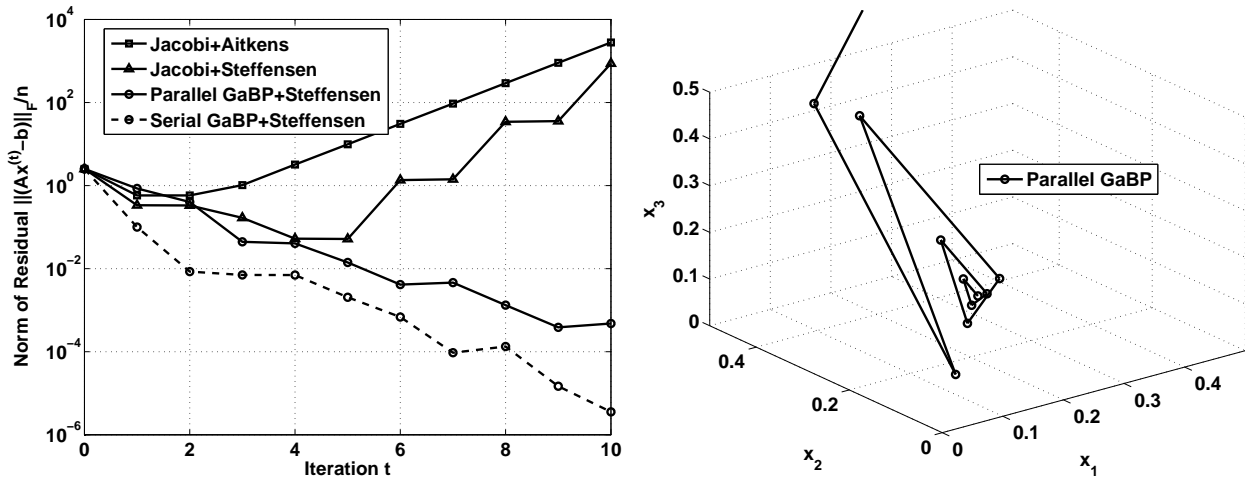


Figure 3.3: The left graph depicts accelerated convergence rate for a 3×3 symmetric non-PSD data matrix. The Frobenius norm of the residual per equation, $\|Ax^t - b\|_F/n$, as a function of the iteration t for Aitkens (squares and solid line) and Steffensen-accelerated (triangles and solid line) Jacobi method, parallel GaBP (circles and solid line) and serial GaBP (circles and dashed line) solvers accelerated by Steffensen iterations. The right graph shows a visualization of parallel GaBP on the same problem, drawn in \mathbb{R}^3 .

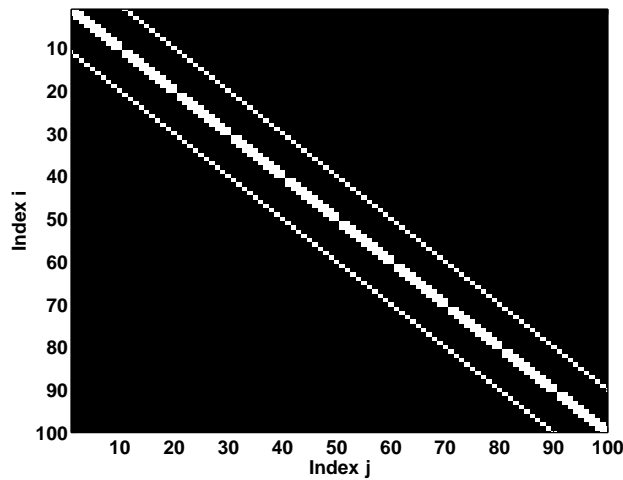


Figure 3.4: Image of the corresponding sparse data matrix for the 2-D discrete Poisson's PDE with $p = 10$. Empty (full) squares denote non-zero (zero) entries.

$U(i, j)$, $\{i, j = 0, \dots, p + 1\}$, be the approximate solution to the PDE at $x = ih$ and $y = jh$.

Approximating the Laplacean by

$$\begin{aligned} \Delta U(x, y) &= \frac{\partial^2(U(x, y))}{\partial x^2} + \frac{\partial^2(U(x, y))}{\partial y^2} \\ &\approx \frac{U(i+1, j) - 2U(i, j) + U(i-1, j)}{h^2} + \frac{U(i, j+1) - 2U(i, j) + U(i, j-1)}{h^2}, \end{aligned}$$

one gets the system of $n = p^2$ linear equations with n unknowns

$$4U(i, j) - U(i-1, j) - U(i+1, j) - U(i, j-1) - U(i, j+1) = b(i, j) \forall i, j = 1, \dots, p, \quad (3.10)$$

where $b(i, j) \triangleq -f(ih, jh)h^2$, the scaled value of the function $f(x, y)$ at the corresponding grid point $\{i, j\}$. Evidently, the accuracy of this approximation to the PDE increases with n .

Choosing a certain ordering of the unknowns $U(i, j)$, the linear system can be written in a matrix-vector form. For example, the natural row ordering (*i.e.*, enumerating the grid points left→right, bottom→up) leads to a linear system with $p^2 \times p^2$ sparse data matrix \mathbf{A} . For example, a Poisson PDE with $p = 3$ generates the following 9×9 linear system

$$\underbrace{\begin{pmatrix} 4 & -1 & & & & & & & \\ -1 & 4 & -1 & & & & & & \\ & -1 & 4 & & & & & & \\ \hline -1 & & & 4 & -1 & & & & \\ & -1 & & -1 & 4 & -1 & & & \\ & & -1 & & -1 & 4 & & & \\ \hline & & & -1 & & & 4 & -1 & \\ & & & & -1 & & -1 & 4 & -1 \\ & & & & & -1 & & -1 & 4 \end{pmatrix}}_{\mathbf{A}} \underbrace{\begin{pmatrix} U(1, 1) \\ U(2, 1) \\ U(3, 1) \\ U(1, 2) \\ U(2, 2) \\ U(3, 2) \\ U(1, 3) \\ U(2, 3) \\ U(3, 3) \end{pmatrix}}_{\mathbf{x}} = \underbrace{\begin{pmatrix} b(1, 1) \\ b(2, 1) \\ b(3, 1) \\ b(1, 2) \\ b(2, 2) \\ b(3, 2) \\ b(1, 3) \\ b(2, 3) \\ b(3, 3) \end{pmatrix}}_{\mathbf{b}}, \quad (3.11)$$

where blank data matrix \mathbf{A} entries denote zeros.

Hence, now we can solve the discretized 2-D Poisson's PDE by utilizing the GaBP algorithm. Note that, in contrast to the other examples, in this case the GaBP solver is applied for solving a sparse, rather than dense, system of linear equations.

In order to evaluate the performance of the GaBP solver, we choose to solve the 2-D Poisson's equation with discretization of $p = 10$. The structure of the corresponding 100×100 sparse data matrix is illustrated in Fig. 3.4.

Algorithm	Iterations t
Jacobi	354
GS	136
Optimal SOR	37
Parallel GaBP	134
Serial GaBP	73
Parallel GaBP+Aitkens	25
Parallel GaBP+Steffensen	56
Serial GaBP+Steffensen	32

Table 3.4: 2-D discrete Poisson's PDE with $p = 3$ and $f(x, y) = -1$. Total number of iterations required for convergence (threshold $\epsilon = 10^{-6}$) for GaBP-based solvers vs. standard methods.

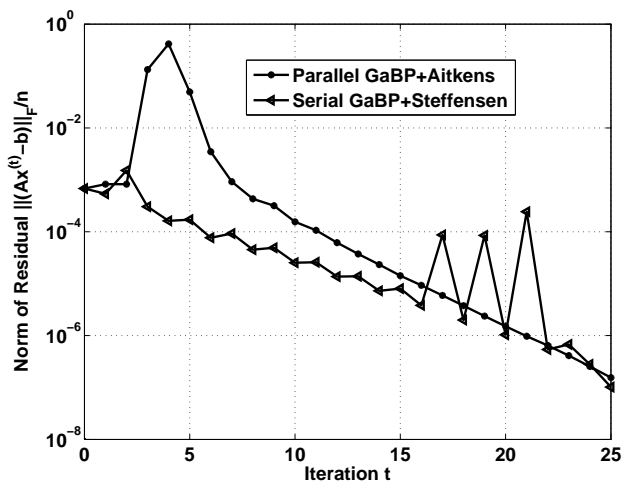


Figure 3.5: Accelerated convergence rate for the 2-D discrete Poisson's PDE with $p = 10$ and $f(x, y) = -1$. The Frobenius norm of the residual, per equation, $\|\mathbf{Ax}^t - b\|_F/n$, as a function of the iteration t for parallel GaBP solver accelerated by Aitkens method (\times -marks and solid line) and serial GaBP solver accelerated by Steffensen iterations (left triangles and dashed line)

Algorithm	Iterations t
Jacobi, GS, SR, Jacobi+Aitkens, Jacobi+Steffensen	—
Parallel GaBP	84
Serial GaBP	30
Parallel GaBP+Steffensen	43
Serial GaBP+Steffensen	17

Table 3.5: Asymmetric 3×3 data matrix. total number of iterations required for convergence (threshold $\epsilon = 10^{-6}$) for GaBP-based solvers vs. standard methods.

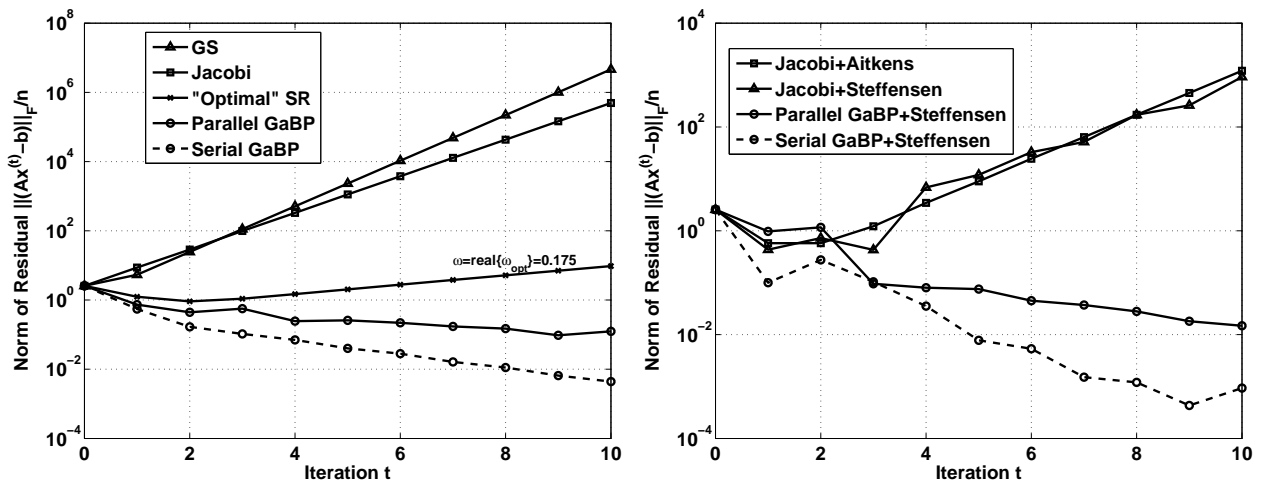


Figure 3.6: Convergence of an asymmetric 3×3 matrix.

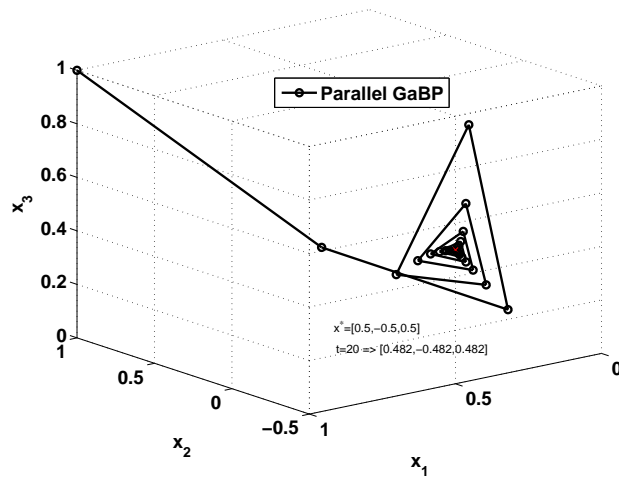


Figure 3.7: Convergence of a 3×3 asymmetric matrix, using 3D plot.

Chapter 4

Relation to other algorithms

In this chapter we discuss the relation between the GaBP algorithm and several other algorithms, and show that all of them are instances of the GaBP algorithm. Thus, a single efficient implementation of GaBP can efficiently compute different cost functions without the need of deriving new update rules. Furthermore, it is easier to find sufficient condition for convergence in our settings.

4.1 Montanari's Linear Detection Algorithm

In this section we show that the Montanari's algorithm [42], which is an iterative algorithm for linear detection is an instance of Gaussian BP. Our improved algorithm for linear detection described in Section 6.1 is more general. First, we allow different noise level for each received bit, unlike his work which uses a single fixed noise for the whole system. In practice, the bits are transmitted using different frequencies, thus suffering from different noise levels. Second, the update rules in his paper are fitted only to the randomly-spreading CDMA codes, where the matrix A contains only values which are drawn uniformly from $\{-1, 1\}$. Assuming binary signalling, he conjectures convergence to the large system limit. Our new convergence proof holds for any CDMA matrices provided that the absolute sum of the chip sequences is one, under weaker conditions on the noise level. Third, we propose in [7] an efficient broadcast version for saving messages in a broadcast supporting network.

The probability distribution of the factor graph used by Montanari is:

$$d\mu_y^{N,K} = \frac{1}{Z_y^{N,K}} \prod_{a=1}^N \exp(-\frac{1}{2}\sigma^2\omega_a^2 + jy_a\omega_a) \prod_{i=1}^K \exp(-\frac{1}{2}x_i^2) \cdot \prod_{i,a} \exp(-\frac{j}{\sqrt{N}}s_{ai}\omega_ax_i)d\omega$$

Extracting the self and edge potentials from the above probability distribution:

$$\psi_{ii}(\mathbf{x}_i) \triangleq \exp(-\frac{1}{2}\mathbf{x}_i^2) \propto \mathcal{N}(\mathbf{x}; 0, 1)$$

$$\psi_{aa}(\omega_a) \triangleq \exp(-\frac{1}{2}\sigma^2\omega_a^2 + jy_a\omega_a) \propto \mathcal{N}(\omega_a; jy_a, \sigma^2)$$

$$\psi_{ia}(\mathbf{x}_i, \omega_a) \triangleq \exp\left(-\frac{j}{\sqrt{N}} s_{ai} \omega_a \mathbf{x}_i\right) \propto \mathcal{N}\left(\mathbf{x}; \frac{j}{\sqrt{N}} s_{ai}, 0\right)$$

For convenience, Table 4.1 provides a translation between the notations used in [7] and that used by Montanari *et al.* in [42]:

Table 4.1: Summary of notations

GaBP [7]	Montanari <i>et al.</i> [42]	Description
P_{ij}	$\lambda_{i \rightarrow a}^{(t+1)}$	precision msg from left to right
	$\hat{\lambda}_{a \rightarrow i}^{(t+1)}$	precision msg from right to left
μ_{ij}	$\gamma_{i \rightarrow a}^{(t+1)}$	mean msg from left to right
	$\hat{\gamma}_{a \rightarrow i}^{(t+1)}$	mean msg from right to left
μ_{ii}	y_i	prior mean of left node
	0	prior mean of right node
P_{ii}	1	prior precision of left node
Ψ_i	σ^2	prior precision of right node
μ_i	$\frac{G_i}{L_i}$	posterior mean of node
P_i	L_i	posterior precision of node
A_{ij}	$\frac{-j s_{ia}}{\sqrt{N}}$	covariance
A_{ji}	$\frac{-j s_{ai}}{\sqrt{N}}$	covariance
	j	$j = \sqrt{-1}$

Theorem 17. *Montanari's update rules are special case of the GaBP algorithm.*

Proof. Now we derive Montanari's update rules. We start with the precision message from left to right:

$$\begin{aligned} \overbrace{\lambda_{i \rightarrow a}^{(t+1)}}^{P_{ij}} &= 1 + \frac{1}{N} \sum_{b \neq a} \frac{s_{ib}^2}{\hat{\lambda}_{b \rightarrow i}^{(t)}} = \overbrace{1}^{P_{ii}} + \sum_{b \neq a} \overbrace{\frac{1}{N} \frac{s_{ib}^2}{\hat{\lambda}_{b \rightarrow i}^{(t)}}}^{P_{ki}} \\ &= \overbrace{1}^{P_{ii}} - \sum_{b \neq a} \frac{-A_{ij}}{\sqrt{N}} \overbrace{\frac{1}{\hat{\lambda}_{b \rightarrow i}^{(t)}}}^{(P_{j \setminus i})^{-1}} \frac{A_{ji}}{\sqrt{N}}. \end{aligned}$$

By looking at Table 4.1, it is easy to verify that this precision update rule is equivalent to 2.11. Using the same logic we get the precision message from right to left:

$$\overbrace{\hat{\lambda}_{i \rightarrow a}^{(t+1)}}^{P_{ji}} = \overbrace{\sigma^2}^{P_{ii}} + \frac{1}{N} \sum_{k \neq i} \overbrace{\frac{s_{ka}^2}{\lambda_{k \rightarrow a}^{(t)}}}^{-A_{ij}^2 P_{j \setminus i}^{-1}}.$$

The mean message from left to right is given by

$$\gamma_{i \rightarrow a}^{(t+1)} = \frac{1}{N} \sum_{b \neq a} \frac{s_{ib}}{\lambda_{b \rightarrow i}^{(t)}} \hat{\gamma}_{b \rightarrow i}^{(t)} = \underbrace{\mu_{ii}}_0 - \sum_{b \neq a} \underbrace{\frac{-A_{ij}}{-j s_{ib}}}_{\frac{P_{j \setminus i}^{-1}}{\lambda_{b \rightarrow i}^{(t)}}} \underbrace{\frac{1}{\lambda_{b \rightarrow i}^{(t)}}}_{\mu_{j \setminus i}} \hat{\gamma}_{b \rightarrow i}^{(t)}.$$

The same calculation is done for the mean from right to left:

$$\hat{\gamma}_{i \rightarrow a}^{(t+1)} = y_a - \frac{1}{N} \sum_{k \neq i} \frac{s_{ka}}{\lambda_{k \rightarrow a}^{(t)}} \gamma_{k \rightarrow a}^{(t)}.$$

Finally, the left nodes calculated the precision and mean by

$$G_i^{(t+1)} = \frac{1}{\sqrt{N}} \sum_b \frac{s_{ib}}{\lambda_{b \rightarrow i}^{(t)}} \hat{\gamma}_{b \rightarrow i}^{(t)}, \quad J_i = G_i^{-1}.$$

$$L_i^{(t+1)} = 1 + \frac{1}{N} \sum_b \frac{s_{ib}^2}{\lambda_{b \rightarrow i}^{(t)}}, \quad \mu_i = L_i G_i^{-1}.$$

□

The key difference between the two constructions is that Montanari uses a directed factor graph while we use an undirected graphical model. As a consequence, our construction provides additional convergence results and simpler update rules.

4.2 Frey's iterative probability propagation algorithm

Frey's local probability propagation [43] was published in 1998, before the work of Weiss on Gaussian Belief propagation. That is why it is interesting to find the relations between those two works. Frey's work deals with the factor analysis learning problem. The factor analyzer network is a two layer densely connected network that models bottom layer sensory inputs as a linear combination of top layer factors plus independent gaussian sensor noise.

In the factor analysis model, the underlying distribution is Gaussian. The prior distribution of the sensors is

$$p(z) = \mathcal{N}(z; 0, I), p(x|z) = \mathcal{N}(z; Sx, \Psi).$$

It is shown that maximum likelihood estimation of S and Ψ performs factor analysis.

The marginal distribution over \mathbf{x} is:

$$p(x) \propto \int_{\mathbf{z}} \mathcal{N}(\mathbf{x}; 0, I) \mathcal{N}(\mathbf{z}; S\mathbf{x}, \Psi) d\mathbf{x} = \mathcal{N}(\mathbf{z}; 0, \mathbf{S}^T \mathbf{S} + \Psi).$$

This distribution is Gaussian as well, with the following parameters:

$$E(\mathbf{z}|\mathbf{x}) = (\mathbf{S}^T \mathbf{S} + \Psi)^{-1} \mathbf{S}^T \mathbf{y},$$

$$Cov(\mathbf{z}|\mathbf{x}) = (\mathbf{S}^T \mathbf{S} + \Psi)^{-1}.$$

Table 4.2: Notations of GaBP (Weiss) and Frey's algorithm

[7]	Frey	comments
P_{ij}^{-1}	$-\phi_{nk}^{(i)}$	precision message from left i to right a
	$\nu_{kn}^{(i)}$	precision message from right a to right i
μ_{ij}	$\mu_{nk}^{(i)}$	mean message from left i to right a
	$\eta_{kn}^{(i)}$	mean message from right a to left i
μ_{ii}	x_n	prior mean of left node i
	0	prior mean of right node a
P_{ii}	1	prior precision of left node i
	ψ_n	prior precision of right node i
μ_i	$\nu_k^{(i)}$	posterior mean of node i
P_i	$\hat{z}_k^{(i)}$	posterior precision of node i
A_{ij}	λ_{nk}	covariance of left node i and right node a
A_{ji}	1	covariance of right node a and left node i

Theorem 18. Frey's iterative propagability propagation in an instance of GaBP

Proof. We start by showing that Frey's update rules are equivalent to the GaBP update rules. From right to left:

$$\underbrace{-P_{ij}^{-1}}_{\phi_{nk}^{(i)}} = \frac{\Psi_n + \sum_k \lambda_{nk}^2 \nu_{kn}^{(i-1)}}{\lambda_{nk}^2} - \nu_{kn}^{(i-1)} = \frac{\overbrace{\Psi_n + \sum_{k \neq j} \nu_{jn}^{(i-1)}}^{P_{i \setminus j}}}{\underbrace{\lambda_{nk}^2}_{A_{ij}^2}},$$

$$\underbrace{\mu_{ij}^{(i)}}_{\mu_{nk}} = \frac{x_n - \sum_k \lambda_{nk} \eta_{kn}^{(i-1)}}{\lambda_{nk}} + \eta_{kn}^{(i-1)} = \frac{\underbrace{\mu_{ii} P_{ii}}_{x_n} - \underbrace{\sum_{j \neq k} \eta_{kn}^{(i-1)}}_{\underbrace{\sum_{j \neq k} -P_{ki} \mu_{ki}}_{A_{ij}}}}{\lambda_{nk}}.$$

And from left to right:

$$\underbrace{P_{ji}^{-1}}_{\eta_{kn}^{(i)}} = 1 / (1 / (1 / (1 + \sum_n 1 / \psi_{nk}^{(i)} - 1 / \psi_{nk}^{(i)}))) = \underbrace{A_{ji}^2}_1 / (\underbrace{P_{ii}}_1 + \underbrace{\sum_{j \neq k} 1 / \psi_{nk}^{(i)}}_{\sum_{j \neq k} -P_{ij}}),$$

$$\begin{aligned} \nu_{kn}^{(i)} &= \eta_{kn}^{(i)} (\sum_n \mu_{nk}^{(i)} / \psi_{nk}^{(i)} - \mu_{nk}^{(i)} / \psi_{nk}^{(i)}) = \eta_{kn}^{(i)} (\sum_{j \neq k} \mu_{nk}^{(i)} / \psi_{nk}^{(i)}) = \\ &= \underbrace{A_{ij}}_1 \underbrace{P_{ij}^{-1}}_{\eta_{kn}^{(i)}} (\underbrace{\mu_{ii} P_{ii}}_0 + \sum_{j \neq k} \underbrace{\mu_{nk}^{(i)} / \psi_{nk}^{(i)}}_{\mu_{nk}^{(i)} / \psi_{nk}^{(i)}}). \end{aligned}$$

Table 4.3: Notations of GaBP (Weiss) and Consensus Propagation

Weiss	CP	comments
P_0	\mathcal{K}	precision of $\psi_{ii}(x_i) \prod_{x_k \in N(x_i) \setminus x_j} m_{ki}(x_i)$
μ_0	$\mu(\mathcal{K})$	mean of $\psi_{ii}(x_i) \prod_{x_k \in N(x_i) \setminus x_j} m_{ki}(x_i)$
P_{ij}	$\mathcal{F}_{ij}(\mathcal{K})$	precision message from i to j
μ_{ij}	$\mathcal{G}_{ij}(\mathcal{K})$	mean message from i to j
μ_{ii}	y_i	prior mean of node i
P_{ii}	1	prior precision of node i
μ_i	\bar{y}	posterior mean of node i (identical for all nodes)
P_i	P_{ii}	posterior precision of node i
b	Q_{ji}	covariance of nodes i and j
b'	Q_{ij}	covariance of nodes i and j
a	0	variance of node i in the pairwise covariance matrix V_{ij}
c	0	variance of node j in the pairwise covariance matrix V_{ij}

It is interesting to note, that in Frey's model the graph is directed. That is why the edges $A_{ji} = 1$ in the update rules from right to left. \square

4.3 Moallami and Van-Roy's Consensus Propagation

The consensus propagation (CP) [44] is a distributed algorithm for calculating the average value in the network. The input to the algorithm is the adjacency graph and the input values y_i . The output is the mean value \bar{y} . The algorithm is based on the GaBP algorithm. In this section we derive the update rules used in CP from the GaBP algorithm (Weiss).

The self potentials of the nodes are

$$\psi_{ii}(x_i) \propto \exp(-(x_i - y_i)^2)$$

The edge potentials are:

$$\psi_{ij}(x_i, x_j) \propto \exp(-\beta Q_{ij}(x_i - x_j)^2)$$

In total, the probability distribution $p(x)$

$$\begin{aligned} p(x) &\propto \prod_i \exp(-(x_i - y_i)^2) \prod_{e \in E} \exp(-\beta Q_{ij}(x_i - x_j)^2) \\ &= \exp(\sum_i (-(x_i - y_i)^2) - \beta \sum_{e \in E} Q_{ij}(x_i - x_j)^2) \end{aligned}$$

We want to find an assignment $x^* = \max_x p(x)$. It is shown in [44] that this assignment conforms to the mean value in the network: $\bar{y} = \frac{1}{n} \sum_i y_i$ when β is very large.

For simplicity of notations, we list the different notations in Table 4.3.

Theorem 19. *The consensus propagation algorithm is an instance of the Gaussian belief propagation algorithm.*

Proof. We prove this theorem by substituting the self and edge potentials used in the CP paper in the belief propagation update rules, deriving the update rules of the CP algorithm.

$$\begin{aligned}
 m_{ij}(x_j) &\propto \int_{x_i} \overbrace{\exp(-(x_i - \mu_{ii})^2)}^{\psi_{ii}(x_i)} \overbrace{\exp(-\beta Q_{ik}(x_i - x_j)^2)}^{\psi_{ij}(x_i, x_j)} \overbrace{\exp(-\sum_k P_{ki}(x_i - \mu_{ki})^2)}^{\prod m_{ki}(x_i)} dx_i = \\
 &\int_{x_i} \exp(-x_i^2 + 2x_i\mu_{ii} - \mu_{ii}^2 - \beta Q_{ik}x_i^2 + 2\beta Q_{ij}x_i x_j - \beta Q_{ij}x_j^2 - \sum_k P_{ki}x_i^2 + \sum_k P_{ki}\mu_{ki} - \sum_k P_{ki}^2\mu_{ki}^2) dx_i = \\
 &\exp(-\mu_{ii}^2 - \beta Q_{ij}x_j^2 + \sum_k P_{ij}^2 m_{ij}^2) \int_{x_i} \overbrace{\exp((1 + \beta Q_{ij} + \sum_k P_{ki})x_i^2)}^{ax^2} \overbrace{\exp(2(\beta Q_{ij}x_j + P_{ki}\mu_{ki} + \mu_{ii})x_i)}^{bx} dx_i \\
 &\hspace{15em} (4.1)
 \end{aligned}$$

Now we use the following integration rule:

$$\int_x \exp(-(ax^2 + bx)) dx = \sqrt{\pi/a} \exp\left(\frac{b^2}{4a}\right)$$

We compute the integral:

$$\begin{aligned}
 &\int_{x_i} \overbrace{\exp(1 + \beta Q_{ij} + \sum_k P_{ki})x_i^2}^{ax^2} \overbrace{\exp(2(\beta Q_{ij}x_j + P_{ki}\mu_{ki} + \mu_{ii})x_i)}^{bx} dx_i = \\
 &= \sqrt{\pi/a} \exp\left(\frac{b^2}{4a}\right) \propto \exp\left(\frac{\beta^2 Q_{ij}^2 x_j^2 + 2\beta Q_{ij}(P_{ki}\mu_{ki} + \mu_{ii})x_j + (\mu_{ki} + \mu_{ii})^2}{1 + \beta Q_{ki} + \sum_k P_{ki}}\right) \\
 &\hspace{15em} \underbrace{\frac{1}{1 + \beta Q_{ki} + \sum_k P_{kl}}}_{4a}
 \end{aligned}$$

Substituting the result back into (4.1) we get:

$$m_{ij}(x_j) \propto \exp(-\mu_{ii}^2 - \beta Q_{ij}x_j^2 + \sum_k P_{ij}^2 m_{ij}^2) \exp\left(\frac{\beta^2 Q_{ij}^2 x_j^2 + 2\beta Q_{ij}(P_{ki}\mu_{ki} + \mu_{ii})x_j + (\mu_{ki} + \mu_{ii})^2}{1 + \beta Q_{ki} + \sum_k P_{ki}}\right) \quad (4.2)$$

For computing the precision, we take all the terms of x_j^2 from (4.2) and we get:

$$P_{ij}(x_j) \propto \exp\left(-\beta Q_{ij} + \frac{\beta^2 Q_{ij}^2}{1 + \beta Q_{ij} + \sum P_{ki}}\right) =$$

$$\begin{aligned}
& \frac{-\beta Q_{ij}(1 + \beta Q_{ij} + \Sigma P_{ki}) + \beta^2 Q_{ij}^2}{1 + \beta Q_{ij} + \Sigma P_{ki}} = \\
& \frac{-\beta Q_{ij} - \beta^2 Q_{ij}^2 - \beta Q_{ij} \Sigma P_{ki} + \beta^2 Q_{ij}^2}{1 + \beta Q_{ij} + \Sigma P_{ki}} = \\
& = \frac{1 + \Sigma P_{ki}}{\beta Q_{ij} + 1 + \Sigma P_{ki}}
\end{aligned}$$

The same is done for computing the mean, taking all the terms of x_j from equation (4.2):

$$\mu_{ij}(x_j) \propto \frac{\beta Q_{ij}(\mu_{ii} + \Sigma P_{ki} \mu_{ki})}{1 + \beta Q_{ij} + \Sigma P_{ki}} = \frac{\mu_{ii} + \Sigma P_{ki} \mu_{ki}}{1 + \frac{1 + \Sigma P_{ki}}{\beta Q_{ij}}}$$

□

4.4 Quadratic Min-Sum Message Passing algorithm

The quadratic Min-Sum message passing algorithm was initially presented in [6]. It is a variant of the max-product algorithm, with underlying Gaussian distributions. The quadratic Min-Sum algorithm is an iterative algorithm for solving a quadratic cost function. Not surprisingly, as we have shown in Section 2.4 that the Max-Product and the Sum-Product algorithms are identical when the underlying distributions are Gaussians. In this contribution, we show that the quadratic Min-Sum algorithm is identical to the GaBP algorithm, although it was derived differently.

In [6] the authors discuss the application for solving linear system of equations using the Min-Sum algorithm. Our work [7] was done in parallel to their work, where both papers appeared in the 45th Allerton 2007 conference.

Theorem 20. *The Quadratic Min-Sum algorithm is an instance of the GaBP algorithm.*

Proof. We start in the quadratic parameter updates:

$$\gamma_{ij} = \frac{1}{1 - \Sigma_{u \in N(i) \setminus j} \Gamma_{ui}^2 \gamma_{ui}} = \overbrace{\left(\underbrace{1}_{A_{ii}} - \Sigma_{u \in N(i) \setminus j} \underbrace{\Gamma_{ui}}_{A_{ui}} \underbrace{\gamma_{ui}}_{\Gamma_{ui}^{-1}} \underbrace{\Gamma_{iu}}_{A_{iu}} \right)^{-1}}^{P_{i \setminus j}^{-1}}$$

Which is equivalent to 2.11. Regarding the mean parameters,

$$z_{ij} = \frac{\Gamma_{ij}}{1 - \Sigma_{u \in N(i) \setminus j} \Gamma_{ui}^2 \gamma_{ui}} (h_i - \Sigma_{u \in N(i) \setminus j} z_{ui}) = \overbrace{\left(\underbrace{\Gamma_{ij}}_{A_{ij}} \underbrace{\Gamma_{ij}^{-1}}_{(P_{i \setminus j})^{-1}} \underbrace{(h_i - \Sigma_{u \in N(i) \setminus j} z_{ui})}_{b_i} \right)}^{\mu_{i \setminus j}}$$

Which is equivalent to 2.12. □

Table 4.4: Notations of Min-Sum [6] vs. GaBP

Min-Sum [6]	GaBP [7]	comments
$\gamma_{ij}^{(t+1)}$	$P_{i \setminus j}^{-1}$	quadratic parameters / product rule precision from i to j
$z_{ij}^{(t+1)}$	$\mu_{i \setminus j}$	linear parameters / product rule mean from i to j
h_i	b_i	prior mean of node i
A_{ii}	1	prior precision of node i
x_i	x_i	posterior mean of node i
—	P_i	posterior precision of node i
Γ_{ij}	A_{ij}	covariance of nodes i and j

For simplicity of notations, we list the different notations in Table 4.4. As shown in Table 4.4, the Min-Sum algorithm assumes the covariance matrix Γ is first normalized s.t. the main diagonal entries (the variances) are all one. The messages sent in the Min-Sum algorithm are called linear parameters (which are equivalent to the mean messages in GaBP) and quadratic parameters (which are equivalent to variances). The difference between the algorithm is that in the GaBP algorithm, a node computes the product rule and the integral, and sends the result to its neighbor. In the Min-Sum algorithm, a node computes the product rule, sends the intermediate result, and the receiving node computes the integral. In other words, the same computation is performed but on different locations. In the Min-Sum algorithm terminology, the messages are linear and quadratic parameters vs. Gaussians in our terminology.

Part 2: Applications

Chapter 5

Rating users and data items in social networks

We propose to utilize the distributed GaBP solver presented in Chapter 2 to efficiently and distributively compute a solution to a family of quadratic cost functions described below. By implementing our algorithm once, and choosing the computed cost function dynamically on the run we allow a high flexibility in the selection of the rating method deployed in the Peer-to-Peer network.

We propose a unifying family of quadratic cost functions to be used in Peer-to-Peer ratings. We show that our approach is general since it captures many of the existing algorithms in the fields of visual layout, collaborative filtering and Peer-to-Peer rating, among them Koren spectral layout algorithm, Katz method, Spatial ranking, Personalized PageRank and Information Centrality. Besides of the theoretical interest in finding common basis of algorithms that were not linked before, we allow a single efficient implementation for computing those various rating methods.

Using simulations over real social network topologies obtained from various sources, including the MSN Messenger social network, we demonstrate the applicability of our approach. We report simulation results using networks of millions of nodes.

Whether you are browsing for a hotel, searching the web, or looking for a recommendation on a local doctor, what your friends like will bear great significance for you. This vision of virtual social communities underlies the stellar success of a growing body of recent web services, e.g., <http://www.flickr.com>, <http://del.icio.us>, <http://www.myspace.com>, and others. However, while all of these services are centralized, the full flexibility of social information-sharing can often be better realized through direct sharing between peers.

This chapter presents a mechanism for sharing user *ratings* (e.g., on movies, doctors, and vendors) in a social network. It introduces distributed mechanisms for computing by the network itself individual ratings that incorporate rating-information from the network. Our approach utilizes message-passing algorithms from the domain of Gaussian graphical models. In our system, information remains in the network, and is never “shipped” to a centralized server for any global computation. Our algorithms provide each user in the network with an individualized rating per object (e.g., per vendor). The end-result is a local rating per user which minimizes her cost

function from her own rating (if exists) and, at the same time, benefits from incorporating ratings from her network vicinity. Our rating converges quickly to an approximate optimal value even in sizable networks.

Sharing views over a social network has many advantages. By taking a peer-to-peer approach the user information is shared and stored only within its community. Thus, there is no need for trusted centralized authority, which could be biased by economic and/or political forces. Likewise, a user can constrain information pulling from its trusted social circle. This prevents spammers from penetrating the system with false recommendations.

5.1 Our general framework

The social network is represented by a directed, weighted communication graph $G = (V, E)$. Nodes $V = \{1, 2, \dots, n\}$ are users. Edges express social ties, where a non-negative edge weight w_{ij} indicates a measure of the mutual trust between the endpoint nodes i and j . Our goal is to compute an output rating $\mathbf{x} \in R^n$ to each data item (or node) where x_i is the output rating computed locally in node i . The vector \mathbf{x} is a solution that minimizes some cost function. Next, we propose such a cost function, and show that many of the existing rating algorithms conform to our proposed cost function.

We consider a single instance of the rating problem that concerns an individual item (e.g., a movie or a user). In practice, the system maintains ratings of many objects concurrently, but presently, we do not discuss any correlations across items. A straight forward generalization to our method for collaborative filtering, to rank m (possibly correlated) items, as done in [45].

In this chapter, we methodically derive the following quadratic cost function, that quantifies the Peer-to-Peer rating problem:

$$\min E(x) \triangleq \sum_i w_{ii}(x_i - y_i)^2 + \beta \sum_{i,j \in E} w_{ij}(x_i - x_j)^2, \quad (5.1)$$

where x_i is a desired rating computed locally by node i , \mathbf{y} is an optional prior rating, where y_i is a local input to node i (in case there is no prior information, \mathbf{y} is a vector of zeros).

We demonstrate the generality of the above cost function by proving that many of the existing algorithms for visual layouts, collaborative filtering and ranking of nodes in Peer-to-Peer networks are special cases of our general framework:

1. **Eigen-Projection method.** Setting $y_i = 1, w_{ii} = 1, w_{ij} = 1$ we get the Eigen-Projection method [46] in a single dimension, an algorithm for ranking network nodes for creating a intuitive visual layout.
2. **Koren's spectral layout method.** Recently, Dell'Amico proposed to use Koren's visual layout algorithm for ranking nodes in a social network [47]. We will show that this ranking method is a special case of our cost function, setting: $w_{ii} = deg(i)$.

3. **Average computation.** By setting the prior inputs y_i to be the input of node i and taking $\beta \rightarrow \infty$ we get $x_i = 1/n \sum_i y_i$, the average value of \mathbf{y} . This construction, Consensus Propagation, was proposed by Moallemi and Van-Roy in [44].
4. **Peer-to-Peer Rating.** By generalizing the Consensus Propagation algorithm above and supporting weighted graph edges, and finite β values we derive a new algorithm for Peer-to-Peer rating [19].
5. **Spatial Ranking.** We propose a generalization of the Katz method [48], for computing a personalized ranking of peers in a social network. By setting $y_i = 1, w_{ii} = 1$ and regarding the weights w_{ij} as the probability of following a link of an absorbing Markov-chain, we formulate the spatial ranking method [19] based on the work of [49].
6. **Personalized PageRank.** We show how the PageRank and personalized PageRank algorithms fits within our framework [50, 51].
7. **Information Centrality.** In the information centrality node ranking method [52], the non-negative weighted graph $G = (V, E)$ is considered as an electrical network, where edge weights is taken to be the electrical conductance. We show that this measure can be modelled using our cost function as well.

Furthermore, we propose to utilize the Gaussian Belief Propagation algorithm (GaBP) - an algorithm from the probabilistic graphical models domain - for efficient and distributed computation of a solution minimizing a single cost function drawn from our family of quadratic cost functions. We explicitly show the relation between the algorithm to our proposed cost function by deriving it from the cost function.

Empirically, our algorithm demonstrates faster convergence than the compared algorithms, including conjugate gradient algorithms that were proposed in [47, 45] to be used in Peer-to-Peer environments. For comparative study of those methods see [7].

5.2 Unifying family of quadratic cost functions

We derive a family of unifying cost functions following the intuitive explanation of Koren [53]. His work addresses graphic visualization of networks using spectral graph properties. Recently, Dell'Amico proposed in [47] to use Koren visual layout algorithm for computing a distance metric that enables ranking nodes in a social network. We further extend this approach by finding a common base to many of the ranking algorithms that are used in graph visualization, collaborative filtering and in Peer-to-Peer rating. Besides of the theoretical interest in finding a unifying framework to algorithms that were not related before, we enable also a single efficient distributed implementation that takes the specific cost function as input and solves it.

Given a directed graph $G = (V, E)$ we would like to find an output rating $\mathbf{x} \in R^n$ to each item where x_i is the output rating computed locally in node i . \mathbf{x} can be expressed as the solution

as the following constraint minimization problem:

$$\min E(\mathbf{x}) \triangleq \sum_{i,j \in E} w_{ij} (x_i - x_j)^2, \quad (5.2)$$

$$\text{Given } \text{Var}(\mathbf{x}) = 1, \text{ Mean}(\mathbf{x}) = 0.$$

The cost function $E(x)$ is combined of weighted sums of interactions between neighbors. From the one hand, "heavy" edges w_{ij} force nodes to have a similar output rating. From the other hand, the variance condition prevents a trivial solution of all x_i converging to a single value. In other words, we would like the rating of an item to be scaled. The value of the variance determines the scale of computed ratings, and is arbitrarily set to one. Since the problem is invariant under translation, we add also the mean constraint to force a unique solution. The mean is arbitrarily set to zero.

In this chapter, we address visual layout computed for a single dimension. The work of Koren and Dell'Amico is more general than ours since it discusses rating in k dimensions. A possible future extension to this work is to extend our work to k dimensions.

From the visual layout perspective, "stronger" edges w_{ij} let neighboring nodes appear closer in the layout. The variance condition forces a scaling on the drawing.

From the statistical mechanics perspective, the cost function $E(x)$ is considered as the system energy that we would like to minimize, the weighted sums are called "attractive forces" and the variance constraint is a "repulsive force".

One of the most important observations we make is that using Koren's framework, the chosen values of the variance and mean are arbitrary and could be changed. This is because the variance influences the scaling of the layout and the mean the translation of the result. Without the loss of generality, in some of the proofs we change the values of the mean and variance to reflect easier mathematical derivation. However, normalization of rated values can be always done at the end, if needed.

Using the equation $\text{Var}(x) \triangleq \sum_i (x_i - \bar{x})^2$ where $\bar{x} \triangleq \frac{1}{n} \sum_i x_i$, we can compute the lagrangian of (2):

$$\begin{aligned} \mathcal{L}(\mathbf{x}, \beta) &= \sum_{i,j \in E} w_{ij} (x_i - x_j)^2 + \beta \sum_i (x_i - \bar{x})^2 \quad (5.3) \\ &= \sum_{i,j \in E} w_{ij} (x_i - x_j)^2 + \beta \left(\sum_i x_i^2 - 2 \sum_i x_i \bar{x} + \sum_i \bar{x}^2 \right). \end{aligned}$$

The algorithm which solves the above cost function, taking the Lagrange multiplier $\beta = 1$ is called "the Eigen-Projection method" [46]: using linear algebra notations we get:

$$\mathcal{L}(x, \beta) = \mathbf{x}^T L \mathbf{x} - 2 \bar{\mathbf{x}} \mathbf{x} + \bar{\mathbf{x}}^T I \bar{\mathbf{x}},$$

where L is the graph Laplacian. Since $\mathcal{L}(\cdot)$ is a convex quadratic function of \mathbf{x} we can find the minimizing \mathbf{x} from the optimality condition:

$$\nabla_{\mathbf{x}} \mathcal{L}(\mathbf{x}, \beta) = 2 \mathbf{x}^T L - 2 \bar{\mathbf{x}} = 0$$

which yields

$$x = L^{-1}\bar{x}.$$

Following, we generalize Koren's method to support a larger variety of cost functions. The main observation we have, is that the variance condition is used only for scaling the rating, without relating to the specific problem at hand. We propose to add a second constraint which is local to each node:

$$\sum_i w_{ii}(x_i - y_i)^2 + \beta \sum_{i,j \in E} w_{ij}(x_i - x_j)^2. \quad (5.4)$$

Thus we allow higher flexibility, since we allow y_i can be regarded as *prior information* in the case of Peer-to-Peer rating, where each node has some initial input it adds to the computation. In other cases, y_i can be some function computed on x like $y_i = \frac{1}{N} \sum_{i=1}^N x_i$ or a function computed on the graph: $y_i = \sum_{N(i)} \frac{w_{ij}}{\text{deg}(i)}$.

Theorem 21. *The Eigen-Projection method is an instance of the cost function 5.1 when $w_{ij} = 1, w_{ii} = 1, \beta = 1, y_i = 0$.*

Proof is found in Appendix 8.5.

Theorem 22. *The Koren spectral layout algorithm/Del'Amicco method in a single dimension, is an instance of the cost function 5.1 when $w_{ii} = 1, \beta = 1, y_i = \text{deg}(i)$, where $\text{deg}(i) \triangleq \sum_{j \in N(i)} w_{ij}$, up to a translation.*

Proof is found in Appendix 8.6.

5.2.1 Peer-to-Peer rating

In [19] we have proposed to generalize the Consensus Propagation (CP) algorithm [44] to solve the general cost function (5.1).

The CP algorithm is a distributed algorithm for calculating the network average, assuming each node has an initial value. We have extended the CP algorithm in several ways. First, in the original paper the authors propose to use a very large β for calculating the network average. As mentioned, large β forces all the nodes to converge to the same value. We remove this restriction by allowing a flexible selection of β based on the application needs. As β becomes small the calculation is done in a closer and closer vicinity of the node.

Second, we have extended the CP algorithm to support null value, adapting it to omit the term $(y_i - x_i)^2$ when $y_i = \perp$, i.e., when node i has no initial rating. This construction is reported in [19] and not repeated here.

Third, we use non-uniform edge weights w_{ij} , which in our settings represent mutual trust among nodes. This makes the rating local to certain vicinities, since we believe there is no meaning for getting a global rating in a very large network. This extension allows also asymmetric

links where the trust assigned between neighbors is not symmetric. In that case we get an approximation to the original problem.

Fourth, we introduce node weights, where node with higher weight has an increasing linear contribution to the output of the computation.

The Peer-to-Peer rating algorithm was reported in detail in [19].

Theorem 23. *The Consensus propagation algorithm is an instance of our cost function 5.1 with $w_{ii} = 1, \beta \rightarrow \infty$.*

The proof is given in Chapter 4.3

Theorem 24. *The Peer-to-Peer rating algorithm is an instance of our cost function 5.1.*

The proof is given in [19].

5.2.2 Spatial Ranking

In [19] we presented a new ranking method called Spatial Ranking, based on the work of Jason K. Johnson *et al.* [49]. Recently, we found out that a related method was proposed in 1953 in the social sciences field by Leo Katz [48]. The Spatial Ranking method described below is a generalization of the Katz method, since it allows weighted trust values between social network nodes (unlike the Katz method which deals with binary relations). Furthermore, we propose a new efficient implementation for a distributed computation of the Spatial Ranking method.

In our method, each node ranks itself the list of all other nodes based on its network topology and creates a personalized ranking of its own.

We propose to model the network as a Markov chain with a transition matrix R , and calculate the *fundamental matrix* P , where the entry P_{ij} is the expected number of times of a random walk starting from node i visits node j [54].

We take the local value P_{ii} of the fundamental matrix P , computed in node i , as node i 's global importance. Intuitively, the value signifies the weight of infinite number of random walks that start and end in node i . Unlike the PageRank ranking method, we explicitly bias the computation towards node i , since we force the random walks to start from it. This captures the local importance node i has when we compute a personalized rating of the network locally by node i . Figure 5.1 captures this bias using a simple network of 10 nodes.

The fundamental matrix can be calculated by summing the expectations of random walks of length one, two, three etc., $R + R^2 + R^3 + \dots$. Assuming that the spectral radius $\rho(R) < 1$, we get $\sum_{l=1}^{\infty} R^l = (I - R)^{-1}$. Since R is stochastic, the inverse $(I - R)^{-1}$ does not exist. We therefore slightly change the problem: we select a parameter $\alpha < 1$, to initialize the matrix $J = I - \alpha R$ where I is the identity matrix. We know that $\rho(\alpha R) < 1$ and thus $\alpha R + \alpha^2 R^2 + \alpha^3 R^3 + \dots$ converges to $(I - \alpha R)^{-1}$.

Theorem 25. *The Spatial Ranking method is an instance of the cost function 5.1, when $y_i = 0, w_{ii} = 1$, and w_{ij} are entries in an absorbing Markov chain R .*

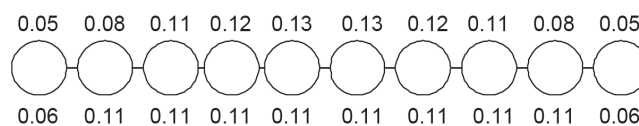


Figure 5.1: Example output of the Spatial ranking (on top) vs. PageRank (bottom) over a network of 10 nodes. In the Spatial ranking method node rank is biased towards the center, where in the PageRank method, non-leaf nodes have equal rank. This can be explained by the fact that the sum of self-returning random walks increases towards the center.

Proof is found in Appendix 8.7.

We have shown that the Spatial Ranking algorithm fits well within our unifying family of cost functions. Setting \mathbf{y} to a fixed constant, means there is no individual prior input at the nodes, thus we measure mainly the topological influence in ranking the nodes. In case that we use $w_{ii} \neq 1$ we will get a biased ranking, where nodes with higher weight have higher influence at result of the computation.

5.2.3 Personalized PageRank

The PageRank algorithm is a fundamental algorithm in computing node ranks in the network [50]. The personalized PageRank algorithm is a variant described in [51]. In a nutshell, the Markov-chain transition probability matrix \mathbf{M} is constructed out of the web links graph. A prior probability \mathbf{x} is taken to weight the result. The personalized PageRank calculation can be computed [51]:

$$PR(x) = (1 - \alpha)(I - \alpha\mathbf{M})^{-1}\mathbf{x},$$

where α is a weighting constant which determines the speed of convergence in trade-off with the accuracy of the solution and I is the identity matrix.

Theorem 26. *The Personalized PageRank algorithm can be expressed using our cost function 5.1, up to a translation.*

Proof is found in Appendix 8.8.

5.2.4 Information Centrality

In the information centrality (IC) node ranking method [52], the non-negative weighted graph $G = (V, E)$ is considered as an electrical network, where edge weights is taken to be the electrical conductance. A vector of supply b is given as input, and the question is to compute the electrical

Topology	Nodes	Edges	Data Source
MSN Messenger graph	1M	9.4M	Microsoft
Blogs Web Crawl	1.5M	8M	IBM
DIMES	300K	2.2M	DIMES Internet measurements
US Government documents	12M	64M	Web research collection

Table 5.1: Topologies used for experimentation

potentials vector p . This is done by computing the graph Laplacian and solving the set of linear equations $Lp = b$. The IC method (a.k.a current flow betweenness centrality) is defined by:

$$IC(i) = \frac{n - 1}{\sum_{i \neq j} p_{ij}(i) - p_{ij}(j)}.$$

The motivation behind this definition is that a centrality of node is measured by inverse proportion to the effective resistance between a node to all other nodes. In case the effective resistance is lower, there is a higher electrical current flow in the network, thus making the node more "socially influential".

One can easily show that the IC method can be derived from our cost function, by calculating $(L + J)^{-1}$ where L is the graph Laplacian and J is a matrix of all ones. Note that the inverted matrix is not sparse, unlike all the previous constructions. Hence, a special construction which transforms this matrix into a sparse matrix is needed. This topic is of scope of this work.

5.3 Experimental results

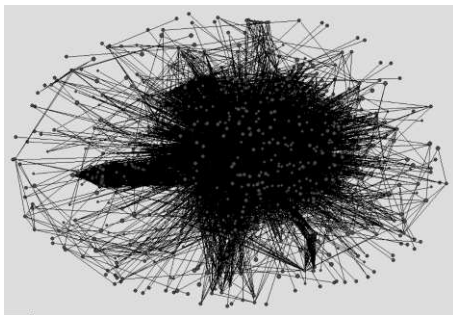


Figure 5.2: Blog network topology

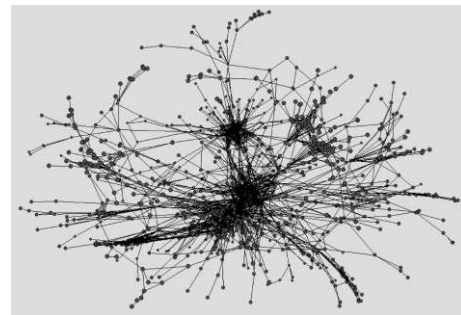


Figure 5.3: DIMES Internet topology

We have shown that various ranking methods can be computed by solving a linear system of equations. We propose to use the GaBP algorithm, for efficiently computing the ranking methods distributively by the network nodes. Next, we bring simulation results which show that for very large networks the GaBP algorithm performs remarkably well.

For evaluating the feasibility and efficiency of our rating system, we used several types of large scale social networks topologies:

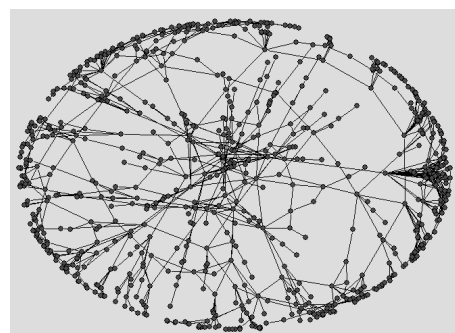
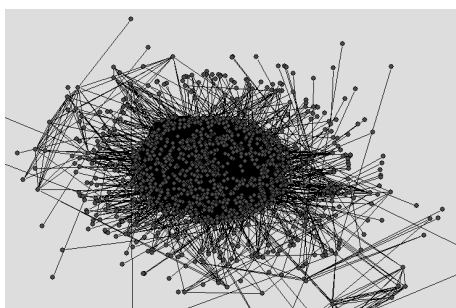


Figure 5.4: US gov documents topology

Figure 5.5: MSN Messenger topology

Figures 2-5 illustrate subgraphs taken from the different topologies plotted using the Pajek software [55]. Despite the different graph characteristics, the GaBP performed very well on all tested topologies

1. **MSN Live Messenger.** We used anonymized data obtained from Windows Live Messenger that represents Messenger users' buddy relationships. The Messenger network is rather large for simulation (over two hundred million users), and so we cut sub-graphs by starting at a random node, and taking a BFS cut of about one million nodes. The diameter of the sampled graph is five on average.
2. **Blog crawl data.** We used blog crawl data of a network of about 1.5M bloggers, and 8M directed links to other blogs. This data was provided thanks to Elad Yom-Tov from IBM Research Labs, Haifa, Israel.
3. **DIMES Internet measurements.** We used a snapshot of an Internet topology from January 2007 captured by the DIMES project [56]. The 300K nodes are routers and the 2.2M edges are communication lines.
4. **US gov document repository.** We used a crawl of 12M pdf documents of US government, where the links are links within the pdf documents pointing to other documents within the repository [57].

One of the interesting questions, is the practical convergence speed of our rating methods. The results are given using the MSN Messenger social network's topology, since all of the other topologies tested obtained similar convergence results. We have tested the Peer-to-Peer rating algorithm. We have drawn the input ratings y_i and edge weights w_{ij} in uniformly at random in the range $[0 - 1]$. We have repeated this experiment with different initializations for the input rating and the edge weights and got similar convergence results. We have tested other cost functions, including PageRank and Spatial Ranking and got the same convergence results.

Figure 5.6 shows the convergence speed of the Peer-to-Peer rating algorithm. The x-axis represents round numbers. The rounds are given only for reference, in practice there is no need for the nodes to be synchronized in rounds as shown in [58]. The y-axis represents the sum-total of change in ratings relative to the previous round. We can see that the node ratings converge

very fast towards the optimal rating derived from the cost function. After only five iterations, the total change in nodes ratings is about 1 (which means an average change of 1×10^{-6} per node).

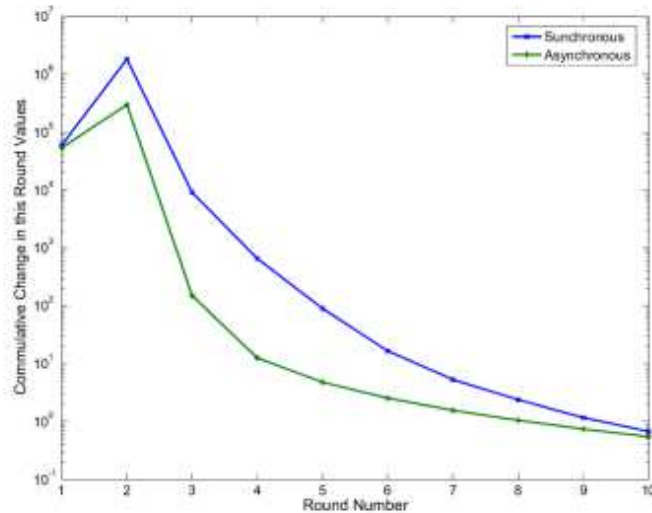


Figure 5.6: Convergence of rating over a social network of 1M nodes and 9.4M edges. Note, that using asynchronous rounds, the algorithm converges faster, as discussed in [58]

5.3.1 Rating Benchmark

For demonstrating the applicability of our proposed cost functions, we have chosen to implement a “benchmark” that evaluates the effectiveness of the various cost functions. Demonstrating this requires a quantitative measure beyond mere speed and scalability. The benchmark approach we take is as follows. First, we produce a ladder of “social influence” that is inferred from the network topology, and rank nodes by this ladder, using the Spatial ranking cost function. Next, we test our Peer-to-Peer rating method in the following settings. Some nodes are initialized with rate values, while other nodes are initialized with empty ratings. Influential nodes are given different initial ratings than non-influential nodes. The expected result is that the ratings of influential nodes should affect the ratings of the rest of the network so long as they are not vastly outnumbered by opposite ratings.

As a remark, we note that we can use the social ranks additionally as trust indicators, giving higher trust values to edges which are incident to high ranking nodes, and vice versa. This has the nice effect of initially placing low trust on intruders, which by assumption, cannot appear influential.

For performing our benchmark tests, we once again used simulation over the 1 million node sub-graph of the Messenger network. Using the ranks produced by our spatial ranking, we selected the seven highest ranking nodes and assigned them an initial rating value 5. We also selected

seven of the lowest ranking nodes and initialized them with rating value 1. All other nodes started with null input. The results of the rating system in this settings are given in Figure 3. After about ten rounds, a majority of the nodes converged to a rating very close to the one proposed by the influential nodes. We ran a variety of similar tests and obtained similar results in all cases where the influential nodes were not totally outnumbered by opposite initial ratings; for brevity, we report only one such test here.

The conclusion we draw from this test is that a combination of applying our GaBP solver for computing first the rating of nodes, and then using this rating for choosing influential nodes and spreading their beliefs in the network has the desired effect of fast and influential dissemination of the socially influential nodes. This effect can have a lot of applications in practice, including targeted commercials to certain zones in the social network.

Quite importantly, our experiment shows that our framework provide good protection against malicious infiltrators: Assuming that intruders have low connectivity to the rest of the network, we demonstrate that it is hard for them to influence the rating values in the system. Furthermore, we note that this property will be reinforced if the trust values on edges are reduced due to their low ranks, and using users satisfaction feedback.

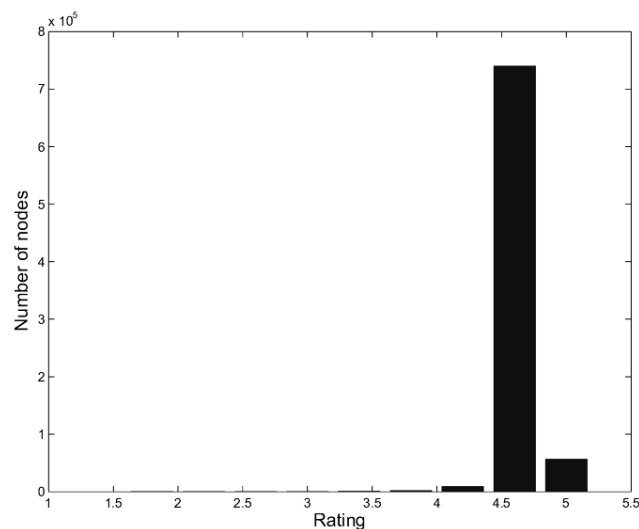


Figure 5.7: Final rating values in a network of 1M nodes. Initially, 7 highest ranking nodes rate 5 and 7 lowest ranking nodes rate 1.

Chapter 6

Linear Detection

Consider a discrete-time channel with a real input vector $\mathbf{x} = \{x_1, \dots, x_K\}^T$ governed by an arbitrary prior distribution, $P_{\mathbf{x}}$, and a corresponding real output vector $\mathbf{y} = \{y_1, \dots, y_K\}^T = f\{\mathbf{x}^T\} \in \mathbb{R}^K$.¹ Here, the function $f\{\cdot\}$ denotes the channel transformation. By definition, linear detection compels the decision rule to be

$$\hat{\mathbf{x}} = \Delta\{\mathbf{x}^*\} = \Delta\{\mathbf{A}^{-1}\mathbf{b}\}, \quad (6.1)$$

where $\mathbf{b} = \mathbf{y}$ is the $K \times 1$ observation vector and the $K \times K$ matrix \mathbf{A} is a positive-definite symmetric matrix approximating the channel transformation. The vector \mathbf{x}^* is the solution (over \mathbb{R}) to $\mathbf{A}\mathbf{x} = \mathbf{b}$. Estimation is completed by adjusting the (inverse) matrix-vector product to the input alphabet, dictated by $P_{\mathbf{x}}$, accomplished by using a proper clipping function $\Delta\{\cdot\}$ (e.g., for binary signaling $\Delta\{\cdot\}$ is the sign function).

For example, linear channels, which appear extensively in many applications in communication and data storage systems, are characterized by the linear relation

$$\mathbf{y} = f\{\mathbf{x}\} = \mathbf{R}\mathbf{x} + \mathbf{n}, \quad (6.2)$$

where \mathbf{n} is a $K \times 1$ additive noise vector and $\mathbf{R} = \mathbf{S}^T\mathbf{S}$ is a positive-definite symmetric matrix, often known as the correlation matrix. The $N \times K$ matrix \mathbf{S} describes the physical channel medium while the vector \mathbf{y} corresponds to the output of a bank of filters matched to the physical channel \mathbf{S} .

Due to the vast applicability of linear channels, in Section 3 we focus in our experimental study on such channels, although our paradigm is not limited to this case. Assuming linear channels with AWGN with variance σ^2 as the ambient noise, the general linear detection rule (6.1) can describe known linear detectors. For example [59, 60]:

- The conventional matched filter (MF) detector is obtained by taking $\mathbf{A} \triangleq \mathbf{I}_K$ and $\mathbf{b} = \mathbf{y}$. This detector is optimal, in the MAP-sense, for the case of zero cross-correlations, *i.e.*, $\mathbf{R} = \mathbf{I}_K$, as happens for orthogonal CDMA or when there is no ISI effect.

¹An extension to the complex domain is straightforward.

- The decorrelator (zero forcing equalizer) is achieved by substituting $\mathbf{A} \triangleq \mathbf{R}$ and $\mathbf{b} = \mathbf{y}$. It is optimal in the noiseless case.
- The linear minimum mean-square error (MMSE) detector can also be described by using $\mathbf{A} = \mathbf{R} + \sigma^2 \mathbf{I}_K$ and $\mathbf{b} = \mathbf{y}$. This detector is known to be optimal when the input distribution $P_{\mathbf{x}}$ is Gaussian.

In general, linear detection is suboptimal because of its deterministic underlying mechanism (*i.e.*, solving a given set of linear equations), in contrast to other estimation schemes, such as MAP or maximum likelihood, that emerge from an optimization criterion. In the following section we implement the linear detection operation, in its general form (6.1), in an efficient message-passing fashion.

The essence of detection theory is to estimate a hidden input to a channel from empirically-observed outputs. An important class of practical sub-optimal detectors is based on linear detection. This class includes, for instance, the conventional single-user matched filter, the decorrelator (also, called the zero-forcing equalizer), the linear minimum mean-square error (MMSE) detector, and many other detectors with widespread applicability [59, 60]. In general terms, given a probabilistic estimation problem, linear detection solves a deterministic system of linear equations derived from the original problem, thereby providing a sub-optimal, but often useful, estimate of the unknown input.

Applying the GaBP solver to linear detection, we establish a new and explicit link between BP and linear detection. This link strengthens the connection between message-passing inference and estimation theory, previously seen in the context of optimal maximum a-posteriori (MAP) detection [61, 62] and several sub-optimal nonlinear detection techniques [63] applied in the context of both dense and sparse [64, 65] graphical models.

In the following experimental study, we examine the implementation of a decorrelator detector in a noiseless synchronous CDMA system with binary signaling and spreading codes based upon Gold sequences of length $m = 7$.² Two system setups are simulated, corresponding to $n = 3$ and $n = 4$ users, resulting in the cross-correlation matrices

$$\mathbf{R}_3 = \frac{1}{7} \begin{pmatrix} 7 & -1 & 3 \\ -1 & 7 & -5 \\ 3 & -5 & 7 \end{pmatrix}, \quad (6.3)$$

and

$$\mathbf{R}_4 = \frac{1}{7} \begin{pmatrix} 7 & -1 & 3 & 3 \\ -1 & 7 & 3 & -1 \\ 3 & 3 & 7 & -1 \\ 3 & -1 & -1 & 7 \end{pmatrix}, \quad (6.4)$$

respectively.³

²In this case, as long as the system is not overloaded, *i.e.* the number of active users n is not greater than the spreading code's length m , the decorrelator detector yields optimal detection decisions.

³These particular correlation settings were taken from the simulation setup of Yener *et al.* [13].

Algorithm	Iterations $t(\mathbf{R}_3)$	Iterations $t(\mathbf{R}_4)$
Jacobi	111	24
GS	26	26
Parallel GaBP	23	24
Optimal SOR	17	14
Serial GaBP	16	13

Table 6.1: Decorrelator for $K = 3, 4$ -user, $N = 7$ Gold code CDMA. Total number of iterations required for convergence (threshold $\epsilon = 10^{-6}$) for GaBP-based solvers vs. standard methods.

The decorrelator detector, a member of the family of linear detectors, solves a system of linear equations, $\mathbf{A}\mathbf{x} = \mathbf{b}$, where the matrix \mathbf{A} is equal to the $n \times n$ correlation matrix \mathbf{R} , and the observation vector \mathbf{b} is identical to the n -length CDMA channel output vector \mathbf{y} . Thus the vector of decorrelator decisions is determined by taking the signum of the vector $\mathbf{A}^{-1}\mathbf{b} = \mathbf{R}^{-1}\mathbf{y}$. Note that \mathbf{R}_3 and \mathbf{R}_4 are not strictly diagonally dominant, but their spectral radii are less than unity, since $\rho(|\mathbf{I}_3 - \mathbf{R}_3|) = 0.9008 < 1$ and $\rho(|\mathbf{I}_4 - \mathbf{R}_4|) = 0.8747 < 1$, respectively. In all of the experiments, we assumed the output vector was the all-ones vector.

Table 6.1 compares the proposed GaBP algorithm with standard iterative solution methods [2] (using random initial guesses), previously employed for CDMA multiuser detectors (MUD). Specifically, MUD algorithms based on the algorithms of Jacobi, Gauss-Seidel (GS) and (optimally weighted) successive over-relaxation (SOR)⁴ were investigated [11, 12]. The table lists the convergence rates for the two Gold code-based CDMA settings. Convergence is identified and declared when the differences in all the iterated values are less than 10^{-6} . We see that, in comparison with the previously proposed detectors based upon the Jacobi and GS algorithms, the GaBP detectors converge more rapidly for both $n = 3$ and $n = 4$. The serial (asynchronous) GaBP algorithm achieves the best overall convergence rate, surpassing even the SOR-based detector.

Further speed-up of GaBP can be achieved by adapting known acceleration techniques from linear algebra, such as Aitken's method and Steffensen's iterations [14]. Consider a sequence $\{x_n\}$ (e.g., obtained by using GaBP iterations) linearly converging to the limit \hat{x} , and $x_n \neq \hat{x}$ for $n \geq 0$. According to Aitken's method, if there exists a real number a such that $|a| < 1$ and $\lim_{n \rightarrow \infty} (x_n - \hat{x}) / (x_{n-1} - \hat{x}) = a$, then the sequence $\{y_n\}$ defined by

$$y_n = x_n - \frac{(x_{n+1} - x_n)^2}{x_{n+2} - 2x_{n+1} + x_n}.$$

⁴This moving average improvement of Jacobi and GS algorithms is equivalent to what is known in the BP literature as 'damping' [41].

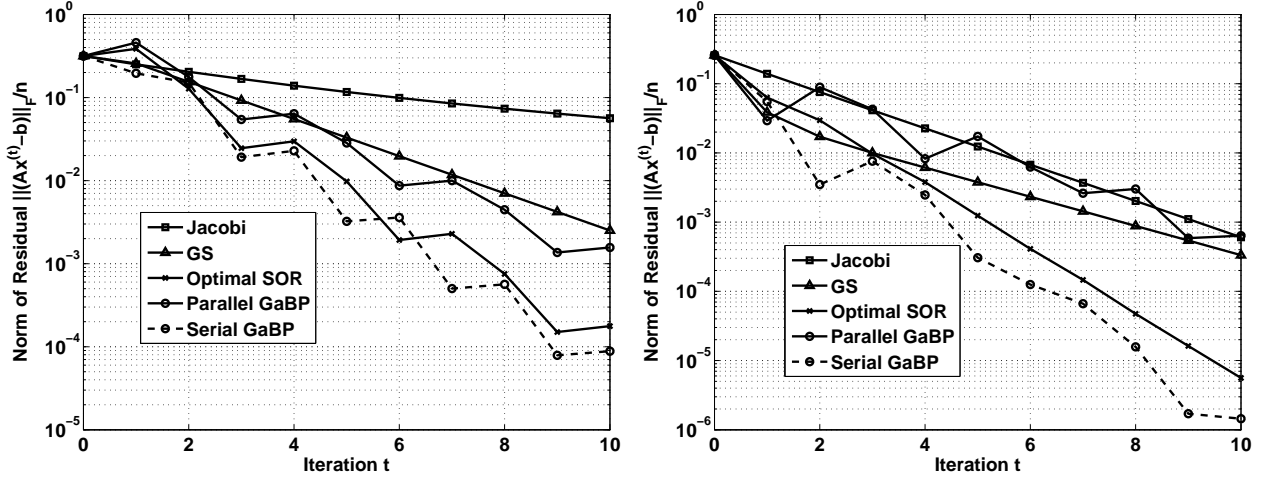


Figure 6.1: Convergence of the two gold CDMA matrices. To the left R_3 , to the right, R_4 .

Algorithm	R_3	R_4
Jacobi+Steffensen ⁵	59	—
Parallel GaBP+Steffensen	13	13
Serial GaBP+Steffensen	9	7

Table 6.2: Decorrelator for $K = 3, 4$ -user, $N = 7$ Gold code CDMA. Total number of iterations required for convergence (threshold $\epsilon = 10^{-6}$) for Jacobi, parallel and serial GaBP solvers accelerated by Steffensen iterations.

converges to \hat{x} faster than $\{x_n\}$ in the sense that $\lim_{n \rightarrow \infty} |(\hat{x} - y_n)/(\hat{x} - x_n)| = 0$. Aitken's method can be viewed as a generalization of over-relaxation, since one uses values from three, rather than two, consecutive iteration rounds. This method can be easily implemented in GaBP as every node computes values based only on its own history.

Steffensen's iterations incorporate Aitken's method. Starting with x_n , two iterations are run to get x_{n+1} and x_{n+2} . Next, Aitken's method is used to compute y_n , this value replaces the original x_n , and GaBP is executed again to get a new value of x_{n+1} . This process is repeated iteratively until convergence. Table 6.2 demonstrates the speed-up of GaBP obtained by using these acceleration methods, in comparison with that achieved by the similarly modified Jacobi algorithm.⁶ We remark that, although the convergence rate is improved with these enhanced

⁶Application of Aitken and Steffensen's methods for speeding-up the convergence of standard (non-BP) iterative solution algorithms in the context of MUD was introduced by Leibig *et al.* [66].

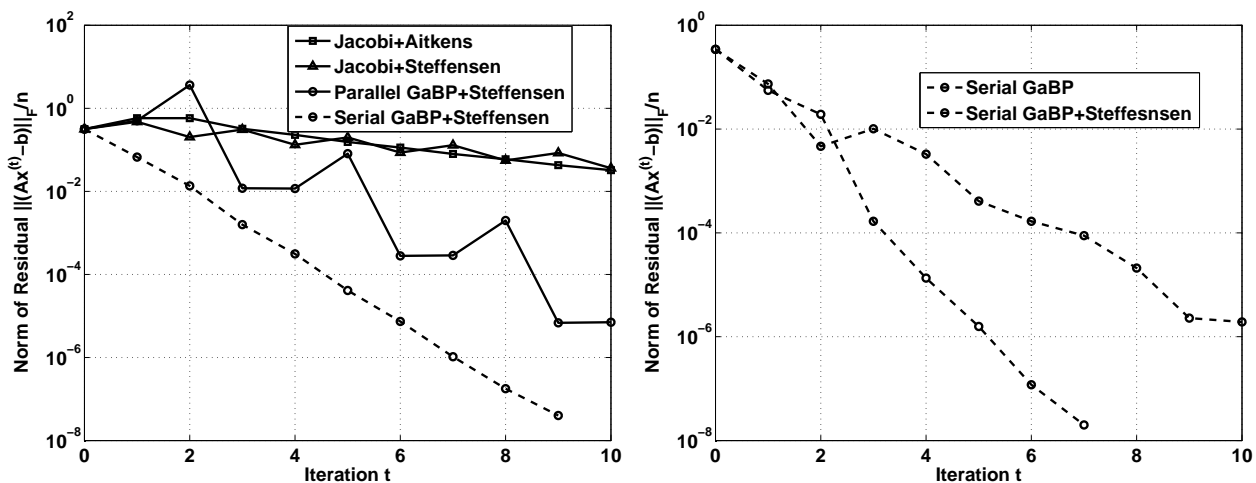


Figure 6.2: Convergence acceleration of the GaBP algorithm using Aitken and Steffensen methods. The left graph depicts a 3×3 gold CDMA matrix, the right graph 4×4 gold CDMA matrix. Further details regarding simulation setup are found in Section 6.

algorithms, the region of convergence of the accelerated GaBP solver remains unchanged.

For the algorithms we examined, 6.6 displays the Euclidean distance between the tentative (intermediate) results and the fixed-point solution as a function of the number of iterations. As expected, all linear algorithms exhibit a logarithmic convergence behavior. Note that GaBP converges faster on average, although there are some fluctuations in the GaBP curves, in contrast to the monotonicity of the other curves.

An interesting question concerns the origin of this convergence speed-up associated with GaBP. Better understanding may be gained by visualizing the iterations of the different methods for the matrix \mathbf{R}_3 case. The convergence contours are plotted in the space of $\{x_1, x_2, x_3\}$ in Fig. 6.3. As expected, the Jacobi algorithm converges in zigzags towards the fixed point (this behavior is well-explained in Bertsekas and Tsitsiklis [40]). The fastest algorithm is serial GaBP. It is interesting to note that GaBP convergence is in a spiral shape, hinting that despite the overall convergence improvement, performance improvement is not guaranteed in successive iteration rounds. In this case the system was simulated with a specific \mathbf{R} matrix for which Jacobi algorithm and other standard methods did not even converge. Using Aitken's method, a further speed-up in GaBP convergence was obtained.

Despite the fact that the examples considered correspond to small multi-user systems, we believe that the results reflect the typical behavior of the algorithms, and that similar qualitative results would be observed in larger systems. In support of this belief, we note, in passing, that GaBP was experimentally shown to converge in a logarithmic number of iterations in the cases of very large matrices both dense (with up to hundreds of thousands of dimensions [67]) and sparse (with up to millions of dimensions [19]).

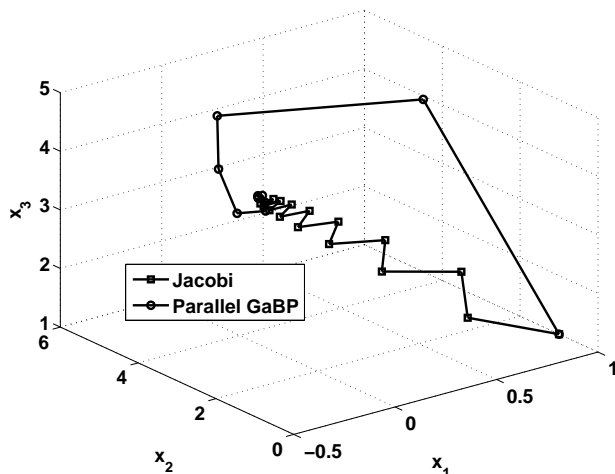


Figure 6.3: Convergence of the GaBP algorithm vs. Jacobi on a 3×3 gold CDMA matrix. Each dimension shows one coordinate of the solution. Jacobi converges in zigzags while GaBP has spiral convergence.

As a final remark on the linear detection example, we mention that, in the case of a channel with Gaussian input signals, for which linear detection is optimal, it can be easily shown that the proposed GaBP scheme reduces to the BP-based MUD scheme, recently introduced by Montanari *et al.* [42]. Their BP scheme, tailored specifically for Gaussian signaling, has been proven to converge to the MMSE (and optimal) solution for any arbitrarily loaded, randomly-spread CDMA system (*i.e.*, a system where $\rho(\mathbf{I}_n - \mathbf{R}) \lesssim 1$).⁷ Thus Gaussian-input additive white Gaussian noise CDMA is another example for which the proposed GaBP solver converges to the MAP decisions for any $m \times n$ random spreading matrix \mathbf{S} , regardless of the spectral radius.

6.1 Extending GaBP to support non-square matrices

In the previous Section, linear detection has been explicitly linked to BP [7], using a Gaussian belief propagation (GaBP) algorithm. This allows for a distributed implementation of the linear detector [15], circumventing the need of, potentially cumbersome, direct matrix inversion (via, *e.g.*, Gaussian elimination). The derived iterative framework was compared quantitatively with ‘classical’ iterative methods for solving systems of linear equations, such as those investigated in the context of linear implementation of CDMA demodulation [11, 12, 13]. GaBP is shown to yield faster convergence than these standard methods. Another important work is the BP-based MUD, recently derived and analyzed by Montanari *et al.* [42] for Gaussian input symbols.

There are several drawbacks to the linear detection technique presented earlier [7]. First, the

⁷For non-Gaussian signaling, *e.g.* with binary input alphabet, this BP-based detector is conjectured to converge only in the large-system limit, as $n, m \rightarrow \infty$ [42].

input matrix $\mathbf{R}_{n \times n} = \mathbf{S}_{n \times k}^T \mathbf{S}_{k \times n}$ (the chip correlation matrix) needs to be computed prior to running the algorithm. This computation requires $n^2 k$ operations. In case where the matrix \mathbf{S} is sparse [65], the matrix \mathbf{R} might not no longer be sparse. Second, GaBP uses $2n^2$ memory to store the messages. For a large n this could be prohibitive.

In this Section, we propose a new construction that addresses those two drawbacks. In our improved construction, given a non-rectangular CDMA matrix $\mathbf{S}_{n \times k}$, we compute the MMSE detector $x = (\mathbf{S}^T \mathbf{S} + \Psi)^{-1} \mathbf{S}^T y$ where Ψ is the AWGN diagonal covariance matrix. We utilize the GaBP algorithm which is an efficient iterative distributed algorithm. The new construction uses only $2nk$ memory for storing the messages. When $k \ll n$ this represents significant saving relative to the $2n^2$ in our previously proposed algorithm. Furthermore, we do not explicitly compute $\mathbf{S}^T \mathbf{S}$, saving an extra $n^2 k$ overhead.

In Chapter 4.1 we show that Montanari's algorithm [42] is an instance of our method. By showing this, we are able to prove new convergence results for Montanari's algorithm. Montanari proves that his method converges on normalized random-spreading CDMA sequences, assuming Gaussian signaling. Using binary signaling, he conjectures convergence to the large system limit. Here, we extend Montanari's result, to show that his algorithm converges also for non-random CDMA sequences when binary signaling is used, under weaker conditions. Another advantage of our work is that we allow different noise levels per bit transmitted.

6.1.1 Distributed Iterative Computation of the MMSE Detector

In this section, we efficiently extend the applicability of the proposed GaBP-based solver for systems with symmetric matrices [7] to systems with any square (*i.e.*, also nonsymmetric) or rectangular matrix. We first construct a new symmetric data matrix $\tilde{\mathbf{R}}$ based on an arbitrary (non-rectangular) matrix $\mathbf{S} \in \mathbb{R}^{k \times n}$

$$\tilde{\mathbf{R}} \triangleq \begin{pmatrix} \mathbf{I}_k & \mathbf{S}^T \\ \mathbf{S} & -\Psi \end{pmatrix} \in \mathbb{R}^{(k+n) \times (k+n)}. \quad (6.5)$$

Additionally, we define a new vector of variables $\tilde{\mathbf{x}} \triangleq \{\hat{\mathbf{x}}^T, \mathbf{z}^T\}^T \in \mathbb{R}^{(k+n) \times 1}$, where $\hat{\mathbf{x}} \in \mathbb{R}^{k \times 1}$ is the (to be shown) solution vector and $\mathbf{z} \in \mathbb{R}^{n \times 1}$ is an auxiliary hidden vector, and a new observation vector $\tilde{\mathbf{y}} \triangleq \{\mathbf{0}^T, \mathbf{y}^T\}^T \in \mathbb{R}^{(k+n) \times 1}$.

Now, we would like to show that solving the symmetric linear system $\tilde{\mathbf{R}} \tilde{\mathbf{x}} = \tilde{\mathbf{y}}$ and taking the first k entries of the corresponding solution vector $\tilde{\mathbf{x}}$ is equivalent to solving the original (not necessarily symmetric) system $\mathbf{R} \mathbf{x} = \mathbf{y}$. Note that in the new construction the matrix $\tilde{\mathbf{R}}$ is sparse again, and has only $2nk$ off-diagonal nonzero elements. When running the GaBP algorithm we have only $2nk$ messages, instead of n^2 in the previous construction.

Writing explicitly the symmetric linear system's equations, we get

$$\hat{\mathbf{x}} + \mathbf{S}^T \mathbf{z} = \mathbf{0}, \quad \mathbf{S} \hat{\mathbf{x}} - \Psi \mathbf{z} = \mathbf{y}.$$

Thus,

$$\hat{\mathbf{x}} = \Psi^{-1} \mathbf{S}^T (\mathbf{y} - \mathbf{S} \hat{\mathbf{x}}),$$

and extracting $\hat{\mathbf{x}}$ we have

$$\hat{\mathbf{x}} = (\mathbf{S}^T \mathbf{S} + \Psi)^{-1} \mathbf{S}^T \mathbf{y}.$$

Note, that when the noise level is zero, $\Psi = 0_{m \times m}$, we get the Moore-Penrose pseudoinverse solution

$$\hat{\mathbf{x}} = (\mathbf{S}^T \mathbf{S})^{-1} \mathbf{S}^T \mathbf{y} = \mathbf{S}^\dagger \mathbf{y}.$$

6.1.2 Relation to factor graph

In this section we give an alternate proof of the correctness of our construction. Given the inverse covariance matrix $\tilde{\mathbf{R}}$ defined in (6.5), and the shift vector $\tilde{\mathbf{x}}$ we can derive the matching self and edge potentials

$$\begin{aligned} \psi_{ij}(x_i, x_j) &\triangleq \exp(-x_i R_{ij} x_j), \\ \phi_i(x_i) &\triangleq \exp(-1/2 x_i R_{ii}^2 x_i - x_i y_i). \end{aligned}$$

which is a factorization of the Gaussian system distribution

$$\begin{aligned} p(\mathbf{x}) &\propto \prod_i \phi_i(x_i) \prod_{i,j} \psi_{ij}(x_i, x_j) = \prod_{i \leq k} \phi_i(x_i) \prod_{i > k} \phi_i(x_i) \prod_{i,j} \psi_{ij}(x_i, x_j) = \\ &= \prod_{i \leq k} \overbrace{\exp(-\frac{1}{2} x_i^2)}^{\text{prior on } x} \prod_{i > k} \exp(-\frac{1}{2} \Psi_i x_i^2 - x_i y_i) \prod_{i,j} \exp(-x_i \overbrace{S_{ij}}^{R_{ij}} x_j). \end{aligned}$$

Next, we show the relation of our construction to a factor graph. We will use a factor graph with k nodes to the left (the bits transmitted) and n nodes to the right (the signal received), shown in Fig. 1. Using the definition $\tilde{\mathbf{x}} \triangleq \{\hat{\mathbf{x}}^T, \mathbf{z}^T\}^T \in \mathbb{R}^{(k+n) \times 1}$ the vector $\hat{\mathbf{x}}$ represents the k input bits and the vector \mathbf{z} represents the signal received. Now we can write the system probability as:

$$p(\tilde{\mathbf{x}}) \propto \int_{\hat{\mathbf{x}}} \mathcal{N}(\hat{\mathbf{x}}; 0, I) \mathcal{N}(\mathbf{z}; S\hat{\mathbf{x}}, \Psi) d\hat{\mathbf{x}}$$

It is known that the marginal distribution over \mathbf{z} is:

$$= \mathcal{N}(\mathbf{z}; 0, \mathbf{S}^T \mathbf{S} + \Psi).$$

This distribution is Gaussian, with the following parameters:

$$E(\mathbf{z} | \hat{\mathbf{x}}) = (\mathbf{S}^T \mathbf{S} + \Psi)^{-1} \mathbf{S}^T \mathbf{y},$$

$$Cov(\mathbf{z} | \hat{\mathbf{x}}) = (\mathbf{S}^T \mathbf{S} + \Psi)^{-1}.$$

It is interesting to note that a similar construction was used by Frey [68] in his seminal 1999 work when discussing the factor analysis learning problem. Comparison to Frey's work is found in Chapter 4.2.

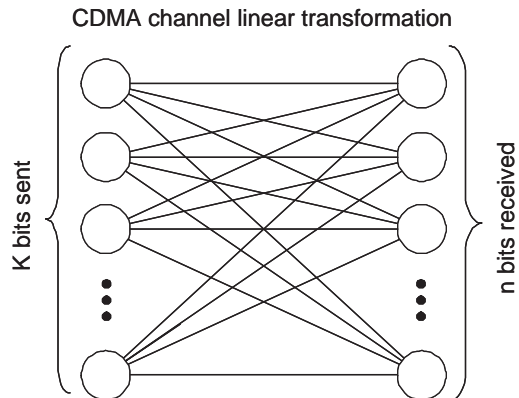


Figure 6.4: Factor graph describing the linear channel

6.1.3 New convergence results

One of the benefits of using our new construction is that we propose a new mechanism to provide future convergence results. In the Appendix we prove that Montanari's algorithm is an instance of our algorithm, thus our convergence results apply to Montanari's algorithm as well.

We know that if the matrix $\tilde{\mathbf{R}}$ is strictly diagonally dominant, then GaBP converges and the marginal means converge to the true means [8, Claim 4]. Noting that the matrix $\tilde{\mathbf{R}}$ is symmetric, we can determine the applicability of this condition by examining its columns. Referring to (4) we see that in the first k columns, we have the k CDMA sequences. We assume random-spreading binary CDMA sequences where the total system power is normalized to one. In other words, the absolute sum of each column is 1. By adding ϵ to the main diagonal, we insure that the first k columns are diagonally dominant. In the next n columns of the matrix $\tilde{\mathbf{R}}$, we have the diagonal covariance matrix Ψ with different noise levels per bit in the main diagonal, and zero elsewhere. The absolute sum of each column of S is k/n , thus when the noise level of each bit satisfies $\Psi_i > k/n$, we have a convergence guarantee. Note, that the convergence condition is a *sufficient condition*. Based on Montanari's work, we also know that in the large system limit, the algorithm converges for binary signaling, even in the absence of noise.

An area of future work is to utilize this observation to identify CDMA schemes with matrices \mathbf{S} that when fitted into the matrix $\tilde{\mathbf{R}}$ are either DD, or comply to the spectral radius convergence condition of [9].

$$\left(\begin{array}{cccc|cccc} 1 & 0 & \cdots & 0 & 1/n & -1/n & -1/n & 1/n & \cdots & 1/n \\ 0 & 1 & & 0 & & & & & & \\ \cdots & & \ddots & & & & & & & \\ 0 & 0 & \cdots & 1 & 1/n & -1/n & 1/n & -1/n & \cdots & -1/n \\ \hline 1/n & \cdots & & 1/n & \Psi_1 & 0 & 0 & & \cdots & 0 \\ -1/n & & & -1/n & 0 & \Psi_2 & & & & \cdots \\ -1/n & & & 1/n & & & & & & \\ 1/n & & & -1/n & & & & & & \\ \vdots & & & \vdots & & & & & \ddots & 0 \\ 1/n & & & -1/n & & & & \cdots & 0 & \Psi_n \end{array} \right)$$

Figure 6.5: An example randomly spreading CDMA sequences matrices using our new construction. Using this illustration, it is easy to give a sufficient convergence proof to the GaBP algorithm. Namely, when the above matrix is diagonally dominant.

Chapter 7

Support vector regression

Support-vector machines (SVMs) are a class of algorithms that have, in recent years, exhibited superior performance compared to other pattern classification algorithms. There are several formulations of the SVM problem, depending on the specific application of the SVM (e.g., classification, regression, etc.).

One of the difficulties in using SVMs is that building an SVM requires solving a constrained quadratic programming problem, whose size is quadratic in the number of training examples. This fact has led to much research on efficient SVM solvers. Recently, several researchers have suggested using multiple computing nodes in order to increase the computational power available for solving SVMs.

In this chapter, we introduce a distributed SVM solver based on the Gaussian Belief Propagation (GaBP) algorithm. We improve on the original GaBP algorithm by reducing the communication load, as represented by the number of messages sent in each optimization iteration, from n^2 to n aggregated messages, where n is the number of data points. Previously, it was known that the GaBP algorithm is very efficient for sparse matrices. Using our novel construction, we demonstrate that the algorithm exhibits very good performance for dense matrices as well. We also show that the GaBP algorithm can be used with kernels, thus making the algorithm more powerful than previously possible.

Using extensive simulation we demonstrate the applicability of our protocol vs. the state-of-the-art existing parallel SVM solvers. Using a Linux cluster of up to a hundred machines and the IBM Blue Gene supercomputer we managed to solve very large data sets up to hundreds of thousands data point, using up to 1,024 CPUs working in parallel. Our comparison shows that the proposed algorithm is just as accurate as these solvers, while being significantly faster.

7.1 Classification Using Support Vector Machines

We begin by formulating the SVM problem. Consider a training set:

$$D = \{(\mathbf{x}_i, y_i), \quad i = 1, \dots, N, \quad \mathbf{x}_i \in \mathbb{R}^m, \quad y_i \in \{-1, 1\}\}. \quad (7.1)$$

The goal of the SVM is to learn a mapping from \mathbf{x}_i to y_i such that the error in mapping, as measured on a new dataset, would be minimal. SVMs learn to find the linear weight vector that separates the two classes so that

$$y_i(\mathbf{x}_i \cdot \mathbf{w} + b) \geq 1 \text{ for } i = 1, \dots, N. \quad (7.2)$$

There may exist many hyperplanes that achieve such separation, but SVMs find a weight vector \mathbf{w} and a bias term b that maximize the margin $2/\|\mathbf{w}\|$. Therefore, the optimization problem that needs to be solved is

$$\min J_D(\mathbf{w}) = \frac{1}{2} \|\mathbf{w}\|, \quad (7.3)$$

$$\text{Subject to } y_i(\mathbf{x}_i \cdot \mathbf{w} + b) \geq 1 \text{ for } i = 1, \dots, N. \quad (7.4)$$

Any points lying on the hyperplane $y_i(\mathbf{x}_i \cdot \mathbf{w} + b) = 1$ are called support vectors.

If the data cannot be separated using a linear separator, a slack variable $\xi \geq 0$ is introduced and the constraint is relaxed to:

$$y_i(\mathbf{x}_i \cdot \mathbf{w} + b) \geq 1 - \xi_i \text{ for } i = 1, \dots, N. \quad (7.5)$$

The optimization problem then becomes:

$$\min J_D(\mathbf{w}) = \frac{1}{2} \|\mathbf{w}\| + C \sum_{i=1}^N \xi_i, \quad (7.6)$$

$$\text{Subject to } y_i(\mathbf{x}_i \cdot \mathbf{w} + b) \geq 1 \text{ for } i = 1, \dots, N, \quad (7.7)$$

$$\xi_i \geq 0 \text{ for } i = 1, \dots, N. \quad (7.8)$$

The weights of the linear function can be found directly or by converting the problem into its dual optimization problem, which is usually easier to solve.

Using the notation of Vijayakumar and Wu [69], the dual problem is thus:

$$\max L_D(h) = \sum_i h_i - \frac{1}{2} h^T D h \quad (7.9)$$

$$\text{subject to } 0 \leq h_i \leq C, \quad i = 1, \dots, N, \quad (7.10)$$

$$\sum_i h_i y_i = 0 \quad (7.11)$$

where D is a matrix such that $D_{ij} = y_i y_j K(\mathbf{x}_i, \mathbf{x}_j)$ and $K(\cdot, \cdot)$ is either an inner product of the samples or a function of these samples. In the latter case, this function is known as the kernel function, which can be any function that complies with the Mercer conditions [70]. For example, these may be polynomial functions, radial-basis (Gaussian) functions, or hyperbolic tangents. If the data is not separable, C is a tradeoff between maximizing the margin and reducing the number of misclassifications.

The classification of a new data point is then computed using the following equation:

$$(x) = \text{sign} \left(\sum_{i \in SV} h_i y_i K(x_i, x) + b \right) \quad (7.12)$$

7.2 Kernel Ridge Regression problem

Kernel Ridge Regression (KRR) implements a regularized form of the least squares method useful for both regression and classification. The non-linear version of KRR is similar to the Support-Vector Machine (SVM) problem. However, in the latter, special emphasis is given to points close to the decision boundary, which is not provided by the cost function used by KRR.

Given training data

$$\mathcal{D} = \{\mathbf{x}_i, y_i\}_{i=1}^l, \mathbf{x}_i \in R^d, y_i \in R$$

the KRR algorithm determines the parameter vector $\mathbf{w} \in R^d$ of a non-linear model (using the “kernel trick”), via minimization of the following objective function: [67]:

$$\min \lambda \|\mathbf{w}\|^2 + \sum_{i=1}^l (y_i - \mathbf{w}^T \Phi(\mathbf{x}_i))^2$$

where λ is a tradeoff parameter between the two terms of the optimization function, and $\Phi(\cdot)$ is a (possible non-linear) mapping of the training patterns.

One can show that the dual form of this optimization problem is given by:

$$\max W(\alpha) = \mathbf{y}^T \alpha + 1/4 \lambda \alpha^T \mathbf{K} \alpha - 1/4 \alpha^T \alpha \quad (7.13)$$

where \mathbf{K} is a matrix whose (i, j) -th entry is the kernel function $\mathbf{K}_{i,j} = \Phi(\mathbf{x}_i)^T \Phi(\mathbf{x}_j)$.

The optimal solution to this optimization problem is:

$$\alpha = 2\lambda(\mathbf{K} + \lambda\mathbf{I})^{-1}\mathbf{y}$$

The corresponding prediction function is given by:

$$f(\mathbf{x}) = \mathbf{w}^T \Phi(\mathbf{x}) = \mathbf{y}^T (\mathbf{K} + \lambda\mathbf{I})^{-1} \mathbf{K}(\mathbf{x}_i, \mathbf{x}).$$

7.3 Previous Approaches for Solving Parallel SVMs

There are several main methods for finding a solution to an SVM problem on a single-node computer. (See Chapter 10 of [70]) for a taxonomy of such methods.) However, since solving an SVM is quadratic in time and cubic in memory, these methods encounter difficulty when scaling to datasets that have many examples and support vectors. The latter two are not synonymous. A large dataset with many repeated examples might be solved using sub-sampling approaches, while a highly non-separable dataset with many support vectors will require an altogether different solution strategy. The literature covers several attempts at solving SVMs in parallel, which allow for greater computational power and larger memory size. In Collobert et al. [71] the SVM solver is parallelized by training multiple SVMs, each on a subset of the training data, and aggregating the resulting classifiers into a single classifier. The training data is then redistributed to the classifiers according their performance and the process is iterated until convergence is reached. The need to

re-divide the data among the SVM classifiers means that the data must be moved between nodes several times; this rules out the use of an approach where bandwidth is a concern. A more low-level approach is taken by Zanghirati et al. [72], where the quadratic optimization problem is divided into smaller quadratic programs (similar to the Active Set methods), each of which is solved on a different node. The results are aggregated and the process is repeated until convergence. The performance of this method has a strong dependence on the caching architecture of the cluster. Graf et al. [73] partition the data and solve an SVM for each partition. The support vectors from each pair of classifiers are then aggregated into a new training set for which an SVM is solved. The process continues until a single classifier remains. The aggregation process can be iterated, using the support vectors of the final classifier in the previous iteration to seed the new classifiers. One problem with this approach is that the data must be repeatedly shared between nodes, meaning that once again the goal of data distribution cannot be attained. The second problem, which might be more severe, is that the number of possible support vectors is restricted by the capacity of a single SVM solver. Yom Tov [74] proposed modifying the sequential algorithm developed in [69] to batch mode. In this way, the complete kernel matrix is held in distributed memory and the Lagrange multipliers are computed iteratively. This method has the advantage that it can efficiently solve difficult SVM problems that have many support vectors to their solution. Based on that work, we show in this paper how an SVM solution can be obtained by adapting a Gaussian Belief Propagation algorithm to the solution of the algorithm proposed in [69].

Recently, Hazan *et al.* proposed an iterative algorithm for parallel decomposition based on Fenchel Duality [75]. Zanni *et al.* proposes a decomposition method for computing SVM in parallel [76]. We compare our run time results to both systems in Section 7.6.

For our proposed solution, we take the exponent of dual SVM formulation given in equation (7.9) and solve $\max \exp(L_D(h))$. Since $\exp(L_D(h))$ is convex, the solution of $\max \exp(L_D(h))$ is a global maximum that also satisfies $\max L_D(h)$ since the matrix D is symmetric and positive definite. Now we can relate to the new problem formulation as a probability density function, which is in itself Gaussian:

$$p(h) \propto \exp\left(-\frac{1}{2}h^T D h + h^T \mathbf{1}\right),$$

where $\mathbf{1}$ is a vector of $(1, 1, \dots, 1)$ and find the assignment of $\hat{h} = \arg \max p(h)$. It is known [77] that in Gaussian models finding the MAP assignment is equivalent to solving the inference problem. To solve the inference problem, namely computing the marginals \hat{h} , we propose using the GaBP algorithm, which is a distributed message passing algorithm. We take the computed \hat{h} as the Lagrange multiplier weights of the support vectors of the original SVM data points and apply a threshold for choosing data points with non-zero weight as support vectors.

Note that using this formulation we ignore the remaining constraints 7.10, 7.11. In other words we do not solve the SVM problem, but the kernel ridge regression problem. Nevertheless, empirical results presented in Section 7.6 show that we achieve very good classification vs. state-of-the-art SVM solvers.

Finally, following [69], we remove the explicit bias term b and instead add another dimension to the pattern vector \mathbf{x}_i such that $\hat{\mathbf{x}}_i = (x_1, x_2, \dots, x_N, \lambda)$, where λ is a scalar constant. The mod-

ified weight vector, which incorporates the bias term, is written as $\hat{\mathbf{w}} = (w_1, w_2, \dots, w_N, b/\lambda)$. However, this modification causes a change to the optimized margin. Vijayakumar and Wu [69] discuss the effect of this modification and reach the conclusion that “setting the augmenting term to zero (equivalent to neglecting the bias term) in high dimensional kernels gives satisfactory results on real world data”. We did not completely neglect the bias term and in our experiments, which used the Radial Basis Kernel, set it to $1/N$, as proposed in [74].

7.4 GaBP Algorithm Convergence

In order to force the algorithm to converge, we artificially weight the main diagonal of the kernel matrix D to make it diagonally dominant. Section 7.6 outlines our empirical results showing that this modification did not significantly affect the error in classifications on all tested data sets.

A partial justification for weighting the main diagonal is found in [67]. In the 2-Norm soft margin formulation of the SVM problem, the sum of squared slack variables is minimized:

$$\begin{aligned} \min_{\xi, w, b} \|\mathbf{w}\|_2^2 + C \sum_i \xi_i^2 \\ \text{s.t. } y_i(\mathbf{w} \cdot \mathbf{x}_i + b) \geq 1 - \xi_i \end{aligned}$$

The dual problem is derived:

$$W(h) = \sum_i h_i - \frac{1}{2} \sum_{i,j} y_i y_j h_i h_j (\mathbf{x}_i \cdot \mathbf{x}_j + \frac{1}{C} \delta_{ij}),$$

where δ_{ij} is the Kronecker δ defined to be 1 when $i = j$, and zero elsewhere. It is shown that the only change relative to the 1-Norm soft margin SVM is the addition of $1/C$ to the diagonal of the inner product matrix associated with the training set. This has the effect of adding $1/C$ to the eigenvalues, rendering the kernel matrix (and thus the GaBP problem) better conditioned [67].

7.5 Convergence in Asynchronous Settings

One of the desired properties of a large scale algorithm is that it should converge in asynchronous settings as well as in synchronous settings. This is because in a large-scale communication network, clocks are not synchronized accurately and some nodes may be slower than others, while some nodes experience longer communication delays.

Corollary 27. *Assuming one of the convergence conditions (Theorems 12, 13) holds, the GaBP algorithm convergence using serial (asynchronous) scheduling as well.*

Proof. The quadratic Min-Sum algorithm [6] provides a convergence proof in the asynchronous case. In Section 4.4 we show equivalence of both algorithms. Thus, assuming one of the convergence conditions holds, the GaBP algorithm converges using serial scheduling as well. \square

Recent work by Koller et. al [58] defines conditions for the convergence of belief propagation. This work defines a distance metric on the space of BP messages; if this metric forms a max-norm construction, the BP algorithm converges under some assumptions. Using experiments on various network sizes, up to a sparse matrix of one million over one million nodes, the algorithm converged asynchronously in all cases where it converged in synchronous settings. Furthermore, as noted in [58], in asynchronous settings the algorithm converges faster as compared to synchronous settings.

7.6 Experimental Results

We implemented our proposed algorithm using approximately 1,000 lines of code in C. We implemented communication between the nodes using the MPICH2 message passing interface¹. Each node was responsible for d data points out of the total n data points in the dataset.

Our implementation used synchronous communication rounds because of MPI limitations. In Section 7.7 we further elaborate on this issue.

Each node was assigned several examples from the input file. Then, the kernel matrix D was computed by the nodes in a distributed fashion, so that each node computed the rows of the kernel matrix related to its assigned data points. After computing the relevant parts of the matrix D , the nodes weighted the diagonal of the matrix D , as discussed in Section 7.4. Then, several rounds of communication between the nodes were run. In each round, using our optimization, a total of n sums were calculated using MPI_Allreduce system call. Finally, each node output the solution x , which was the mean of the input Gaussian that matched its own data points. Each x_i signified the weight of the data point i for being chosen as a support vector.

To compare our algorithm performance, we used two algorithms: Sequential SVM (SVMSeq) [69] and SVMlight [78]. We used the SVMSeq implementation provided within the IBM Parallel Machine Learning (PML) toolbox [79]. The PML implements the same algorithm by Vijaykumar and Wu [69] that our GaBP solver is based on, but the implementation is through a master-slave architecture as described in [74]. SVMlight is a single computing node solver.

Table 7.1 describes the seven datasets we used to compare the algorithms and the classification accuracy obtained. These computations were done using five processing nodes (3.5GHz Intel Pentium machines, running the Linux operating system) for each of the parallel solvers. All datasets were taken from the UCI repository [80]. We used medium-sized datasets so that run-times using SVMlight would not be prohibitively high. All algorithms were run with an RBF kernel. The parameters of the algorithm (kernel width and misclassification cost) were optimized using a line-search algorithm, as detailed in [81].

Note that SVMlight is a single node solver, which we use mainly as a comparison for the accuracy in classification.

Using the Friedman test [82], we did not detect any statistically significant difference between the performance of the algorithms with regards to accuracy ($p < 0.10^{-3}$).

¹<http://www-unix.mcs.anl.gov/mpi/mpich/>

Dataset	Dimension	Train	Test	ERROR (%)		
				GaBP	Sequential	SVMLight
Isolet	617	6238	1559	7.06	5.84	49.97
Letter	16	20000		2.06	2.06	2.3
Mushroom	117	8124		0.04	0.05	0.02
Nursery	25	12960		4.16	5.29	0.02
Pageblocks	10	5473		3.86	4.08	2.74
Pen digits	16	7494	3498	1.66	1.37	1.57
Spambase	57	4601		16.3	16.5	6.57

Table 7.1: Error rates of the GaBP solver versus those of the parallel sequential solver and SVMlight

Dataset	RUN TIMES (SEC)	
	GaBP	Sequential
Isolet	228	1328
Letter	468	601
Mushroom	226	176
Nursery	221	297
Pageblocks	26	37
Pen digits	45	155
Spambase	49	79

Table 7.2: Running times (in seconds) of the GaBP solver (working in a distributed environment) compared to that of the IBM parallel solver

Figure 7.1 shows the speedup results of the algorithm when running the GaBP algorithm on a Blue Gene supercomputer. The speedup with N nodes is computed as the run time of the algorithm on a single node, divided by the run time using N nodes. Obviously, it is desirable to obtain linear speedup, i.e., doubling computational power halves the processing time, but this is limited by the communication load and by parts of the algorithm that cannot be parallelized. Since Blue Gene is currently limited to 0.5 GB of memory at each node, most datasets could not be run on a single node. We therefore show speedup compared to two nodes. As the figure shows, in most cases we get a linear speedup up to 256 CPUs, which means that the running time is linearly proportional to one over the number of used CPUs. When using 512 - 1024 CPUs, the communication overhead reduces the efficiency of the parallel computation. We identified this problem as an area for future research into optimizing the performance for larger scale grids.

We also tested the ability to build classifiers for larger datasets. Table 7.3 shows the run times of the GaBP algorithm using 1024 CPUs on two larger datasets, both from the UCI repository. This demonstrates the ability of the algorithm to process very large datasets in a reasonably short amount of time. We compare our running time to state-of-the-art parallel decomposition method

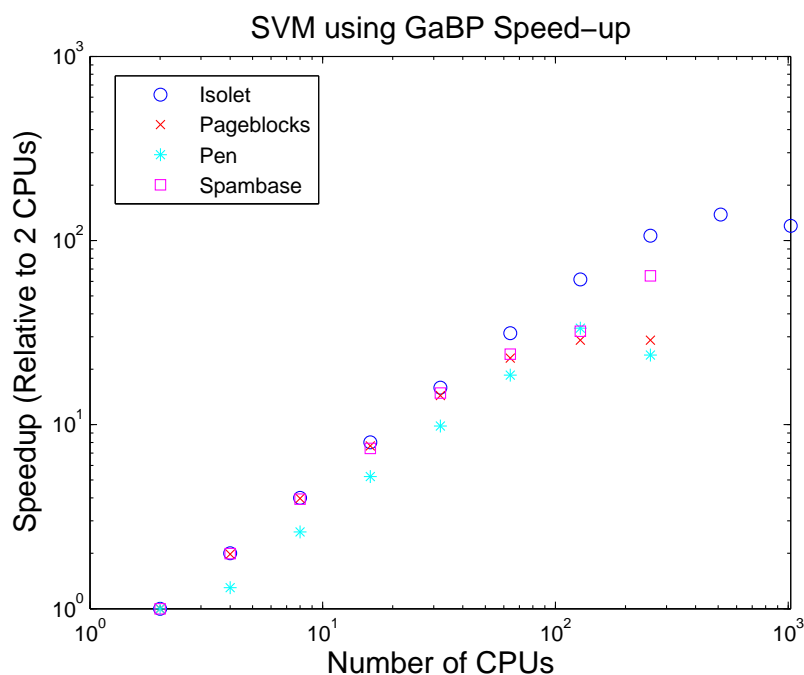


Figure 7.1: Speedup of the GaBP algorithm vs. 2 CPUS

Dataset	Dim	Num of examples	Run time GaBP (sec)	Run time [76] (sec)	Run time [75]
Coverttype	54	150,000/300,000	468	24365	16742
MNIST	784	60,000	756	359	18

Table 7.3: Running times of the GaBP solver for large data sets using 1024 CPUs on an IBM Blue Gene supercomputer. Running time results are compared to two state-of-the-art solvers: [76] and [75].

by Zanni *et al.* [76] and Hazan *et al.*. Using the MNIST dataset we were considerably slower by a factor of two, but in the larger Coverttype dataset we have a superior performance. Note that it is hard to compare running times since the machines used for experimentation are different. Zanni used 16 Pentium IV machines with 16Gb memory, Hazan used 10 Pentium IV machines with 4Gb memory while we used a larger number of weaker Pentium IV machines with 400Mb of memory. Furthermore, in the Coverttype dataset we used only 150,000 data points while Zanni and Hazan used the full dataset which is twice larger.

7.7 Discussion

In this chapter we demonstrated the application of the Gaussian Belief Propagation to the solution of SVM problems. Our experiments demonstrate the usefulness of this solver, being both accurate and scalable.

We implemented our algorithm using a synchronous communication model mainly because MPICH2 does not support asynchronous communication. While synchronous communication is the mode of choice for supercomputers such as Blue Gene, in many cases such as heterogeneous grid environments, asynchronous communication will be preferred. We believe that the next challenging goal will be to implement the proposed algorithm in asynchronous settings, where algorithm rounds will no longer be synchronized.

Our initial experiments with very large sparse kernel matrices (millions of data points) show that asynchronous settings converge faster. Recent work by Koller [58] supports this claim by showing that in many cases the BP algorithm converges faster in asynchronous settings.

Another challenging task would involve scaling to data sets of millions of data points. Currently the full kernel matrix is computed by the nodes. While this is effective for problems with many support vectors [74], it is not required in many problems which are either easily separable or else where the classification error is less important compared to the time required to learn the mode. Thus, solvers scaling to much larger datasets may have to diverge from the current strategy of computing the full kernel matrix and instead sparsify the kernel matrix as is commonly done in single node solvers.

Finally, it remains an open question whether SVMs can be solved efficiently in Peer-to-Peer environments, where each node can (efficiently) obtain data from only several close peers. Future work will be required in order to verify how the GaBP algorithm performs in such an environment, where only partial segments of the kernel matrix can be computed by each node.

Chapter 8

Appendices

8.1 Proof of Lemma 10

Proof. Taking the product of the two Gaussian probability density functions

$$f_1(x)f_2(x) = \frac{\sqrt{P_1P_2}}{2\pi} \exp\left(-\frac{(P_1(x - \mu_1)^2 + P_2(x - \mu_2)^2)}{2}\right) \quad (8.1)$$

and completing the square, one gets

$$f_1(x)f_2(x) = \frac{C\sqrt{P}}{2\pi} \exp\left(-\frac{P(x - \mu)^2}{2}\right), \quad (8.2)$$

with

$$P \triangleq P_1 + P_2, \quad (8.3)$$

$$\mu \triangleq P^{-1}(\mu_1P_1 + \mu_2P_2) \quad (8.4)$$

and the scalar constant determined by

$$C \triangleq \sqrt{\frac{P}{P_1P_2}} \exp\left(\frac{(P_1\mu_1^2(P^{-1}P_1 - 1) + P_2\mu_2^2(P^{-1}P_2 - 1) + 2P^{-1}P_1P_2\mu_1\mu_2)}{2}\right). \quad (8.5)$$

Hence, the product of the two Gaussian densities is $C \cdot \mathcal{N}(\mu, P^{-1})$. □

8.2 Integrating over x_i

Proof.

$$m_{ij}(x_j) \propto \int_{x_i} \psi_{ij}(x_i, x_j) \phi_i(x_i) \prod_{k \in \mathcal{N}(i) \setminus j} m_{ki}(x_i) dx_i \quad (8.6)$$

$$\propto \int_{x_i} \overbrace{\exp(-x_i A_{ij} x_j)}^{\psi_{ij}(x_i, x_j)} \overbrace{\exp(-P_{i \setminus j}(x_i^2/2 - \mu_{i \setminus j} x_i))}^{\phi_i(x_i) \prod_{k \in \mathcal{N}(i) \setminus j} m_{ki}(x_i)} dx_i \quad (8.7)$$

$$= \int_{x_i} \exp((-P_{i \setminus j} x_i^2/2) + (P_{i \setminus j} \mu_{i \setminus j} - A_{ij} x_j) x_i) dx_i \quad (8.8)$$

$$\propto \exp((P_{i \setminus j} \mu_{i \setminus j} - A_{ij} x_j)^2 / (2P_{i \setminus j})) \quad (8.9)$$

$$\propto \mathcal{N}(\mu_{ij} = -P_{ij}^{-1} A_{ij} \mu_{i \setminus j}, P_{ij}^{-1} = -A_{ij}^{-2} P_{i \setminus j}^{-1}), \quad (8.10)$$

where the exponent (8.9) is obtained by using the Gaussian integral (2.13). \square

8.3 Maximizing over x_i

Proof.

$$m_{ij}(x_j) \propto \arg \max_{x_i} \psi_{ij}(x_i, x_j) \phi_i(x_i) \prod_{k \in \mathcal{N}(i) \setminus j} m_{ki}(x_i) \quad (8.11)$$

$$\propto \arg \max_{x_i} \overbrace{\exp(-x_i A_{ij} x_j)}^{\psi_{ij}(x_i, x_j)} \overbrace{\exp(-P_{i \setminus j}(x_i^2/2 - \mu_{i \setminus j} x_i))}^{\phi_i(x_i) \prod_{k \in \mathcal{N}(i) \setminus j} m_{ki}(x_i)} \quad (8.12)$$

$$= \arg \max_{x_i} \exp((-P_{i \setminus j} x_i^2/2) + (P_{i \setminus j} \mu_{i \setminus j} - A_{ij} x_j) x_i). \quad (8.13)$$

Hence, x_i^{\max} , the value of x_i maximizing the product $\psi_{ij}(x_i, x_j) \phi_i(x_i) \prod_{k \in \mathcal{N}(i) \setminus j} m_{ki}(x_i)$ is given by equating its derivative w.r.t. x_i to zero, yielding

$$x_i^{\max} = \frac{P_{i \setminus j} \mu_{i \setminus j} - A_{ij} x_j}{P_{i \setminus j}}. \quad (8.14)$$

Substituting x_i^{\max} back into the product, we get

$$m_{ij}(x_j) \propto \exp((P_{i \setminus j} \mu_{i \setminus j} - A_{ij} x_j)^2 / (2P_{i \setminus j})) \quad (8.15)$$

$$\propto \mathcal{N}(\mu_{ij} = -P_{ij}^{-1} A_{ij} \mu_{i \setminus j}, P_{ij}^{-1} = -A_{ij}^{-2} P_{i \setminus j}), \quad (8.16)$$

which is identical to the result obtained when eliminating x_i via integration (8.10). \square

8.4 Equivalence of Weiss and Johnson formulations

In [77] it is shown that one of the possible ways of converting the information form to pairwise potentials form is when the covariance matrices used are of the type:

$$V_{ij} = \begin{pmatrix} 0 & J_{ij} \\ J_{ji} & 0 \end{pmatrix}$$

Where the terms $J_{ij} = J_{ji}$ are the entries of the covariance matrix J in the information form. First we list the equivalent notations in the two papers:

Weiss	Johnson	comments
P_0	$\hat{J}_{i \setminus j}$	precision of $\psi_{ii}(x_i) \prod_{x_k \in N(x_i) \setminus x_j} m_{ki}(x_i)$
μ_0	$\hat{h}_{i \setminus j}$	mean of $\psi_{ii}(x_i) \prod_{x_k \in N(x_i) \setminus x_j} m_{ki}(x_i)$
P_{ij}	$\Delta J_{i \rightarrow j}$	precision message from i to j
μ_{ij}	$\Delta h_{i \rightarrow j}$	mean message from i to j
μ_{ii}	h_i	prior mean of node i
P_{ii}	J_{ii}	prior precision of node i
P_i	$(P_{ii})^{-1}$	posterior precision of node i
μ_i	μ_i	posterior mean of node i
b	J_{ji}	covariance of nodes i and j
b'	J_{ij}	covariance of nodes i and j
a	0	variance of node i in the pairwise covariance matrix V_{ij}
c	0	variance of node j in the pairwise covariance matrix V_{ij}

Using this fact we can derive again the BP equations (above are the same equation using Weiss' notation).

$$\underbrace{\mu_0}_{\hat{h}_{i \setminus j}} = \underbrace{\mu_{ii}}_{h_i} + \sum_{k \in N(i) \setminus j} \underbrace{\mu_{ki}}_{\Delta h_{k \rightarrow i}}, \quad \underbrace{P_0}_{\hat{J}_{i \setminus j}} = \underbrace{P_{ii}}_{J_{ii}} + \sum_{k \in N(i) \setminus j} \underbrace{P_{ki}}_{\Delta J_{k \rightarrow i}}, \quad (8.17)$$

$$\underbrace{\mu_{ij}}_{\Delta h_{i \rightarrow j}} = - \underbrace{b}_{J_{ji}} \underbrace{(a+P_0)^{-1}}_{(J_{i \setminus j})^{-1}} \underbrace{\mu_0}_{\hat{h}_{i \setminus j}}, \quad \underbrace{P_{ij}}_{\Delta J_{i \rightarrow j}} = \underbrace{c}_0 - \underbrace{b}_{J_{ji}} \underbrace{(a+P_0)^{-1}}_{(0+J_{i \setminus j})^{-1}} \underbrace{b'}_{J_{ij}}. \quad (8.18)$$

Finally:

$$\begin{aligned} \hat{h}_i &= h_{ii} + \sum_{k \in N(i)} \Delta h_{k \rightarrow i}, \quad \hat{J}_i = J_{ii} + \sum_{k \in N(i)} \Delta J_{k \rightarrow i}, \\ \mu_i &= \hat{J}_i^{-1} h_i, \quad P_{ii} = \hat{J}_i^{-1}. \end{aligned}$$

8.5 Proof of Theorem 21

It is shown in [46] that the optimal solution to the cost function is $\mathbf{x} = L^{-1}$ where L is the graph Laplacian. Substitute $\beta = 1, w_{ii} = 1, w_{ij} = 1, y_i = 1$ in the cost function 5.1 :

$$\min E(x) \triangleq \sum_i 1 * (x_i - 1)^2 - 1 * \sum_{i,j \in E} (x_i - x_j)^2.$$

The same cost function in linear algebra form:

$$\min E(\mathbf{x}) \triangleq \mathbf{x}^T L \mathbf{x} - 2\mathbf{x}\mathbf{1} + n.$$

Now we calculate the derivative and compare to zero and get

$$\begin{aligned} \nabla_{\mathbf{x}} E(\mathbf{x}) &= 2\mathbf{x}^T L - 2\mathbf{x}\mathbf{1}, \\ \mathbf{x} &= (L)^{-1}. \quad \square. \end{aligned}$$

8.6 Proof of Theorem 22

Using the notations of [47] the cost function of Koren's spectral layout algorithm is:

$$\begin{aligned} \min \sum_{ij} w_{ij}(x_i - x_j)^2, \\ \text{s.t. } \sum_i \text{deg}(i)x_i^2 = n, \sum_i \text{deg}(i)x_i = 0. \end{aligned}$$

We compute the Lagrangian:

$$\mathcal{L}(\mathbf{x}, \beta, \gamma) = \sum_{ij} w_{ij}(x_i - x_j)^2 - \beta \left(\sum_i \text{deg}(i)x_i^2 - n \right) - \gamma \sum_i \text{deg}(i)x_i.$$

Substitute $\beta = 1, \gamma = 1/2$ we get:

$$= \sum_{ij} w_{ij}(x_i - x_j)^2 - \sum_i \text{deg}(i)(x_i^2 - 1)^2,$$

Reverting to our cost function formulation we get:

$$= \sum_i \text{deg}(i)(x_i - 1)^2 + \sum_{ij} w_{ij}(x_i - x_j)^2.$$

In other words, we substitute $w_{ii} = \text{deg}(i), y_i = 1, \beta = 1$ and we get Koren's formulation. \square

It is interesting to note, that the optimal solution according to Koren's work is $x_i = \sum_{j \in N(i)} \frac{w_{ij}x_j}{\text{deg}(i)}$ which is equivalent to the thin plate model image processing and PDEs [83].

8.7 Proof of Theorem 25

We have shown that the fundamental matrix is equal to $(I - R)^{-1}$. Assume that the edge weights are probabilities of Markov-chain transitions (which means the matrix is stochastic), substitute $\beta = \alpha$, $w_{ii} = 1$, $y_i = 1$ in the cost function (5.1):

$$\min E(x) \triangleq \sum_i 1 * (x_i - 1)^2 - \alpha \sum_{i,j \in E} w_{ij} (x_i - x_j)^2.$$

The same cost function in linear algebra form:

$$\min E(x) \triangleq \mathbf{x}I\mathbf{x} - \alpha\mathbf{x}^T R\mathbf{x} - 2\mathbf{x}.$$

Now we calculate the derivative and compare to zero and get

$$\mathbf{x} = (I - \alpha R)^{-1}. \square$$

8.8 Proof of Theorem 26

The proof is similar to the Spatial Ranking proof. There are two differences: the first is that the prior distribution \mathbf{x} is set in \mathbf{y} to weight the output towards the prior. Second, in the the Personalized PageRank algorithm the result is multiplied by the constant $(1 - \alpha)$, which we omit in our cost function. This computation can be done locally at each node after the algorithm terminates, since α is a known fixed system parameter.

8.9 GaBP code in matlab

Latest code appears on the web on: [\[84\]](#).

8.9.1 The file gabp.m

```
% Implementation of the Gaussian BP algorithm, as given in:
% Linear Detection via Belief Propagation
% By Danny Bickson, Danny Dolev, Ori Shental, Paul H. Siegel and Jack K. Wolf.
% In the 45th Annual Allerton Conference on Communication, Control and Computing,
% Allerton House, Illinois, Sept. 07'
%
%
% Written by Danny Bickson.
% updated: 24-Aug-2008
%
% input: A - square matrix nxn
```

```

% b - vector nx1
% max_iter - maximal number of iterations
% epsilon - convergence threshold
% output: x - vector of size nx1, which is the solution to linear systems
           of equations  $A x = b$ 
%         Pf - vector of size nx1, which is an approximation to the main
%         diagonal of  $\text{inv}(A)$ 
function [x,Pf] = gabp(A, b, max_iter, epsilon)

% Stage 1 - initialize
P = diag(diag(A));
U = diag(b./diag(A));
n = length(A);

% Stage 2 - iterate
for l=1:max_iter
    % record last round messages for convergence detection
    old_U = U;

    for i=1:n
        for j=1:n
            % Compute  $P_{i \setminus j}$  - line 2
            if (i~=j && A(i,j) ~= 0)
                p_i_minus_j = sum(P(:,i)) - P(j,i); %
                assert(p_i_minus_j ~= 0);
                %iterate - line 3
                P(i,j) = -A(i,j) * A(j,i) / p_i_minus_j;
                % Compute  $U_{i \setminus j}$  - line 2
                h_i_minus_j = (sum(P(:,i).*U(:,i)) - P(j,i)*U(j,i)) / p_i_minus_j;
                %iterate - line 3
                U(i,j) = - A(i,j) * h_i_minus_j / P(i,j);
            end
        end
    end
end

% Stage 3 - convergence detection
if (sum(sum((U - old_U).^2)) < epsilon)
    disp(['GABP converged in round ', num2str(l)]);
    break;
end

```

```

end % iterate

% Stage 4 - infer
Pf = zeros(1,n);
x = zeros(1,n);
for i = 1:n
    Pf(i) = sum(P(:,i));
    x(i) = sum(U(:,i).*P(:,i))./Pf(i);
end

end

```

8.9.2 The file run_gabp.m

```

% example for running the gabp algorithm, for computing the solution to Ax = b
% Written by Danny Bickson

% Initialize

%format long;
n = 3; A = [1 0.3 0.1;0.3 1 0.1;0.1 0.1 1]; b = [1 1 1]'; x =
inv(A)*b; max_iter = 20; epsilon = 0.000001;

[x1, p] = gabp(A, b, max_iter, epsilon);

disp('x computed by gabp is: ');

x1

disp('x computed by matrix inversion is : ');

x'

disp('diag(inv(A)) computed by gabp is: (this is an
approximation!) ');

p

disp('diag(inv(A)) computed by matrix inverse is: ');

```

```
diag(inv(A))'
```

Bibliography

- [1] G. H. Golub and C. F. V. Loan, Eds., *Matrix Computation*, 3rd ed. The Johns Hopkins University Press, 1996.
- [2] O. Axelsson, *Iterative Solution Methods*. Cambridge, UK: Cambridge University Press, 1994.
- [3] Y. Saad, Ed., *Iterative methods for Sparse Linear Systems*. PWS Publishing company, 1996.
- [4] J. Pearl, *Probabilistic Reasoning in Intelligent Systems: Networks of Plausible Inference*. San Francisco: Morgan Kaufmann, 1988.
- [5] M. I. Jordan, Ed., *Learning in Graphical Models*. Cambridge, MA: The MIT Press, 1999.
- [6] C. Moallemi and B. V. Roy, "Convergence of the min-sum algorithm for convex optimization," in *Proc. of the 45th Allerton Conference on Communication, Control and Computing*, Monticello, IL, September 2007.
- [7] D. Bickson, O. Shental, P. H. Siegel, J. K. Wolf, and D. Dolev, "Linear detection via belief propagation," in *Proc. 45th Allerton Conf. on Communications, Control and Computing*, Monticello, IL, USA, Sept. 2007.
- [8] Y. Weiss and W. T. Freeman, "Correctness of belief propagation in Gaussian graphical models of arbitrary topology," *Neural Computation*, vol. 13, no. 10, pp. 2173–2200, 2001.
- [9] J. K. Johnson, D. M. Malioutov, and A. S. Willsky, "Walk-sum interpretation and analysis of Gaussian belief propagation," in *Advances in Neural Information Processing Systems 18*, Y. Weiss, B. Schölkopf, and J. Platt, Eds. Cambridge, MA: MIT Press, 2006, pp. 579–586.
- [10] D. M. Malioutov, J. K. Johnson, and A. S. Willsky, "Walk-sums and belief propagation in Gaussian graphical models," *Journal of Machine Learning Research*, vol. 7, Oct. 2006.
- [11] A. Grant and C. Schlegel, "Iterative implementations for linear multiuser detectors," *IEEE Trans. Commun.*, vol. 49, no. 10, pp. 1824–1834, Oct. 2001.
- [12] P. H. Tan and L. K. Rasmussen, "Linear interference cancellation in CDMA based on iterative techniques for linear equation systems," *IEEE Trans. Commun.*, vol. 48, no. 12, pp. 2099–2108, Dec. 2000.
- [13] A. Yener, R. D. Yates, , and S. Ulukus, "CDMA multiuser detection: A nonlinear programming approach," *IEEE Trans. Commun.*, vol. 50, no. 6, pp. 1016–1024, June 2002.
- [14] P. Henrici, *Elements of Numerical Analysis*. John Wiley and Sons, 1964.
- [15] O. Shental, D. Bickson, P. H. Siegel, J. K. Wolf, and D. Dolev, "Gaussian belief propagation solver for systems of linear equations," in *IEEE Int. Symp. on Inform. Theory (ISIT)*, Toronto, Canada, July 2008.
- [16] —, "Gaussian belief propagation for solving systems of linear equations: Theory and application," in *IEEE Transactions on Information Theory*, submitted for publication, June 2008.
- [17] —, "A message-passing solver for linear systems," in *Information Theory and Applications (ITA) Workshop*, San Diego, CA, USA, January 2008.

- [18] D. Bickson, O. Shental, P. H. Siegel, J. K. Wolf, and D. Dolev, "Gaussian belief propagation based multiuser detection," in *IEEE Int. Symp. on Inform. Theory (ISIT)*, Toronto, Canada, July 2008.
- [19] D. Bickson, D. Malkhi, and L. Zhou, "Peer to peer rating," in *the 7th IEEE Peer-to-Peer Computing, Galway, Ireland, Sept. 2007*.
- [20] D. Bickson and D. Malkhi, "A unifying framework for rating users and data items in peer-to-peer and social networks," in *Peer-to-Peer Networking and Applications (PPNA) Journal, Springer-Verlag*, April 2008.
- [21] D. Bickson, D. Dolev, and E. Yom-Tov, "Solving large scale kernel ridge regression using a gaussian belief propagation solver," in *NIPS Workshop on Efficient Machine Learning*, Canada, 2007.
- [22] D. Bickson, D. Dolev, and E. Yom-Tov, "A gaussian belief propagation solver for large scale support vector machines," in *5th European Conference on Complex Systems*, Jerusalem, Sept. 2008.
- [23] T. Anker, D. Bickson, D. Dolev, and B. Hod, "Efficient clustering for improving network performance in wireless sensor networks," in *European Conference on Wireless Sensor Networks (EWSN'08)*.
- [24] K. Aberer, D. Bickson, D. Dolev, M. Hauswirth, and Y. Weiss, "Indexing data-oriented overlay networks using belief propagation," in *7th Workshop of distributed algorithms and data structures (WDAS 06)*, SF, CA, Jan. 2006.
- [25] —, "Extended data indexing in overlay networks using the belief propagation algorithm. (invited paper)," in *In the Peer-to-peer Data Management in the Complex Systems Perspective Workshop (ECCS 05')*, Paris, Nov. 2005.
- [26] D. Bickson, D. Dolev, and Y. Weiss, "Resilient peer-to-peer streaming," in *submitted for publication*, 2007.
- [27] —, "Modified belief propagation for energy saving in wireless and sensor networks," in *Leibniz Center TR-2005-85, School of Computer Science and Engineering, The Hebrew University*, 2005. [Online]. Available: <http://leibniz.cs.huji.ac.il/tr/842.pdf>
- [28] D. Bickson and D. Malkhi, "The Julia content distribution network," in *2nd Usenix Workshop on Real, Large Distributed Systems (WORLDS '05)*, SF, CA, Dec. 2005.
- [29] D. Bickson, D. Malkhi, and D. Rabinowitz, "Efficient large scale content distribution," in *6th Workshop on Distributed Data and Structures (WDAS '04)*, Lausanne, Switzerland, 2004.
- [30] D. Bickson and R. Borer, "Bitcode: A bittorrent clone using network coding," in *7th IEEE Peer-to-Peer Computing*, Galway, Ireland, 9 2007.
- [31] I. Abraham, A. Badola, D. Bickson, D. Malkhi, S. Maloo, and S. Ron, "Practical locality-awareness for large scale information sharing," in *4th Annual International Workshop on Peer-To-Peer Systems (IPTPS '05)*, 2005.
- [32] Y. Kulbak and D. Bickson, "The emule protocol specification," in *Leibniz Center TR-2005-03, School of Computer Science and Engineering, The Hebrew University*, 2005.
- [33] E. Jaffe, D. Bickson, and S. Kirkpatrick, "Everlab - a production platform for research in network experimentation and computation," in *21st Large Installation System Administration Conference (LISA '07)*, Dallas, Texas, 11 2007.
- [34] S. M. Aji and R. J. McEliece, "The generalized distributive law," *IEEE Trans. Inform. Theory*, vol. 46, no. 2, pp. 325–343, Mar. 2000.
- [35] F. Kschischang, B. Frey, and H. A. Loeliger, "Factor graphs and the sum-product algorithm," *IEEE Trans. Inform. Theory*, vol. 47, pp. 498–519, Feb. 2001.
- [36] G. Elidan, McGraw, and D. Koller, "Residual belief propagation: Informed scheduling for asynchronous message passing," July 2006.

- [37] Y. Weiss and W. T. Freeman, "On the optimality of solutions of the max-product belief-propagation algorithm in arbitrary graphs," *Information Theory, IEEE Transactions on*, vol. 47, no. 2, pp. 736–744, 2001.
- [38] L. R. Bahl, J. Cocke, F. Jelinek, and J. Raviv, "Optimal decoding of linear codes for minimizing symbol error rate," *IEEE Trans. Inform. Theory*, vol. 20, no. 3, pp. 284–287, Mar. 1974.
- [39] A. Viterbi, "Error bounds for convolutional codes and an asymptotically optimum decoding algorithm," *Information Theory, IEEE Transactions on*, vol. 13, no. 2, pp. 260–269, 1967.
- [40] D. P. Bertsekas and J. N. Tsitsiklis, *Parallel and Distributed Calculation. Numerical Methods*. Prentice Hall, 1989.
- [41] K. M. Murphy, Y. Weiss, and M. I. Jordan, "Loopy belief propagation for approximate inference: An empirical study," in *Proc. of UAI*, 1999.
- [42] A. Montanari, B. Prabhakar, and D. Tse, "Belief propagation based multi-user detection," in *Proc. 43th Allerton Conf. on Communications, Control and Computing*, Monticello, IL, USA, Sept. 2005.
- [43] B. Frey, "Local probability propagation for factor analysis," in *NEURAL INFORMATION PROCESSING SYSTEMS 2003*, 1999.
- [44] C. C. Moallemi and B. V. Roy, "Consensus propagation," in *IEEE Transactions on Information Theory*, vol. 52, no. 11, 2006, pp. 4753–4766.
- [45] R. Bell and Y. Koren, "Scalable collaborative filtering with jointly derived neighborhood interpolation weights," in *IEEE International Conference on Data Mining (ICDM'07)*, IEEE, 2007.
- [46] K. M. Hall, "An r-dimensional quadratic placement algorithm," in *Management Science*, vol. 17, 1970, pp. 219–229.
- [47] M. DellAmico, "Mapping small worlds," in *the 7th IEEE Peer-to-Peer Computing*, Galway, Ireland, Sept. 2007.
- [48] L. Katz, "A new status index derived from sociometric analysis," in *Psychometrika*, vol. 18, 1953, pp. 39–43.
- [49] J. Johnson, D. Malioutov, and A. Willsky, "Walk-sum interpretation and analysis of gaussian belief propagation," in *NIPS 05*.
- [50] S. Brin and L. Page, "The anatomy of a large-scale hypertextual web search engine," in *Proceedings of the seventh international conference on World Wide Web 7*, 1998, pp. 107–117.
- [51] A. B. K. Csalogany and T. Sarlos, "On the feasibility of low-rank approximation for personalized pagerank," in *Poster Proceedings of the 14th International World Wide Web Conference (WWW)*, 2005, pp. 972–973.
- [52] U. Brandes and D. Fleisch, "Centrality measures based on current flow," in *STACS 2005, LNCS 3404*, 2005, pp. 533–544.
- [53] Y. Koren, "On spectral graph drawing," in *Proceedings of the 9th International Computing and Combinatorics Conference (COCOON'03), Lecture Notes in Computer Science, Vol. 2697*, Springer Verlag, 2003, pp. 496–508.
- [54] C. M. Grinstead and J. L. Snell, "Introduction to probability. the chance project. chapter 11 - markov chains." [Online]. Available: http://www.dartmouth.edu/~chance/teaching_aids/books_articles/probability_book/pdf.html
- [55] Pajek - A program for large network analysis.
<http://vlado.fmf.unilj.si/pub/networks/pajek/>.
- [56] Y. Shavitt and E. Shir, "Dimes: Let the internet measure itself," *ACM SIGCOMM Computer Communications Review*, vol. 35, no. 5, pp. 71–74, 2005.

- [57] "Web research collections. http://ir.dcs.gla.ac.uk/test_collections."
- [58] G. Elidan, I. McGraw, and D. Koller, "Residual belief propagation: Informed scheduling for asynchronous message passing," in *Proceedings of the Twenty-second Conference on Uncertainty in AI (UAI)*, Boston, Massachusetts, 2006.
- [59] S. Verdú, *Multiuser Detection*. Cambridge, UK: Cambridge University Press, 1998.
- [60] J. G. Proakis, *Digital Communications*, 4th ed. New York, USA: McGraw-Hill, 2000.
- [61] Y. Kabashima, "A CDMA multiuser detection algorithm on the basis of belief propagation," *J. Phys. A: Math. Gen.*, vol. 36, pp. 11111–11121, Oct. 2003.
- [62] O. Shental, N. Shental, A. J. Weiss, and Y. Weiss, "Generalized belief propagation receiver for near-optimal detection of two-dimensional channels with memory," in *Proc. IEEE Information Theory Workshop (ITW)*, San Antonio, Texas, USA, Oct. 2004.
- [63] T. Tanaka and M. Okada, "Approximate belief propagation, density evolution, and statistical neurodynamics for CDMA multiuser detection," *IEEE Trans. Inform. Theory*, vol. 51, no. 2, pp. 700–706, Feb. 2005.
- [64] A. Montanari and D. Tse, "Analysis of belief propagation for non-linear problems: The example of CDMA (or: How to prove Tanaka's formula)," in *Proc. IEEE Inform. Theory Workshop (ITW)*, Punta del Este, Uruguay, Mar. 2006.
- [65] C. C. Wang and D. Guo, "Belief propagation is asymptotically equivalent to MAP detection for sparse linear systems," in *Proc. 44th Allerton Conf. on Communications, Control and Computing*, Monticello, IL, USA, Sept. 2006.
- [66] C. Leibig, A. Dekorsy, and J. Fliege, "Power control using Steffensen iterations for CDMA systems with beamforming or multiuser detection," in *Proc. IEEE International Conference on Communications (ICC)*, Seoul, Korea, 2005.
- [67] N. Cristianini and J. Shawe-Taylor, "An introduction to support vector machines and other kernel-based learning methods," in *Cambridge University Press, 2000. ISBN 0-521-78019-5*.
- [68] B. J. Frey, "Local probability propagation for factor analysis," in *Neural Information Processing Systems (NIPS)*, Denver, Colorado, Dec 1999, pp. 442–448.
- [69] S. Vijayakumar and S. Wu, "Sequential support vector classifiers and regression," in *Proc. International Conference on Soft Computing (SOCO'99)*, Genoa, Italy, 1999, pp. 610–619.
- [70] B. Schölkopf and A. J. Smola, "Learning with kernels: Support vector machines, regularization, optimization, and beyond." MIT Press, Cambridge, MA, USA, 2002.
- [71] R. Collobert, S. Bengio, and Y. Bengio, "A parallel mixture of svms for very large scale problems," in *Advances in Neural Information Processing Systems. MIT Press*, 2002.
- [72] G. Zanghirati and L. Zanni, "A parallel solver for large quadratic programs in training support vector machines," in *Parallel computing*, vol. 29, 2003, pp. 535–551.
- [73] H. P. Graf, E. Cosatto, L. Bottou, I. Durdanovic, and V. Vapnik, "Parallel support vector machines: The cascade svm," in *Advances in Neural Information Processing Systems*, 2004.
- [74] E. Yom-Tov, "A distributed sequential solver for large scale svms," in *O. Chapelle, D. DeCoste, J. Weston, L. Bottou: Large scale kernel machines. MIT Press*, 2007, pp. 141–156.
- [75] T. Hazan, A. Man, and A. Shashua, "A parallel decomposition solver for SVM: Distributed dual ascent using fenchel duality," in *Conference on Computer Vision and Pattern Recognition (CVPR)*, Anchorage, June 2008.
- [76] L. Zanni, T. Serafini, and G. Zanghirati, "Parallel software for training large scale support vector machines on multiprocessor systems," *Journal of Machine Learning Research*, vol. 7, pp. 1467–1492, July 2006.

-
- [77] D. M. Malioutov, J. K. Johnson, and A. S. Willsky, "Walk-sums and belief propagation in Gaussian graphical models," in *Journal of Machine Learning Research*, vol. 7, Oct. 2006.
- [78] T. Joachims, "Making large-scale SVM learning practical," in *Advances in Kernel Methods - Support Vector Learning*, B. Scho"lkopf and C. Burges and A. Smola (ed.), MIT Press, 1999.
- [79] IBM parallel toolkit. <http://www.alphaworks.ibm.com/tech/pml> .
- [80] C. L. Blake, E. J. Keogh, and C. J. Merz, "UCI repository of machine learning databases, 1998. <http://www.ics.uci.edu/~mllearn/mlrepository.html>."
- [81] R. Rifkin and A. Klautau, "In defense of One-vs-All classification," in *Journal of Machine Learning Research*, vol. 5, 2004, pp. 101–141.
- [82] J. Demšar, "Statistical comparisons of classifiers over multiple data sets," in *Journal of Machine Learning Research*, vol. 7, 2006, pp. 1–30.
- [83] J. K. Johnson, D. Malioutov, and A. S. Willsky, "Lagrangian relaxation for map estimation in graphical models," in *the 45th Annual Allerton Conference on Communication, Control and Computing*, Allerton house, IL, Sept. 2007.
- [84] Gaussian Belief Propagation implementation in matlab [online] <http://www.cs.huji.ac.il/labs/danss/p2p/gabp/>.